Measuring, modeling and assessing evaporative fluxes over an integrated lake-wetland system in Southern Quebec

Henrique Vieira

A Thesis

in

the Department

of

Building, Civil and Environmental Engineering

Presented in Partial Fulfillment of the Requirements

for the Degree of Master of Applied Science (Civil Engineering) at

Concordia University

Montréal, Québec, Canada

February 2022

CONCORDIA UNIVERSITY
School of Graduate Studies

This is to certify that the thesis prepared

By: Henrique Vieira

Entitled: Measuring, modeling and assessing evaporative fluxes over an integrated lake-wetland system in Southern Quebec

and submitted in partial fulfillment of the requirements for the degree of

Master of Applied Science (Civil Engineering)

complies with the regulations of the University and meets the accepted standards with respect to originality and quality.

Signed by the final examining committee:

Dr. Mazdak Nik-Bakht — Chair

Dr. Zhi Chen — Examiner

_____ — Examiner

Dr. Ali Nazemi — Thesis Supervisor(s)

_____ — Thesis Supervisor(s)

Approved by Dr. Mazdak Nik-Bakht — Chair of Department or Graduate Program Director

Dr. Mourad Debbabi — Dean

Abstract

Measuring, modeling and assessing evaporative fluxes over an integrated lake-wetland system in Southern Quebec

Henrique Vieira

Evapotranspiration (ET) is the second largest component of the hydrological cycle globally and a major factor in surface energy balance. Despite its importance, quantifying evapotranspiration presents high uncertainties due to limitations in available data and modeling approaches. This thesis provides – for the first time – a temporally high-resolution ET dataset (30 minutes) using Eddy Covariance method for a lake-wetland duo in Southern Québec during 2020's growing season, during the Covid-19 pandemic lockdown. In addition, this thesis benchmarks the performance of 40 existing ET models – the largest number of empirical ET models intercompared to date – across different time scales, times of the day and times of the season. The benchmarking effort uses a non-dominated sorting framework with multiple goodness-of-fit measures to rank models. In general, the most non-falsified models in the marsh are Carpenter (aerodynamic), McMillan (aerodynamic), Kimberley-Penman (combination) and Stephens-Stewart (temperature-hybrid). In the lake, Hamon's (temperature) equation remains non-falsified across most scenarios. Comparing continuous simulations in the two landscapes, the expected Nash-Sutcliffe Efficiency of non-falsified models is consistently higher in the marsh across all timescales from half-hour to one month and different times of the season. Considering different diurnal segments, the performance of non-falsified models becomes comparable in daytime and strictly better in the lake during nighttime. ET was better estimated during daytime and nighttime separately than full days. Overestimation of ET was observed during local temperature peaks preceded by prolonged net radiation peaks without precipitation, which potentially points at models' inability to capture the effect of stomata closure of the canopy during heatwaves. Capturing evapotranspiration in wetlands and lakes requires more physically-based parameterizations to represent thermal and biological dynamics at weekly and finer scales. This study also provides evidence for the necessity of using multi-objective ranking to benchmark evapotranspiration and points at strategic directions for future developments.

Résumé

Mesure, modélisation et investigation des flux d'évaporation d'un lac et d'un milieu humide au sud du Québec

Henrique Vieira

L'évapotranspiration (ET) est la deuxième plus importante composante du cycle hydrologique au niveau mondial et un facteur majeur dans le bilan énergétique de surface. Malgré son importance, la quantification de l'évapotranspiration présente de grandes incertitudes en raison des limitations des données disponibles et des approches de modélisation. Ce mémoire fournit - pour la première fois - un ensemble de données d'évapotranspiration à haute résolution temporelle (30 minutes) utilisant la méthode de covariance des flux turbulents pour un duo lac et un milieu humide au sud du Québec pendant la saison de croissance de 2020, durant la période de fermeture de la pandémie Covid-19. De plus, cette recherche compare la performance de 40 modèles d'ET existants - le plus grand nombre de modèles d'ET empiriques comparés dans une étude à ce jour - à différentes échelles de temps, moments de la journée et périodes de la saison. Cette évaluation comparative utilise un cadre de tri non dominé avec de multiples mesures de qualité d'ajustement pour classer les modèles. En général, les modèles les plus non falsifiés dans le marais sont ceux de Carpenter (aérodynamique), McMillan (aérodynamique), Kimberley-Penman (combinaison) et Stephens-Stewart (température-hybride). Dans le lac, l'équation de Hamon (température) reste non falsifiée dans la plupart des scénarios. En comparant les simulations continues dans les deux paysages, l'efficacité attendue de Nash-Sutcliffe des modèles non falsifiés est systématiquement plus élevée dans le marais à toutes les échelles de temps, de la demi-heure au mois, et à différents moments de la saison. En considérant les différents segments diurnes, la performance des modèles non falsifiés devient comparable en journée et strictement meilleure dans le lac pendant la nuit. L'ET a été mieux estimée pendant le jour et la nuit séparément que pendant les journées complètes. Une surestimation de l'ET a été observée lors de pics de température locaux précédés de pics de rayonnement net prolongés sans précipitation, ce qui indique potentiellement l'incapacité des modèles à capturer l'effet de la fermeture des stomates de la canopée pendant les vagues de chaleur. La capture de l'évapotranspiration dans les zones humides et les lacs nécessite des paramétrisations mieux basées sur la physique pour représenter les dynamiques thermiques et biologiques à des échelles hebdomadaires et plus fines. Cette étude fournit également des preuves de la nécessité d'utiliser un classement multi-objectif pour évaluer l'évapotranspiration et indique des directions stratégiques pour les développements futurs.

Acknowledgements

This work is supported by Natural Science and Engineering Research Council of Canada through Discovery Grant, Canadian Foundation for Innovation through John Evans Leader's Fund extended to Dr. Ali Nazemi, as well as Concordia University Scholarships extended to Henrique Vieira during his graduate studies.

I express my gratitude to Prof. Ali Nazemi for his continuous participation, guidance and supervision throughout the research conducted in 2019-2021. I am thankful for the co-workers and colleagues with whom I've shared numerous fruitful professional and personal experiences which had a directly positive impact on this work: Shadi Hatami and Masoud Zaerpour, Samaneh Ashraf, Romaric Desbrousses and Audrey Smith. I extend my gratitude to Prof. Elmira Hassanzadeh from Polytechnique Montréal who has supported and encouraged my work, as well as to my colleagues Ali Sharifinejad, Matheo Kaemo, Hamza Ousoukhman and Sarah Goulet. I am also thankful to my previous professors and tutors who taught me in different water resources engineering classes, namely Prof. Samuel Li, Dr. Atefeh Fazlollahi and Sho Harada.

The important field-based portion of this work has been a success thanks to a collaboration with Josiane Pouliot from the City of Magog, Laura Patriganni from LAMRAC and Ariane Orjikh from Memphremagog Conservation Inc, and many other from the City of Magog who are all committed to supporting research towards environmental conservation. In addition, Prof. Oliver Sonnentag and his team from Université de Montreal were instrumental in the implementation of Eddy Covariance stations and processing routines, namely Gabriel Hould Gosselin and Gesa Meyer. Finally, I thank Jiahong Li from Licor and Marc-Andre Brady from Campbell Scientific for their continuous technical support.

Most of the academic work of this project was conducted in Montreal, which is the traditional land of the Kanien'kehá꞉ka (Mohawk) First Nation, while field work took place in Magog, which is the traditional territory of the Abenaki of the Wabanaki Confederacy.

Dedication

I dedicate this work to my grandfather, who has ignited the spark for the contemplation and understanding of nature during my childhood; to my mother, who is a role model for working hard towards improving livelihoods; to my father, who has always encouraged my progress; to all my friends and family, with whom I have the privilege of sharing and discussing discoveries and learned lessons; and to you, dear reader, hoping that it shall be useful for your own investigation or project. Above all, I dedicate this work to water resources and nature, so that it may constitute another step towards a more sustainable relationship between humans and our environment.

Statement of Contributions

The work related to this thesis was led by Henrique Vieira under supervision of Dr. Ali Nazemi between June 2019 and February 2022. Henrique Vieira joined initially as a research assistant in June 2019. During his time as the research assistant, Henrique Vieira was trained in Dr. Oliver Sonnentag's lab in Université de Montréal on the principles of the Eddy Covariance technique. He officially started his MASc in September 2019.

The main content and materials presented in this thesis is taken from a submitted paper to the *Journal of Hydrology* co-authored by Henrique Vieira, Dr. Ali Nazemi and Dr. Oliver Sonnentag, where Henrique Vieira is the lead author of the submitted paper and is responsible for 100% of data curing, mathematical modeling and numerical analyses that are the backbone of this work. Henrique Vieira also led 100% of the writing of the first draft of the paper, which was reviewed, edited, and commented with Dr. Ali Nazemi through multiple rounds of reviews from May to December 2021. As a result of multiple rounds of revision, the paper has evolved tremendously both in terms of content and the text, which was further consolidated with Dr. Oliver Sonnentag. The paper accordingly was fine tuned according to Dr. Sonnentag's comments on the Eddy Covariance technique and submitted to the *Journal of Hydrology* as "Benchmarking empirical models of evapotranspiration in a lake-wetland duo**"** on December 3rd, 2021**.** The review process is ongoing and a first revision was submitted on January 2022 – prior to the submission of this thesis – for peer review after minor preliminary comments by the Journal of Hydrology's editor such as a title update to "Benchmarking empirical models of evapotranspiration in an integrated lake-wetland system**"**. The detailed breakdown of responsibilities in creating this paper is:

Henrique Vieira: Conceptualization, Methodology, Investigation, Software, Data Curation, Visualization, Validation, Formal analysis, Writing - Original Draft, Writing - Review & Editing.

Ali Nazemi: Conceptualization, Investigation, Methodology, Validation, Writing - Review & Editing, Resources, Funding acquisition, Project administration, Supervision.

Oliver Sonnentag: Methodology, Validation, Writing - Review & Editing.

The rest of the materials in this thesis is the sole work of Henrique Vieira under Dr. Nazemi's guidance. Specific supervisory guidance on the remaining materials of the thesis included restructuring the text, review comments and suggestions, along with multiple edits on the first draft of the thesis, which was finalized by Henrique Vieira.

Henrique Vieira's work has also resulted in one publicly available presentation at the American Geophysical Union annual meeting in 2020 entitled "The Cooling and Heating Impacts of a Lake and a Nearby Wetland Under Current and Changing Climate", and another related to the evapotranspiration part at the Canadian Water Resources Association conference in 2021. A magazine article was also written by Henrique Vieira and Dr. Ali Nazemi in Memphremagog Conservation Inc.'s annual newsletter which was intended for describing the project and informing the local population about preliminary results in March 2020.

TABLE OF CONTENTS

LIST OF FIGURES

LIST OF TABLES

LIST OF SYMBOLS

Symbol	Variable	Units
T	Air temperature	^{o}C
T_{dew}	Dew point temperature	^{o}C
ρ_a	Air density	kg m-3
ρ_w	Water density	m-3
A	Air pressure	kPa
c_a	Specific heat capacity of air	J kg-1 K-1
c_w	Specific heat capacity of water	J kg-1 K-1
a_s	Surface albedo	Unitless
I	Annual heat index	unitless
C_{at}	Atmospheric conductance	m s-1
C_{can}	Canopy conductance	m s-1
D	Day length	h
z	Altitude	m
y	Latitude	Decimal degrees
R_0	Extraterrestrial radiation	W m-2
R_{sin}	Incoming shortwave radiation	W m-2
R_{sout}	Outgoing shortwave radiation	W m-2
R_{lin}	Incoming longwave radiation	W m-2
R_{lout}	Outgoing longwave radiation	W m-2
R_n	Net radiation	W m-2
λE	Latent heat flux	W m-2
H	Sensible heat flux	W m-2
G	Ground heat flux	W m-2
Q	Heat Storage	W m-2
J_d	Julian day of year	Unitless
λ_v	Latent heat of vaporization	MJ kg-1
γ	Psychrometric constant	kPa $^{o}C^{-1}$
Δ	Temperature slope of saturation vapor pressure relation	kPa $^{o}C^{-1}$
α	Priestley-Taylor coefficient	Unitless
RH	Relative humidity	%
e_a	Vapor pressure of air	kPa
e_s	Vapor pressure at the surface	kPa
e^*	Saturation vapor pressure	kPa
VPD	Vapor pressure deficit	kPa
ρ_v	Absolute humidity (vapor density)	g m-3
u	Wind speed	m s-1
P	Precipitation	mm
PET	Potential Evapotranspiration	mm day-1
ET	Evapotranspiration	mm day-1

1 Introduction

1.1 Background and motivation

Evapotranspiration (ET) is the second largest component of the hydrological cycle, and often accounts for more than half of the water budget at global and local scales (Dingman, 2015; Jansen and Teuling, 2020; Pan et al., 2020). Scientific investigations on ET can be traced back to the late 18th/early 19th century (Dalton, 1802). There are multiple angles for societal and environmental importance of ET, ranging from quantifying aridity (Ashraf et al., 2014; Metcalfe et al., 2019; Y. Zhang et al., 2016) and determining water needed for agricultural activities (Ashraf et al., 2021; Hassanzadeh et al., 2016; Liu et al., 2017; Nazemi and Wheater, 2015a), to quantifying the natural loss from surface water reserves (Nazemi and Wheater, 2015b; Nazemi et al., 2002; Zandmoghaddam et al., 2019), from hydrological modeling at the catchment and basin scales (Karimi and Bastiaanssen, 2015; Minville et al., 2014; Seiller and Anctil, 2016), to closing water and energy budgets at the regional to global scales (Allen et al., 2011; Trenberth and Asrar, 2014), and from investigating land-atmosphere interactions (McColl, 2020; Seneviratne et al., 2006), to addressing the impacts of climate change (Bourdeau-Goulet and Hassanzadeh, 2021; Li et al., 2009; Wang and Dickinson, 2012). Despite an enormous relevance, ET remains a poorly captured component of the hydrologic cycle (Minville et al., 2014). Due to this wide relevance, estimating ET forms one of the grand challenges for the science and application of hydroclimatology according to the World Climate Research Programme's Global Water and Energy Exchanges (Cuxart et al., 2019; Verhoef et al., 2020). Addressing this grand challenge consists of a solid step forward for global research, but its benefits can be further magnified by simultaneously providing solutions at a local scale.

Apart from global relevance, ET has also local importance to decision making. For instance recent study in the City of Magog, where this research is conducted, the principal risks identified are related to floods, droughts and heatwaves for example which are all influenced by ET (Côté and Pouliot, 2021). Indeed, evapotranspiration plays a crucial role also at smaller spatial scales due to its influence on land-atmospheric interactions (dos Santos et al., 2020). In addition to the abovementioned impacts to economic activity, evapotranspiration also plays an immediate role in extreme precipitation events such as increasing the intensity of convective precipitation (Prein et al., 2017). In the context of a changing climate, increases in temperature exacerbate downwind convective precipitation by the intensified evapotranspiration rates in North America (Prein et al., 2020), and Magog can be reasonably expected to be subjected to the same effects.

Magog is located in the Saint-François watershed at the downstream end of Lake Memphremagog. The lake is split between American and Canadian waters, which creates international water quantity and quality implications considered by the International Joint Commission (IJC, 2019). The city is composed mainly of residential areas, while commercial and agricultural land is present less than 2 kilometers away from the city center. It is an important tourist attraction in Québec due to its beautiful landscapes, namely its proximity to Mont-Orford's National Park and due to the

lake's presence, where tourists can engage in aquatic activities and fishing. In addition, it is situated upstream of important cities in Québec, namely Sherbrooke and Drummondville along the St-François River, and Trois-Rivières and Québec City along the St-Lawrence River. Considering its hydrological importance, coordinated efforts are required to ensure proper management of the waters also flowing to these downstream cities. The present study stems from a collaboration with local institutions who are working toward this objective, namely the City of Magog and the Cherry River Marsh Association (LAMRAC).

1.2 Objectives and thesis layout

This research provides the first characterization of Eddy Covariance ET in the Cherry River Marsh and Lake Memphremagog, which is a critical step to the advancement of characterizing land-atmosphere interactions in this transboundary lake and its northern-end wetlands. In this study, Eddy Covariance ET is used not only to provide high resolution measurements, but also implemented to validate and benchmark existing ET models forced by the microclimate data in the marsh and lake. The study period is the growing season of 2020.

The main objectives of this thesis are the following:

1. To generate and provide Eddy Covariance evapotranspiration datasets for the marsh and lake according to best processing practices in the literature;
2. Benchmark existing evapotranspiration models in the marsh and the lake at different time scales, times of the day and period within the growing season of 2020, when Covid-19 pandemic stroke the world, Canada and Québec;

The materials provided in the rest of this chapter presents an up-to-date literature review about each of the two keys objectives. Further down in this thesis, Chapter 2 is dedicated to introducing our case study and generating the high-resolution ET measurement datasets for the considered lake-wetland duo. Chapter 2 of this thesis contains (2.1) a site description section associated with the research location and its basic characteristics. It also contains (2.2) the detailed procedure selected for generating ET datasets according to the literature review and the resulting measurements which are used later.

Chapter 3 is dedicated to the second task of this thesis. It demonstrates the considered ET models and presents the results of the benchmarking exercise. It investigates modelling of ET at different time scales, times of the day and times of the year in the marsh and lake. In this effort, our research pioneers the use of non-dominated sorting to simultaneously use multiple goodness of fit measures to benchmark 40 ET models in a more systematic manner than using individual goodness of fit measures separately. Compared to similar studies, it also considers the largest number of models to ensure an adequate representation of existing literature. This benchmarking study and the results presented there are currently under review at the *Journal of Hydrology*.

Chapter 4 presents the concluding remarks and main insights we have obtained through this research effort. It reviews the initial gaps, presents our principal results and discussions related to

the main investigations, and comments on the current state of knowledge and associated gaps. Lastly, it also summarizes future directions for research in the local context of the City of Magog.

The measured data and processed results are publicly available on a GitHub repository (https://github.com/vieirah1/Thes_ET_LakeMemphremagog).

1.3 Understanding and Measuring Evapotranspiration

ET is essentially the sum of the evaporation and transpiration fluxes. On the one hand, evaporation is driven by free and forced convection, governed by available energy at the surface and air turbulence. Surface characteristics such as albedo, roughness, and heat capacity, along with environmental conditions such as wind speed can alter the surface energy balance (see Figure 1 below) and influence the amount of energy available for the evaporative component of the ET flux. On the other hand, biological activities of living organisms, in particular photosynthesis and other physiological functions of vegetation can regulate the transpiration segment of ET (Li et al., 2009; Rasmussen et al., 1995; Sartori, 2000). Despite the nature and/or the cause of ET, whenever water molecules leave the surface through ET, the latent heat is also lost (Liou and Kar, 2014). ET, therefore, is a complex process caused by coupling of the water and energy balance and is affected by surrounding physical and biological environments (Barry and Blanken, 2016; Oke, 1987).

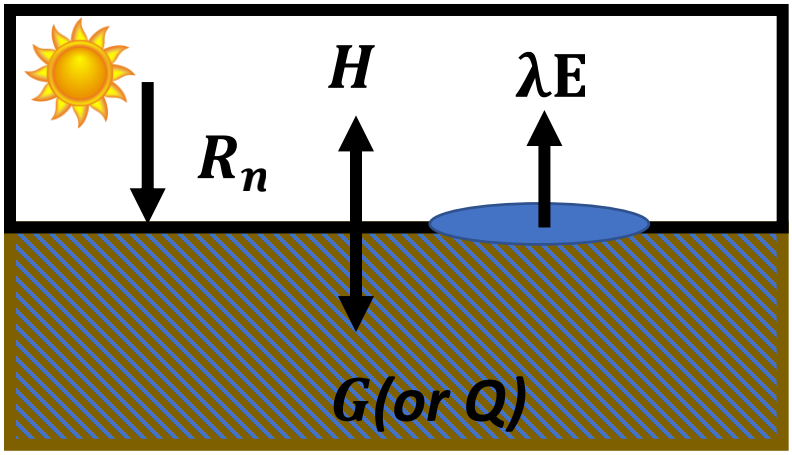

Figure 1. The components of land-atmospheric energy exchanges, which can also describe the evaporative flux ($\boldsymbol{R_n}$: net radiation, $\boldsymbol{H}$: sensible heat flux, $\boldsymbol{\lambda E}$: latent heat flux, $\boldsymbol{G}$: ground heat flux, $\boldsymbol{Q}$: heat storage flux (W m^{-2}).

Difficulties in estimating ET stem from limitations in measuring and modeling the process across different spatial and temporal scales. Measuring ET has been a longstanding challenge in hydrology. Currently, different measurement techniques for ET are available but all are associated with limitations and uncertainties across a range of landscape and/or scales. The simplest approach to measure ET is through evaporation pans (Peterson et al., 1995). Despite being easy to use, pans wholly ignore the transpiration flux and are unable to accurately reflect the impact of radiation and heat exchanges. Pan measurements, therefore, need correction (Bedient et al., 2012). Lysimeters, another widely-used measurement technique since the 1970s, are considered to provide the most accurate measure of local ET (Dingman, 2015). However, lysimeters require a complex and costly setup, and are only relevant locally (Jensen et al., 1990). The eddy covariance (EC) method can be more representative of landscape-scale footprints of tens to hundreds of square meters. As EC is representative of a larger footprint, it is well suitable for microclimatic studies (Karimi and Bastiaanssen, 2015; Rosenberry et al., 2007); however, the method is relatively complex compared to other techniques and also presents errors (Mauder and Foken, 2006; Stannard and Rosenberry, 1991).

Limitations in ET measurements propagate into the development of mathematical models, with which ET is represented and quantified. A true physically-based representation of ET requires coupling partial differential equations, describing energy and water exchanges at the interface between sub-surface, surface and atmosphere (Chu et al., 2019; Hostetler and Bartlein, 1990; Liu and Zhang, 2013; Roderick et al., 2007). In addition, because an important part of ET partitioning is related to transpiration, a detailed representation of ET inevitably requires representing biological processes (Wang and Dickinson, 2012; Wei et al., 2017), and this necessitates representing some other physical phenomena such as the carbon and nutrient cycles (Lott and Hunt, 2001; Rouse, 1998). As in most of cases, neither data supports nor the computational algorithms and/or resources for such detailed representations are available, ET is often parametrized in relation to some conceptual variables, such as Potential ET (hereafter PET) and/or Reference ET (Allen et al., 2011; Penman, 1948; Thornthwaite, 1948). PET is defined as the amount of ET when there is no moisture limitation in the surface (Guo et al., 2016). This definition is very similar to the concept of atmospheric water demand, defined as the ET when soil and/or plant surfaces reach to their holding capacity (Cuxart et al., 2019; Y. Zhang et al., 2016). The agronomy community has heavily applied this definition and included new parameterizations to account heterogeneity in soil, crop, and vegetation conditions in converting PET (or Reference ET) to ET (Allen and Pereira, 1998; Djaman et al., 2015; Doorenbos and Pruitt, 1977).

1.4 The Backbone and State of the Eddy Covariance Technique

Eddy Covariance is a modern methodology applied toward measuring evapotranspiration. The Eddy Covariance technique has emerged and evolved in the past decades to be considered the second most reliable measurement technique after lysimeters. While lysimeters might be the most accurate technique to measure ET, they are representative of a small area. Eddy Covariance towers, however, can be more representative of areas larger than 50m in length (Allen et al., 2011). Some studies indicate statistically-derived accuracies of 10-20% (Mauder and Foken, 2006; Stannard and Rosenberry, 1991). However, review papers after 2005 which investigate actual studies point that closure errors of 20% are common and higher errors of 30% are also observed (Allen et al., 2011; Wang and Dickinson, 2012). Eddy Covariance is useful not only for measuring water vapor fluxes, but also for quantifying the fluxes of different gases, such as carbon dioxide and methane, which makes it an ideal instrument to study land-atmosphere interactions in the context of a changing climate (Gunawardhana et al., 2021). Several Eddy Covariance networks have been established by the scientific community around the globe to facilitate communication of datasets between different researchers and accelerate developments, such as FLUXNET (Wilson et al., 2002), AmeriFlux (Novick et al., 2018), ChinaFLUX (Yuling, 2005). Considering their meso-scale spatial coverage, they are ideal for measuring ET for marshes and lakes, and many studies have done so (Blanken et al., 2000; Guo et al., 2019; Jansen and Teuling, 2020; Lott and Hunt, 2001; Nordbo et al., 2011).

The Eddy Covariance technique consists essentially of using fast (10-Hz) measurements of water vapor concentration and 3-D wind velocity to generate vertical evapotranspiration fluxes by investigating the covariance of wind velocity and water vapor (Aubinet et al., 2012). In simple words, by knowing the wind velocity and water vapor concentration, we can determine how much water is moving upwards or downwards. More precisely, the equation $Flux = \rho_a \overline{w's'}$ illustrates that evaporation fluxes are proportional to the covariance (overbar) of the instantaneous vertical wind velocity (w') and mixing ratio (s') – see Burba (2013). Derivation of instantaneous variables is carried through the use of Reynolds decomposition around variable means (Foken, 2017). Flux calculations comprehend the basis of Eddy Covariance and are automatized in numerous existing software and packages. The main software tools to make the flux calculation are summarized in Table 1 – see Sigut (2017). In addition to designing the towards and maintaining the instrumentation and data, the Eddy Covariance technique relies on extensive routines for pre-processing, processing and post-processing to transform the measured data into research-approved data. Most Eddy Covariance software execute the processing step, while pre-processing and post-processing steps are more site-specific and are often programmed by researchers – this was the case for this research endeavor as a custom MATLAB code was developed with initial support from Université de Montréal's researchers Oliver Sonnentag, Gesa Meyer and Gabriel Hould-Gosselin. However, post-processing and pre-processing assisting software and packages are also available (Sigut, 2017), but careful investigation of the techniques and assumptions used should be carried to ensure they correspond to the landscape and instrumentation configuration. Some of these include hesseflux, esmwfr, fluxpart, bigleaf and FluxnetLSM (see Sigut, 2017 for a complete list and references to available options). Below, we review the many different methods proposed

by the literature and discuss their advantages and disadvantages. In Section 2.2 , a more customized discussion will present which methods were selected in this study, how and why they were applied.

Table 1: Software for implementing Eddy Covariance techniques for land-atmospheric flux calculation

Eddy Covariance Software	**Developer**
EddyPro	Licor
EddySoft	Max-Planck-Institut für Biogeochemie
TK3	Zenodo
EddyUH	University of Helsinki
EdiRe	University of Edinburgh

1.4.1 Tower design and housekeeping

While we can observe heated debates in the literature about different processing techniques, researchers unanimously agree on one fact: proper design of an Eddy Covariance setup and housekeeping of the instrumentation and data are crucial. Detailed literature-derived guidelines have inspired this study and some of the main ones are summarized below (Aubinet et al., 2012; Burba, 2013):

1. Tower location and height should be selected as a function of the size and roughness of the landscape, main wind directions and location availability. A general rule of thumb is to consider 1 m of height for 100 m of landscape footprint and place it ideally at the center of the landscape; if center placement is impossible such as in a lake, it should be placed at the leeward (downwind) edge of the lake and wind direction filtering should be applied when wind direction is not coming from the lake.
2. While a hygrometer and sonic anemometer are sufficient to compute fluxes, other micrometeorological sensors are critical to improving corrections and inspecting punctual events at the site location;
3. Open-path analyzers are ideal for hardly accessible stations thanks to their low power consumption and long-term stability;
4. Frequent inspections, as well as expedient maintenance and calibration when required are paramount to long-term success, but often overlooked.

1.4.2 Eddy Covariance pre-processing

Pre-processing subroutines can be summarized as variable transformations and basic raw data corrections. Different instruments may require different pre-processing steps before their outputs can be used in flux computations, since slow data such as temperature and relative humidity can be useful toward more precise corrections (Aubinet et al., 2012).

Open-path gas analysers such as krypton hygrometers output their signals in electric signals measured in millivolts (*mV).* Consequently, they require a transformation to vapor density in $g\ m^{-3}$ according to the manufacturer's calibration instructions before further processing.

In addition, as mentioned by Burba (2013), one of the most common mistakes by researchers is to underestimate the importance of inspections and maintenance, which increases the likelihood of data loss. However, even detailed maintenance plans are subject to data loss due to the unpredictable nature of field work.

1.4.3 Eddy Covariance processing

Processing subroutines consist of flux computation and corrections, footprint estimation, quality control and filtering. Quality control is critical in the process of developing an ET Eddy Covariance dataset, because the data might be unreliable for many reasons related to instrument malfunction, such as electric issues, raindrops on the hygrometer and damage to the sensors (Aubinet et al., 2012). The processing procedure consists of several steps, executed using EddyPro (LI-COR Inc., 2019).

First, wind filtering is applied at the lake to remove wind from the city to ensure the evaporation signal comes only from the lake. This procedure consists simply of filtering data according to wind direction.

Second, a coordinate rotation, in this case double rotation, is used to correct small shifts in instrumentation angles and to ensure that the coordinate of sonic anemometer is in line with the ground (Gan and Liu, 2020; Wilczak et al., 2001). Although initially sensors are placed parallel to the ground and precisely levelled, small shifts can occur. Therefore, automatic routines have been developed to correct any levelling errors to ensure flux calculations are done with respect to the landscape's coordinate system. The two main coordinate rotation methods are the double rotation and planar-fit methods (Foken, 2017). The first method is the best in flat terrain (Kaimal et al., 1994), while the latter should be favored over sloped terrain (Wilczak et al., 2001).

As sonic wind speed and water vapor cannot be measured at the same point, third, an algorithm is needed to shift the time series before averaging fluxes (Burba, 2013; Fan et al., 1990; Paul-Limoges et al., 2020). This procedure is called time lag compensation and accounts for the lag time associated with the spatial separation between the sonic anemometer and gas analyzer. It is more important in closed-path systems where this distance can be of several meters, in comparison with open-path systems whose separation are only of a few centimeters. Even in open-path systems, time lag must be always compensated. Two main methods are used: constant time lags

and covariance maximization (Aubinet et al., 2012). The former can be used directly in closed-path systems where the flowrate is known and allows calculation of the time lag directly. The latter searches for the time lag which maximizes the covariance between water vapor concentration and vertical wind speed (Fan et al., 1990).

Fourth, 10-Hz sonic wind speeds and water vapor measurements are averaged into half-hourly fluxes by using the block averaging technique (Aubinet et al., 2012). Flux calculations require averaging fluxes, which can be done using block average, linear detrending or autoregressive filtering. This step was heavily debated in the literature because although linear detrending and autoregressive filtering reduced random error, they are theoretically incompatible with the derivation of flux equations, so block averaging is recommended (Finnigan et al., 2003; Foken, 2017; Pilegaard et al., 2003). However, Eddy Covariance averaging causes loss of high-frequency and low-frequency physically plausible data; therefore, computed fluxes must be corrected (Aubinet et al., 2012) according to best practices established by Moncrieff in 2004 and 1997 respectively which are applied through EddyPro (Foken, 2017; Moncrieff et al., 2004, 1997).

At this stage, the computed EC fluxes may capture some error due to fluctuations in water vapor density caused by changes in temperature and relative humidity (Webb et al., 1980). To account for this error and to correct it, fifth, we use the Webb, Pearman and Leuning (WPL) corrections (see Gunawardhana et al., 2021; Lee et al., 2004). The Webb, Pearman and Leuning (WPL) correction is the most important correction, since it addresses false fluctuations in water vapor concentrations (Webb et al., 1980). If uncorrected, the measured water vapor density would reflect not only the actual evapotranspiration fluxes, but also incorrectly account for changes in temperature and relative humidity.

Finally, based on statistical characteristics of spikes and drop-outs, unrealistic fluxes are removed as outliers (Vickers and Mahrt, 1997). Spikes in data are often eliminated by determining if each data point is within physically plausible limits (absolute limits), or very different from than the mean of a selected moving window in terms of standard deviations (Schmid et al., 2000). Other procedures exist to identify spikes using point-to-point autocorrelation (Hojstrup, 1993), or the difference between consecutive points (Clement, 2004), but these have a larger tendency to remove physically plausible data accidentally (Aubinet et al., 2012). In this situation, variable moving windows imply a design choice has to be made about the window's length. While Schmid (2020) used 15-min windows, smaller windows of 5-min are more conservative and often used (Gunawardhana et al., 2021; Nordbo et al., 2011; Vickers and Mahrt, 1997). When spikes occur for more than a certain number of time steps, they are considered discontinuities or drop-outs which usually occur due to data recording issues. Under atmospherically stable conditions, data amplitude may be too small to capture fluctuations and unreliable amplitude resolution are automatically identified by inspecting the frequency distribution of moving windows. Spike detection sometimes misses medium-duration spikes, so an additional flag is created by investigating the skewness and kurtosis of the data; records are flagged as soft or hard flags if outside physically plausible ranges. Using Vickers and Mahrt's method, a flag is also added to inform about the quality of the time lag optimization (Vickers and Mahrt, 1997).

Best practice in Quality Assessment and Quality Control (QA/QC) for Eddy Covariance currently involves a two-step process. The first includes statistical methods that investigate the data for absolute limits, spikes, amplitude resolution, drop-outs, skewness & kurtosis and time lags (Nordbo et al., 2011; Vickers and Mahrt, 1997), while the second evaluates the appropriateness of turbulence conditions for Eddy Covariance (Foken et al., 2004; Ma et al., 2015). Both data analyses have the potential of identifying unreliable data, such that gap-filling these removed time steps during postprocessing will result in a more realistic dataset.

1.4.4 Eddy Covariance post processing

Measuring ET using EC includes implementing standard procedures during post-processing as well (Gunawardhana et al., 2021; Paul-Limoges et al., 2020). The post-processing procedure consists of 4 steps, mainly to filter poor-quality fluxes and fill data gaps. For these we use Reichstein's framework (2005) and friction velocity thresholds recommended by Alavi et al. (2006) – see also Zhou and Zhou (2009) for details.

First, fluxes are removed if the turbulence conditions represented by friction velocity are not sufficient for fluxes to be plausible (Alavi et al., 2006). Foken et al. propose using steady state tests and turbulence tests to verify the respect of Eddy Covariance turbulent conditions (2004). In the steady state test, the covariance of different smaller bins is compared with that of a whole 30-min interval, and flagged for removal if the percent difference is more than 30%. This method has been evaluated, approved and used in several studies (Foken and Wichura, 1996; Gunawardhana et al., 2021; Gurjanov et al., 1984; Paul-Limoges et al., 2020).

Second, de-spiking procedures during processing of instantaneous data are bound to leave some physically unrealistic spikes in the averaged fluxes time series. Therefore, an additional de-spiking procedure should be applied during post-processing to filter out unrealistic fluxes at the averaged time scale (Papale et al., 2006; W. Zhang et al., 2016). Papale's de-spiking procedure is similar to Vickers and Mahrt's (1997) statistical method described above and is widely recommended (Aubinet et al., 2012; W. Zhang et al., 2016).

Third, water droplets on the hygrometer and sonic anemometer distort measurements both according to the literature and manufacturer's technical sheets (Aubinet et al., 2012). Therefore, fluxes must be removed during 30-min periods with precipitation.

Finally, gaps are created due to the different filters mentioned above and must be filled using appropriate techniques. Gap-filling methods can be categorized as empirical or functional (Aubinet et al., 2012). Empirical methods use nearby existing data to fill gaps, while functional methods develop functions to estimate values in gaps. Mean diurnal variation (empirical) is the simplest technique, which replaces missing values by the mean of adjacent days at the same time of the day; although simple, it also presents the worse performance. Look-up tables (empirical) attempt to replace missing fluxes by existing fluxes in nearby days with similar meteorological conditions. Studies have implemented this in different ways, such as creating four tables per year and air temperature to select fluxes in similar conditions (Falge et al., 2001). Other more statistical

(functional) methods such as regressions, artificial neural networks are available, but require gap-filled raw datasets to begin with and add therefore a layer of uncertainty (Aubinet et al., 2012). In 2005, a method has been proposed that combines empirical look-up tables with a more physically sound approach (Gunawardhana et al., 2021; Reichstein et al., 2005). Reichstein's (2005) method fills data gap by searching for nearest data points with similar micrometeorological conditions to the missing data point from which to sample the expected flux and fill the gap. Assuming that fluxes will be similar in nearer time steps and that the more auxiliary data is available, the higher the confidence in their generation of similar fluxes, Reichstein et al. gap-fill fluxes through a systematic framework. It considers net radiation, air temperature, vapor pressure deficit and latent heat flux. Starting with all variables, it attempts to gap-fill based on the smallest time window around the missing data point (7 days) and if successful, signals the highest filling quality. If it fails, the number of variables is decreased and the width of the time window is increased; in doing so, gaps can still be filled but the filling quality drops (Reichstein et al., 2005).

1.5 Modeling Evapotranspiration

The formulation of PET is often based on empirical models, informed by meteorological variables. The advent of empirical models for representing PET/ET can be traced back to the 19th century (Fitzgerald, 1886). Comprehensive reviews of empirical modelling of ET are already available elsewhere (Drexler et al., 2004; Shuttleworth, 2007; Sartori, 2000). In brief, empirical models for PET/ET can be classified into four general categories, namely aerodynamic (mass-transfer), temperature-based, radiation-based, and combination models, each following a set of assumptions to reduce complexity and to allow parameterizations using commonly measured meteorological variables. Aerodynamic models are the oldest type and relate ET to wind speed and vapor pressure deficit (Carpenter, 1888; Dalton, 1802; Fitzgerald, 1886). They do not take into account changes in surface and canopy resistances, nor net radiation or heat storage. In vegetated surfaces this is not the case, as the turbulent fluxes are directly coupled with radiation; and, due to the lack of thermal inertia, simple radiation-based models can well capture ET (Guo et al., 2016; Priestley and Taylor, 1972). Temperature-based models can be seen as proxies of radiation-based models. Similarly, they do not explicitly account for heat storage and usually better correlate with observed ET at larger time scales (M. Valipour, 2015). Combination equations emerged in the attempt of combining radiative and aerodynamic forcing together (Penman, 1948) and later expanded to account for the presence of vegetation (Monteith, 1965).

While calculation of ET based on PET can be limited in landscapes with moisture deficit, it provides a basis for calculation of ET when water limitation is removed; as ET, at least theoretically, would be equal to PET. This assumption has been widely used in the literature particularly in some real-world applications relevant to water resources planning and management, e.g. for calculating irrigation demand, assuming that soil needs to reach field capacity (Harding and Snyder, 2012a, 2012b; Lobell et al., 2006; Nakayama and Shankman, 2013), as well as calculating evaporative losses from open water environments, such as reservoirs and lakes (Hassanzadeh et al., 2017; Nazemi et al., 2020), and surrounding aquatic environments that can be

considered water unlimited (e.g. wetlands; see Lott and Hunt, 2001; Roulet and Woo, 1986). Such representations of ET have been also used in the context of land-atmospheric interactions and assessing the thermal impacts of lakes and wetlands (Emilsson and Sang, 2017).

Although the definition of PET justifies its application for quantifying ET flux from waterbodies, it might deviate from physical realism. In lakes, for example, there is an ideal setting for wind to drive ET (Blanken et al., 2000), however there can be a high heat storage, significantly changing the pattern of ET depending on the volume and the depth of the lake (Harwell, 2012; Tasumi, 2005). The importance of heat storage and how it should be represented is noted as one of the grand challenges for calculating ET in open-water conditions (Cuxart et al., 2019). In vegetated waterbodies such as wetlands, transpiration can play a major role, increasing total ET flux proportionally to incoming radiation and biomass growth, up to a limit governed by vegetation's self-preservation responses to extreme heat (Collatz et al., 1991). In addition, vegetation shelters the wet surface from the wind, reducing the influence of forced convection (Barry and Blanken, 2016; Drexler et al., 2004).

So far, several studies have attempted to benchmark the skills of empirical equations (Rosenberry et al., 2007, 2004; Winter et al., 1995). These attempts are often carried on the basis of a single Goodness-of-fit measure (GoF), which is inherently limited to the definition of the measure chosen. It is, therefore, suggested that no GoF should be used alone (Jia et al., 2021; Legates and McCabe Jr, 1999), and the definition of skills can be dependent to the scale and the time episode in which the observed information are available (Jansen and Teuling, 2020; Li et al., 2009; Tanny et al., 2008; Wang and Dickinson, 2012). However, even when several GoFs across different temporal and spatial scales are considered, they are often investigated independently (Singh and Xu, 1997), or are taken into account using combinatory indices, e.g. index of agreement (Legates and McCabe Jr, 1999). Although combinatory indices may result in finding a model that minimizes the error regarding several error measure (dos Santos et al., 2020; Willmott et al., 1985), they ignore the trade-offs between different GoFs (Bormann et al., 2011).

2 Generation of Evapotranspiration Data in a Lake-Wetland Duo

2.1 Case Study and Site Description

We consider an integrated wetland-lake system in southern Québec, namely Marais de la Rivière-aux-Cerises (in English: the Cherry River Marsh, a 1.4 km^2 freshwater wetland) and Lac Memphrémagog (in English: Lake Memphremagog, a 110 km^2 glacial lake). While Lake Memphremagog is an international lake shared between Canada and US, we measure evaporation in two nearby EC stations within the City of Magog, Québec, Canada in the north end of the lake – see Figure 2 (lake station: 45°16'03.2"N 72°09'41.6"W; marsh station: 45°16'55.8"N 72°09'58.2"W). The two stations are under the same local climate, allowing the local differences in ET fluxes emitted from the two landscapes. The lake has been regulated since 1920 through the construction of a hydroelectric dam, caused water levels to increase and penetrate into the Cherry River Marsh. Today, the lake supplies water to over 170,000 people, and powers up the Centrale Memphremagog, a 1.9 MW hydropower station (Ville de Magog, 2021).

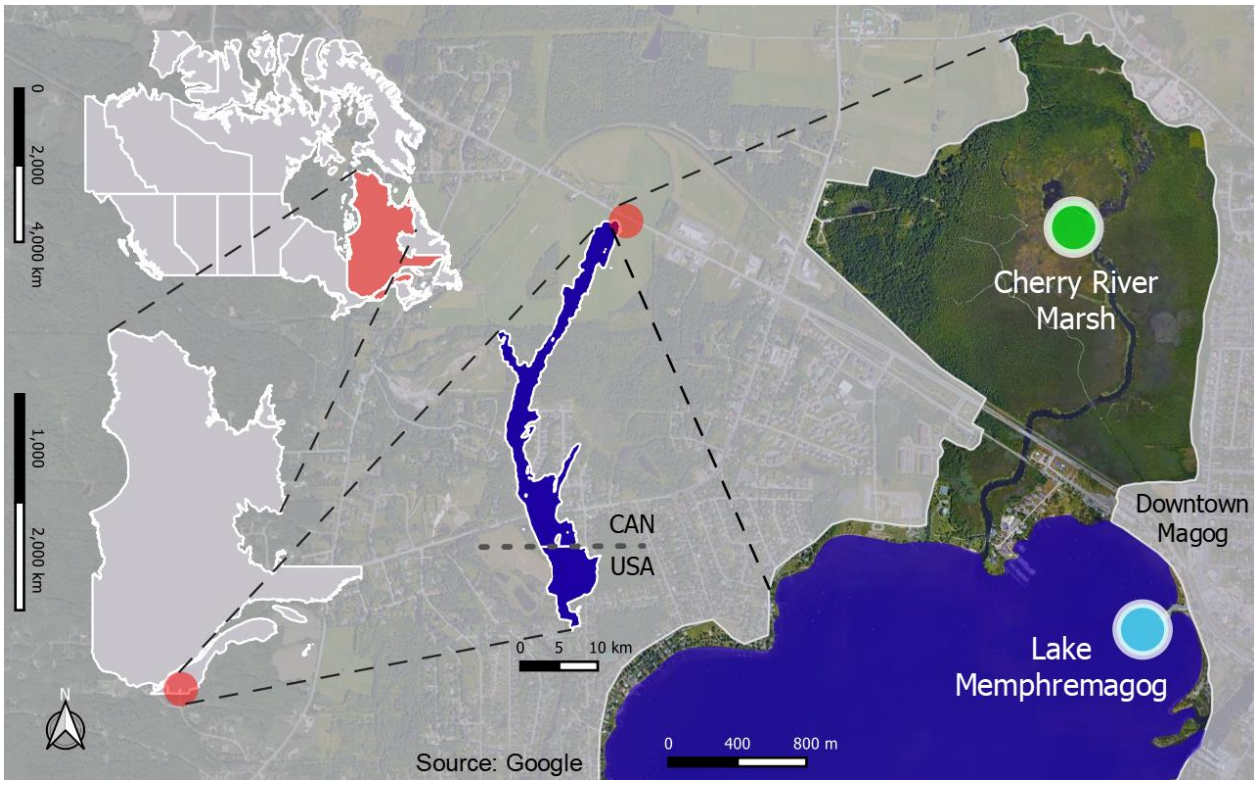

Figure 2. The position of the two Eddy Covariance stations in Lake Memphremagog and Cherry River Marsh, located in Magog, Québec, Canada.

Figure 3 provides a visual description of both stations and their accessibility paths, while their detailed geometry can be consulted in the plans and profiles provided in Appendix A. Both of our stations and their locations have been carefully designed to ensure a representative footprint according to main wind directions and the landscape of the two sites as described below in detail. The two stations are under the same local climate, allowing the local differences in ET fluxes emitted from the two landscapes to be observed (Barry and Blanken, 2016). The duo is situated in a humid continental climate (Köppen and Geiger, 1936; Peel et al., 2007), and have annual mean temperature and annual precipitation of 5.6 °C and 1142.3 mm, respectively (ECCC, 2020).

Figure 3. Photos of lake (left) and marsh (right) stations on top and accessibility at the bottom.

Lake Memphremagog is a glacial lake with a maximum depth of 106 m and an approximate surface of 110 km^2. A dam was constructed at the outlet of the lake in 1920, since when it has been formally regulated and used for hydroelectric power generation by Dominion Textile Ltd. Following construction of the dam, water levels have increased, causing property damage (Anderson-Nichols & Company, Inc., 1978), but also the expansion of the Cherry River Marsh. Today, over 170 000 people are served by the lake's surface waters which extend their services as far as Sherbrooke

situated 27 km away (Ville de Magog, 2021), and powers the Centrale Memphremagog which is a 1.9 MW station. Figure 4 below displays a drone photo showing the lake extending into the horizon and the marsh directly below the drone.

Figure 4. Photo displaying an aerial overview of the Cherry River Marsh and Lake Memphremagog.

The Cherry River Marsh has an area of approximately 1.4 km^2, where we can most often find bushes such as sweet gale (*Tirica gale*) and rosy meadowsweet (*Spiraea tomentosa*), and cattails (*Typha Latifolia*) (Marie-Victorin, 1964), but also other less abundant but diverse species with short seasonal maximum canopy heights under 1 m. It is a biodiversity hotspot, where we can find over 27 species of fish, 26 species of mammals, 12 species of amphibians, 4 species of reptiles, 63 species of invertebrates and 400 species of flowers (LAMRAC, 2021). As a wetland, it provides many ecosystem services including temperature regulation (Bolund and Hunhammar, 1999; Vieira and Nazemi, 2020). Some of the main activities practiced in the marsh by the community and tourists are hiking, bird watching, aquatic sports such as kayaking and guided tours offered by the Cherry River Marsh Association. Although this institution provides services to the community, its main objective is to ensure the conservation of the marsh, which until 1970 had zones which were informally used as garbage dumping grounds, but has been cleaned and now adds environmental and social value to the region.

An overview of the study area's climate is pertinent to shed light on microclimatological of our sites. Although both stations are subject to different microclimates due to landcover differences (i.e. the marsh and the lake), they are under the same local climate (Barry and Blanken, 2016). Two meteorological stations in Magog have allowed the preparation of this climatological portrait. Station Magog from Environment and Climate Change Canada (ECCC) contains daily data from 1948 to 2019 (ECCC, 2020) and Station Lac Memphremagog, from 2001-2019. Precipitation measurements are available from 1948, while temperature maxima, minima, mean and ranges start in 1949. Upon inspection, the data is complete, with the exception of a few episodes of missing data, notably mean temperatures, which are estimated from the average of maxima and minima. Table 2 summarizes data availability in both stations. Seasonality has been computed by averaging values for each month over the data availability period and is presented in Figure 5 for each variable. We can observe that temperature usually peaks in July, which is consistent with the well-known effect of solar radiation heating the air at the surface of the Earth in the northern hemisphere. Precipitation slightly follows temperature patterns, as expected due to increased consequent evapotranspiration. Relative humidity, on the other hand, peaks during the winter and reaches its lowest point in April, which corresponds to the melting of snow. Wind speed is also highest during the winter, and reaches its lowest during the Fall, in September. These variables are all directly related to estimation of evapotranspiration, as will be discussed later in detail.

Table 2: Data available in Magog from Environment and Climate Change Canada.

Station Variable	Station Magog (daily)	Station Memphremagog (hourly)
Temperature	1949-2019	2001-2019
Precipitation	1948-2019	2001-2019
Relative humidity	N/A	2001-2019
Wind speed	N/A	2001-2019

The footprint of the sites is determined based on the parameterization proposed by Kljun et al. (2015), which uses a Lagrangian stochastic particle dispersion model (see also the early work of Kljun et al., 2004). The fetches of the 40%, 60% and 80% footprints in the marsh reach respectively to 26 m, 45 m and 109 m. In the lake site these values are 95 m, 167 m and 390 m (see Figure 6). In the marsh, the dominant wind direction is east, while southeast and northeast winds are not uncommon. The main wind direction in the lake is southeast, but occasional western winds must be filtered due to the station's location at the edge of the lake.

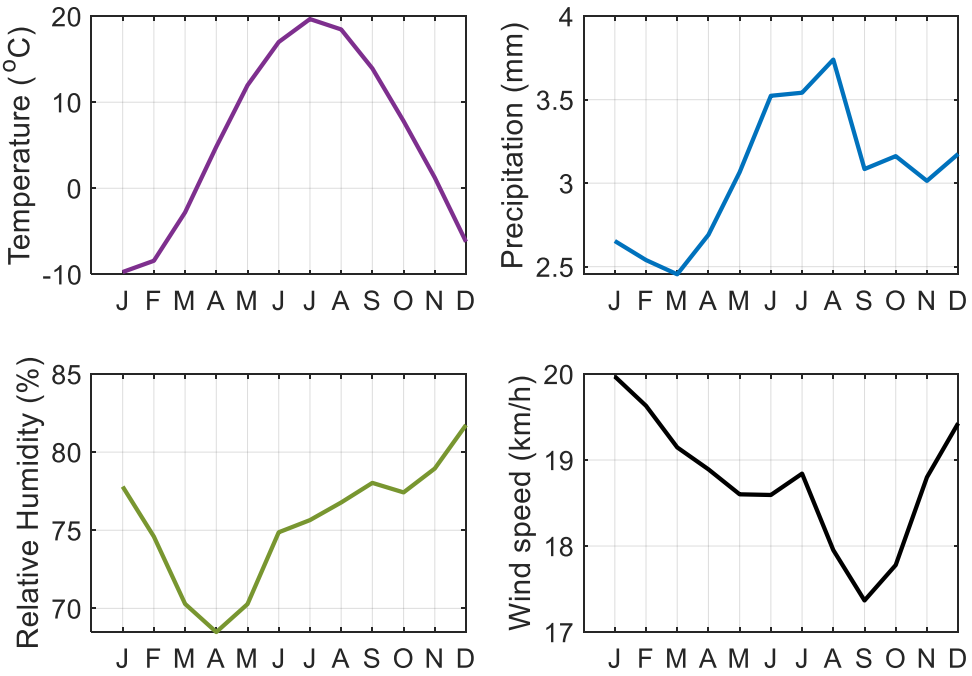

Figure 5. Monthly seasonality of climatic variables available for Magog, Quebec (2001-2019).

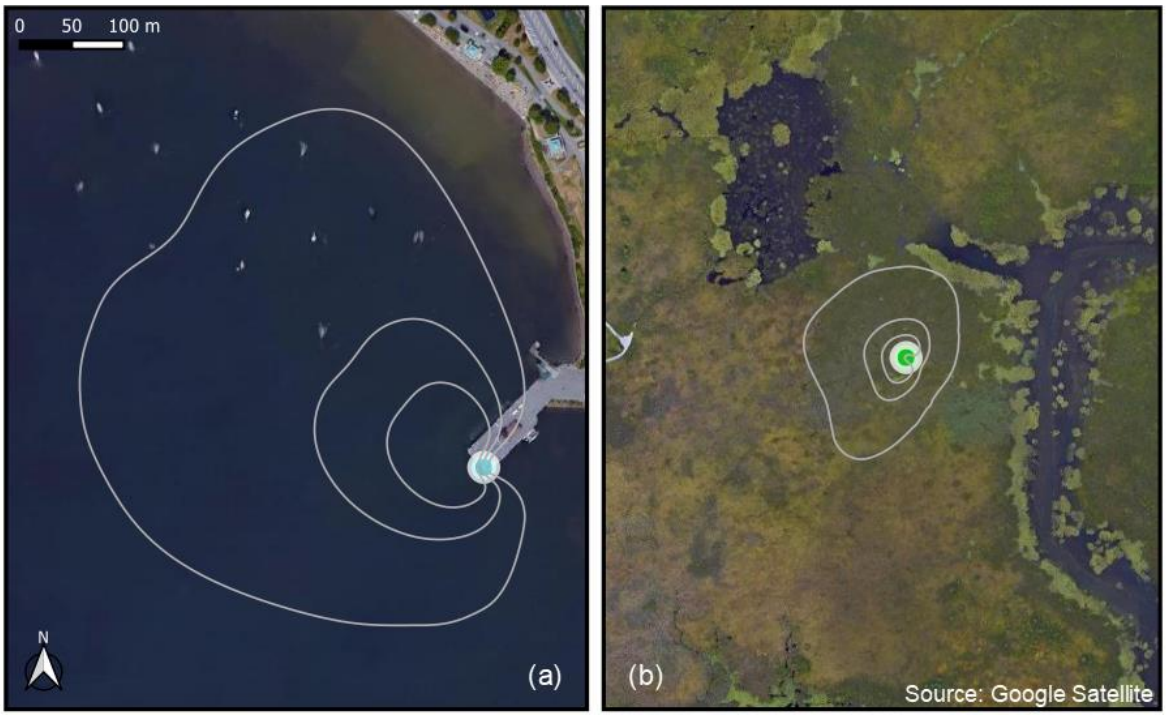

Figure 6. Footprint climatology (a) in Lake Memphremagog and (b) Cherry River Marsh represented by the contour lines of the 40%, 60% and 80% footprints.

2.2 Generating Evapotranspiration Datasets

2.2.1 Instrumentation

This research was possible through the acquisition and continuous maintenance of two full Eddy Covariance meteorological stations. Table 3 below summarizes the different sensors functioning at the marsh and lake stations. The data from all sensors was recorded in both stations on CR6 dataloggers also from Campbell Scientific. Data is collected and stored on 16 GB weather-resistant SD-cards which can endure extreme cold climate. Both stations data can then be accessed remotely for inspections. Regular site visits are required to collect the cards. The marsh station is powered by a solar panel, while the lake station benefits from the proximity to the city's power grid and did not require solar panels. For that reason, the krypton hygrometer is an open-path analyser which consumes less electricity than closed-path analysers, in addition to requiring less corrections during processing. The instrumentation can be broadly categorized in two main types with respect to the frequency of the data acquisition. As we can notice in Table 3, the hygrometer and sonic anemometer collect data every 0.1 seconds (i.e. fast data), while the rest of the instrumentation collects data every half-hour (i.e. slow data). The former category is the primary data source used for Eddy Covariance, while the slow data is used as data support in the processing of EC results or in additional analysis. The design and location selection of the stations were carried according to established criteria in the literature with regards to footprint requirements (Aubinet et al., 2012), and in collaboration with researchers from Dr. Oliver Sonnentag's lab.

The collected data and processed results are publicly available on a GitHub repository (https://github.com/vieirah1/Thes_ET_LakeMemphremagog).

Table 3: Description of Eddy Covariance Measurement Stations in Lake Memphremagog and the Cherry River Marsh

Instrument	Manufacturer (model)	Measured variable	Measurement Frequency	Marsh (height)	Lake (height)
Sonic Anemometer	Campbell Scientific (CSAT-3B)	3-D wind velocity	10 Hz	Yes (2.95 m)	Yes (5.65 m)
Krypton Hygrometer	Campbell Scientific (KH20)	Water vapor concentration	10 Hz	Yes (2.95 m)	Yes (5.65 m)
T-RH probe	Rotronic (HC2S3)	Air temperature, relative humidity	30-min	Yes	Yes
Net radiometer	Kipp & Zonen (CNR4)	Net radiation components	30-min	Yes	Yes
Water level sensor	Campbell Scientific (SR50)	Distance to surface	30-min	Yes	Yes
Rain gauge	Campbell Scientific (TB-4)	Precipitation	30-min	Yes	Yes
Barometer	Vaisala (CS106)	Air pressure	30-min	Yes	Yes
Soil heat flux plates	Hukseflux (HFP01SC15)	Ground heat flux, soil temperature and moisture	30-min	Yes	No
Water temperature sensors	Onset (HOBO TidbiT v2 Temp)	Water temperature	30-min	No	Yes (every 0.3 m up to depth of 2.5 m)

Besides Eddy Covariance stations, a few additional instruments were used to collect data. Water temperatures were measured in the lake by attaching sensors TidbiT® v2 Temp (manufactured by Onset) to chains attached to navigational buoys in Lake Memphremagog.

2.2.2 Setting up and applying Eddy Covariance procedure

Data collection is associated with multiple challenges, such as power issues and instrumental faults. As recommended in the literature (Aubinet et al., 2012), regular monitoring and maintenance were critical to identify any issues early on and minimize data loss. The reader may walk through all major actions executed in this project from data acquisition to post-processed results by referring to the flowchart in Figure 8. A rigorous 3-step data validation approach is adopted to ensure the quality of the resulting datasets. A set of established routines are implemented as recommended by the state-of-the-art Eddy Covariance literature to systematically flag and, as applicable, remove unsuitable data points.

It is important to identify periods when the data might be unreliable and to ensure long-term functioning of the stations. Maintenance procedures were determined according to the factory instruction for each instrument and carried mainly by the author for routine tasks, and by Campbell Scientific technicians for specialized tasks such as replacing, repairing or calibrating sensors. Figure 7 displays sample photos of instrument maintenance site visits. Site visits also included at a brief inspection and photographic report inspired by common practices in the construction industry. These focused on ensuring minimal to no distortion to collected data due to environmental threats such as: structural damage, structure degradation, sensor obstruction, etc.

Figure 7. Sample photos of station maintenance and data collection.

We measure ET using EC by implementing the established methods and computer codes for processing, correcting and post-processing (Gunawardhana et al., 2021; Paul-Limoges et al., 2020).

In Chapter 2, we have discussed in depth the different corrections required, the pros and cons of different techniques in the literature, as well as why and how they are implemented. Therefore, the present section focuses only on justifying the specific methods selected for use in this study.

Pre-processing routines were developed using MATLAB by Mathworks and Loggernet (Campbell Scientific Inc., 2007) to prepare all the data for processing with EddyPro. Automatic routines are critical in Eddy Covariance processing due to the large volume of data processed. Considering that fast measurements are obtained 10 times per second, one year of data results in 315 million lines of data per year; therefore, renaming files, converting data units and even other simple tasks are only feasible with automation. Specific formatting of the data was required for input into EddyPro. In addition, preliminary corrections were required such as day time savings time shifting and wind direction corrections.

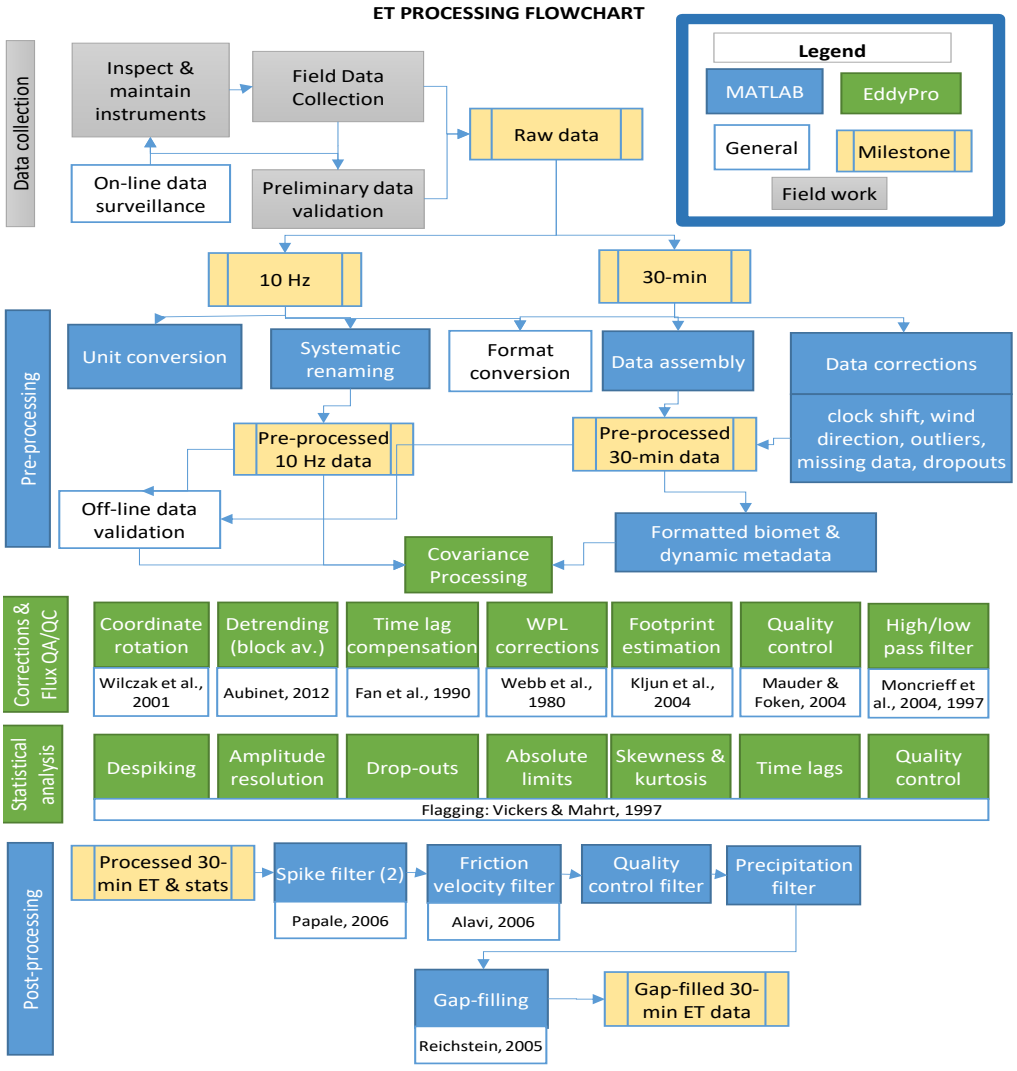

Figure 8. The computational procedure for Eddy Covariance ET flux calculation.

Data processing and corrections were carried using the software EddyPro (LI-COR Inc., 2019). The processing procedure consists of (1) wind filtering to remove wind from the city. (2) Correcting small shifts in instrumentation angles using double rotation approach (Gan and Liu, 2020; Wilczak et al., 2001). The double rotation method is used because of the combination of its simplicity and general dominance over other models (Gan and Liu, 2020; Heinesch et al., 2007; Wilczak et al., 2001). It is only inferior to the planar fit measure in complex terrains, but the topography of the marsh and upwind of the lake station (water) is homogeneous (Aubinet et al., 2012; Heinesch et al., 2007). (3) Accounting for the fact that sonic wind speed and water vapor cannot be measured at the same point using the automatic time lag optimization (Burba, 2013; Fan et al., 1990; Paul-Limoges et al., 2020). This method combines the benefits of a constant time lag and applying covariance maximization (Fan et al., 1990; Paul-Limoges et al., 2020). (4) computing half-hourly fluxes using block averaging (Aubinet et al., 2012); (5) correcting fluctuations in water vapor density using widely used Webb, Pearman and Leuning technique (WPL; Gunawardhana et al., 2021; Lee et al., 2004; Webb et al., 1980); and (6) applying high- and low-pas filters to attenuate computed fluxes (Moncrieff et al., 2004, 1997). Finally, (7) removing of spikes and drop-outs based on statistical characteristics of half-hourly fluxes (Vickers and Mahrt, 1997). Quality assessment and control is carried according to Vickers and Mahrt (1997), and for turbulence conditions according to Foken et al. (2004) as explained in the literature review and summarized in Figure 8.

Data post-processing was carried using the software MATLAB by Mathworks. The post-processing procedure consists of 4 steps, mainly to filter poor-quality fluxes and fill data gaps. In brief, our standard post-processing includes (1) removal of fluxes in which turbulence conditions, represented by friction velocity, are not sufficient for fluxes to be plausible (Alavi et al., 2006); (2) removal of spikes from half-hourly fluxes (Papale et al., 2006; W. Zhang et al., 2016); (3) removal of fluxes when precipitation takes place (Aubinet et al., 2012); and finally (4) gap filling using the nearest data points with similar micrometeorological conditions Reichstein's (2005).

2.2.3 Eddy Covariance Evapotranspiration Dataset

Complete data from our EC stations is available between May 1st to September 30st, 2020. The daily-averaged ET measurements at the two sites are presented in Figure 9. The total ET in the marsh and lake during the whole growing season of 2020 are 330 mm (63 mm, 74 mm, 92 mm, 60 mm and 43 mm from May to September, respectively) and 450 mm (52 mm, 94 mm, 102 mm, 116 mm and 88 mm from May to September, respectively). Based on the measured signals, nearly 90% of seasonal ET in the marsh occurs during daytime, while in the lake this proportion is around 66%, reflecting a higher nighttime ET in the lake (Wang et al., 2014). ET magnitudes reach their maximum in the marsh and the lake around July and August, respectively.

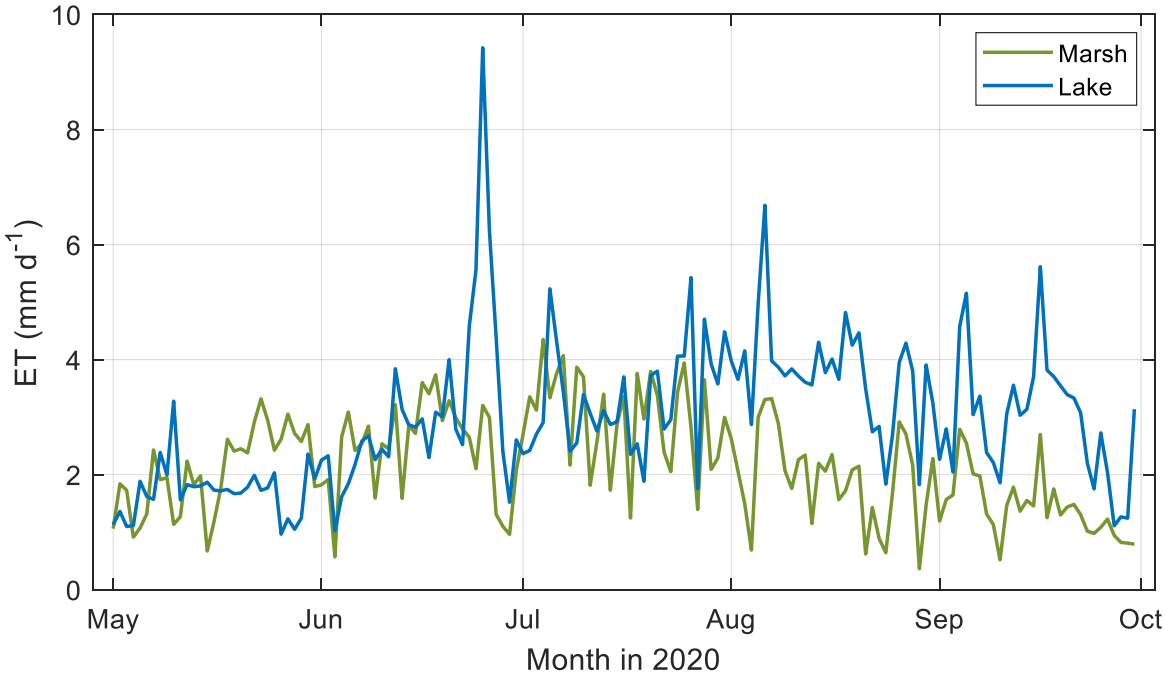

Figure 9. Daily evapotranspiration rate during the study period at the marsh and the lake sites.

Large yet physically-plausible ET spikes are observed in late June in the lake. It has been shown that a large proportion of seasonal evaporation in lakes can happen during short events of high latent heat pulses (Blanken et al., 2000; Liu et al., 2011). For the particular event, high wind speeds, net radiation and air temperature, along with low relative humidity, made an ideal condition for high ET at the lake –see measurements in Figure 10 and anomalies in Figure 11 ($Anomaly = \frac{X-\mu}{\sigma}$). The anomalies displayed in Figure 11 are calculated with respect to the entire growing seaon. We observe that prolonged high values in temperature and net radiation provided a higher free evaporation potential, while the high wind event around June 25 created a strong forced evapotranspiration. This cannot happen in the marsh as the vegetation cover is in its maximum height and shields the surface from the wind.

The accuracy of ET measurements using EC method can be assessed through examining closure of the surface energy balance (Allen et al., 2011; Y. Zhang et al., 2016). This is through checking the balance between available energy ($R_n - G$ for the marsh; $R_n - Q$ for the case of the lake) and the turbulent fluxes ($LE + H$). In reality, this closure is rarely fully satisfied due to multiple sources of errors and unaccounted sources/sinks of heat (Aubinet et al., 2012). In particular, ground heat flux and/or heat storage can account up to 50% misclosure in energy balance (Foken, 2008; Wang and Dickinson, 2012). In our setup at the marsh, ground heat flux is measured directly using an integrated temperature, moisture and heat sensor. Heat storage in the lake is calculated through the method presented in Blanken et al. (2000), and the water temperature data available for September 2020. Temperature is measured using a series of temperature sensors placed over a chain, and spaced at approximately 0.3 m from the water surface to the depth of 2.5 m. Figure 12 shows energy closure at both sites on a daily time scale (Blanken et al., 2000), revealing a closure of 95%

at the lake site and month September. In the marsh the daily closure varies between 41% to 58% in different months, with the expected value of 47% over the whole growing season. While this include large energy imbalance, both FLUXNET (Wilson et al., 2002) and ChinaFLUX (Yuling, 2005) include sites with similar closure ratios. In our case, poor closure in the marsh might be caused by underestimation of ground heat flux due to the absence of solid soil layer, which causes large errors in measuring the stored and emitted heat from the wetland surface (Lee et al., 2004; Foken, 2008).

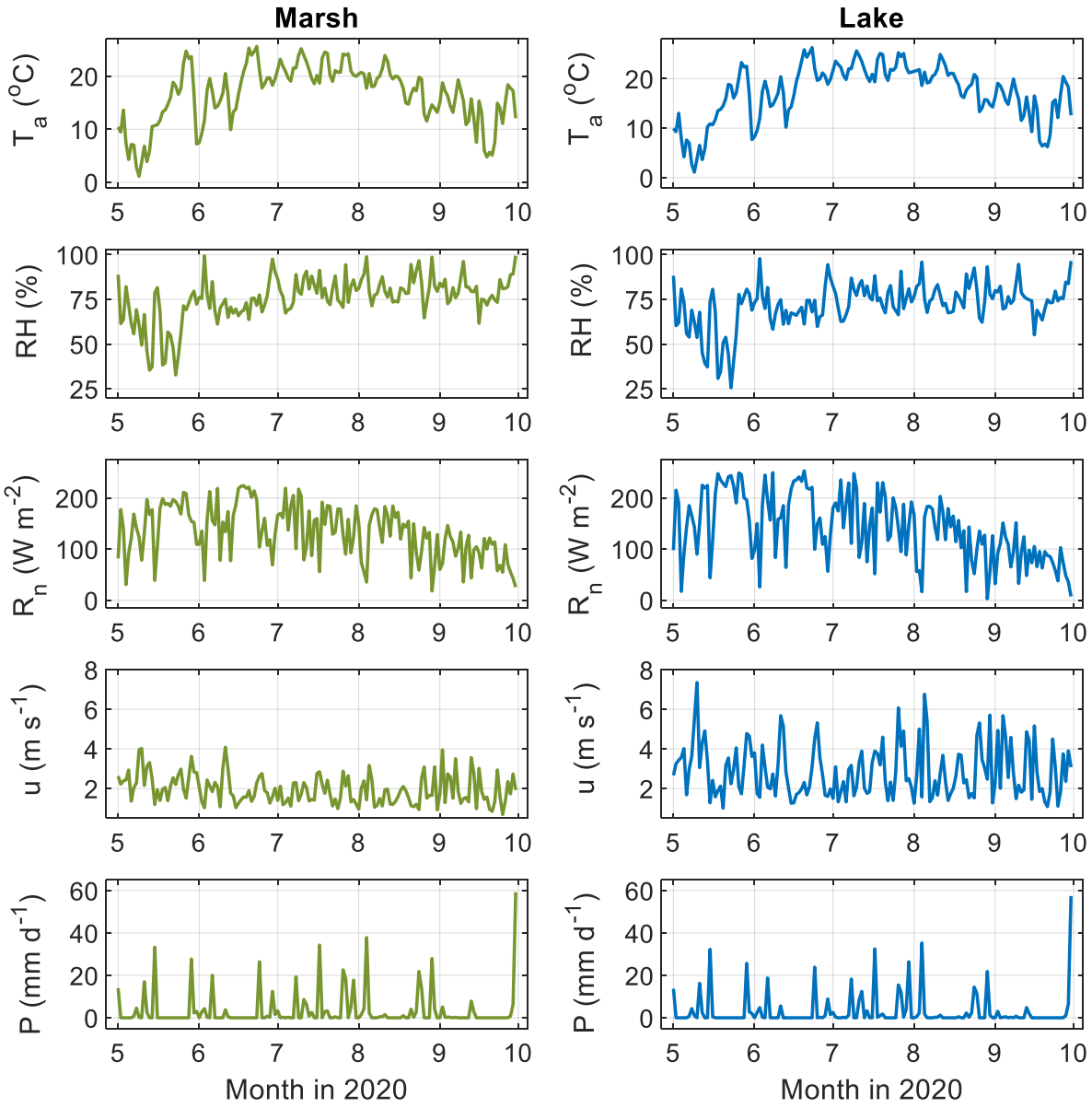

Figure 10. Key microclimatic measurements made in the marsh (left column) and lake (right column) during the study period, averaged at the daily time scale. Symbols are presented in the List of Symbols.

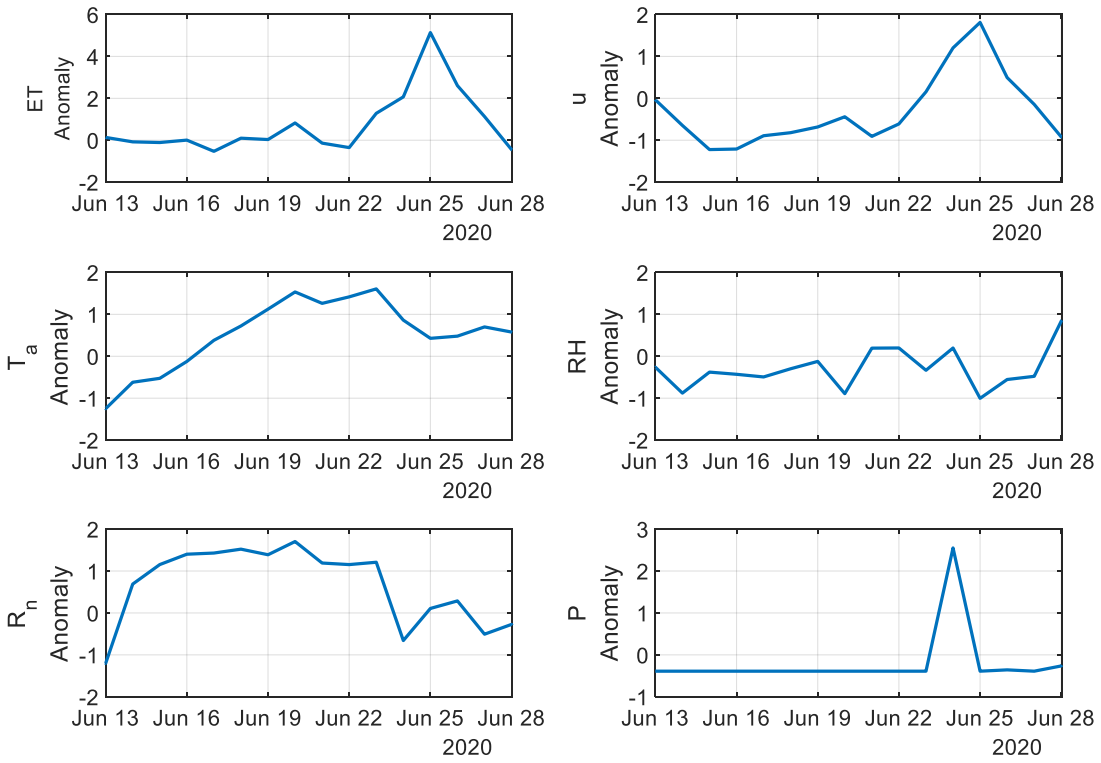

Figure 11. Anomalies in meteorological variables during the high evapotranspiration event in late June in the lake.

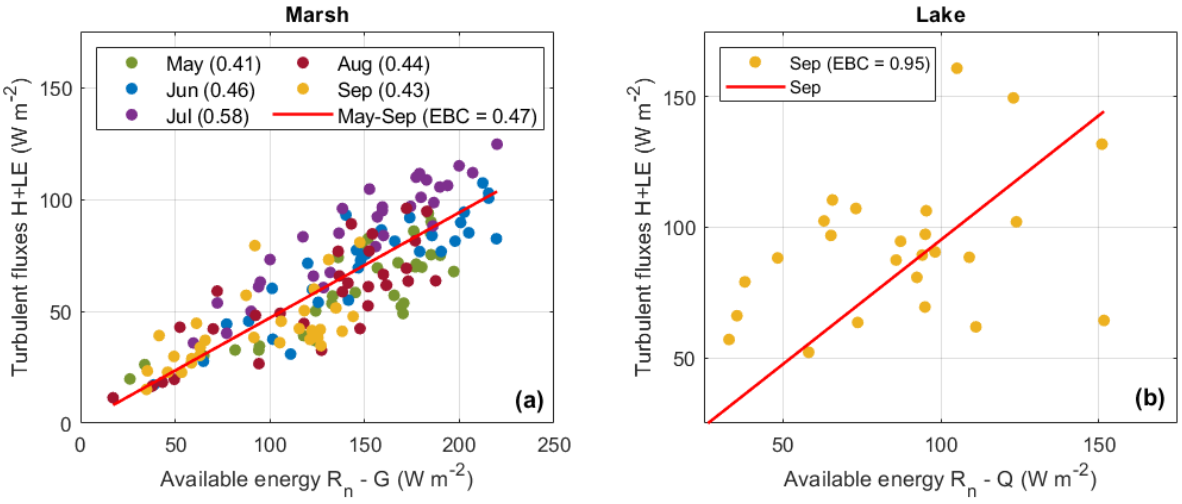

Figure 12. Energy balance closure diagrams showing scatter plots of daily available energy values versus daily turbulent fluxes. The percentage of monthly closure for each month is reported in parenthesis. The line shows the expected closure during the data period.

3 Benchmarking Empirical Models of Evapotranspiration in the Considered Lake-Wetland Duo

By putting in perspective current state of knowledge, the aim here is to understand the skill of empirical PET/ET models in representing the ET fluxes from wetlands and lake. To the best of our knowledge, the most comprehensive intercomparison study is limited to 24 models (Seiller and Anctil, 2016). Here we increase the number of models to 40 and cover empirical equations suggested from Fitzgerald (1886) to McColl (2020) in the time span of 135 years.

3.1 Empirical modelling of evapotranspiration

Our benchmarking study includes 40 empirical ET models, developed in the time span of 135 years. The models are handpicked from all categories of empirical models noted in Section 1 and contain 10 Aerodynamic (A), 8 Combination (C), 8 Temperature-based (T), 6 Temperature hybrid (T+), and 8 Radiation-based (R) models (Table 4). Each model *M* is identified by two indices as M_{number}^{Type}, in which *Type* identifies the model category and the number is the nominator of the model in its own category. Table 4 lists these models, their sources and input meteorological variables.

Each model *M* is identified by two indices as M_{number}^{Type}, in which *Type* identifies the model category and the number is the nominator of the model in its own category. Note that ET models are placed in each category based on their conceptualization, and the way input variables are utilized (Seiller and Anctil, 2016). For example, De Bruin's equation (M_1^C) is considered a combination equation, due to its derivation from Priestley Taylor's equation and inclusion of a radiation coefficient (de Bruin, 1978; Priestley and Taylor, 1972). Also, a temperature-hybrid category is created to distinguish temperature-based equations with and without other supporting meteorological variables such as incoming radiation. 90% of these equations provide an estimate for PET, except for M_4^C, M_5^C, M_6^C, and M_8^C, which compute actual ET. The formulations of these equations are provided in Tables 5 to 9 and are slightly modified to harmonize the units. Thornthwaite's equation, M_8^T, requires long-term records to establish monthly averages (Thornthwaite, 1948), for which we use temperature records from 2001 to 2020 from Environment and Climate Change Canada's climate station at Lake Memphremagog (Climate ID: 702CFGG).

We test the skills of these models in representing ET from a wetland-lake duo, in which ET is measured using an entirely consistent EC approach and instrumentation during growing season 2020, when Covid-19 pandemic hit Québec, Canada and the world.

3.2 Benchmarking approach

We shift the benchmarking approach from single- to multi-objective assessment by implementing a non-dominated sorting algorithm. This allows using multiple GoFs simultaneously and identifying several non-falsified ET models as parallel modeling hypotheses. We repeat our benchmarking across a range of scales as well as diurnal and seasonal segments to reveal how the skill of empirical ET models alters across scales and/or daily to seasonal cycles.

Our benchmarking is based on assessing the skills of empirical ET models against multiple GoFs. The simplest approach to implement multiple GoFs is to assign a corresponding weight to each GoF based on their importance to the problem in hand (which may be subjective), and to combine them through a mathematical operator into a combined GoF (Nazemi et al., 2002).

Although this approach transforms the multi-objective problem into a *quasi*-single objective ranking, it fails to accurately represent dominance (Cheng et al., 2018; Wang et al., 2017). Accordingly, in line with the state-of-the-art (see e.g. Bao et al., 2017; Herman et al., 2018), we consider assessing multiple GoFs using a multi-objective ranking. In this approach, a model dominates another, if and only if it performs better considering all GoFs. This consideration requires implementation of non-dominated sorting (or Pareto ranking) methods (Ghiasi et al., 2011; Nazemi et al., 2006, 2008), and inherently allows the existence of several models at the same front (or dominance level). Here, we consider a fast non-dominated sorting algorithm, which considers the idea of Pareto comparison with a pruning scheme and is used in the context of Nondominated Sort Genetic Algorithm II (NSGA-II; Deb et al., 2002). In brief, the algorithm uses a sequential approach to rank models. First, all ET models are used to determine Pareto front of non-dominated (or non-falsified). The algorithm then removes the Pareto front and repeats the multi-objective ranking to identify the second front and so on until all models are ranked.

We consider four GoFs, namely the Root Mean Square Error (RMSE), Mean Absolute Error (MAE), Mean Error (ME) and index of agreement (d) for multi-objective ranking. These GoFs have been frequently used in intercomparison studies (Bormann et al., 2011; Herman et al., 2018; Legates and McCabe Jr, 1999; Willmott et al., 1985). The experimentation methodology can be clearly followed up to this point in the flowchart presented below in Figure 13. We also use two other GoFs to independently monitor the uncertainty and skills of the first-rank models. To evaluate the uncertainty, we measure the expected range of non-falsified simulations of ET per day, termed here as Standardized Mean Range per Day (SMRD). A large (small) SMRD indicates low (high) agreement between non-falsified models, and therefore high (low) uncertainty. We also use Nash Sutcliffe coefficient of Efficiency (NSE) to independently evaluate the skills of non-falsified models. NSE values have the upper bound of 1, indicating a perfect fit and a critical value of 0, below which the simulated values are practically useless as they are not even as informative as long-term average of the observed signal. Table 10 summarizes the formulation of the GoFs used, in which ET_{mod} and ET_{obs} are the modelled and observed ET signals, N is the number of data points and Δt is the simulation timestep per day.

Table 4: Summary of the 40 empirical evapotranspiration models and their meteorological variables, namely air temperature (T), relative humidity (RH), wind speed (u), atmospheric pressure (P), incoming and outgoing shortwave radiation ($\boldsymbol{R_{in}^s}$, $\boldsymbol{R_{out}^s}$), net radiation (R_n), ground heat flux (G) and extraterrestrial radiation (R_0). Models that are recommended for daily and larger time scales are identified with an asterisk sign (*) after their reference.

Category	Reference	Abbreviation	Meteorological Variables
Aerodynamic models (A)	Brutsaert and Yu (1968)	M_1^A	T, RH, u
	Carpenter (1888)	M_2^A	T, RH, u
	Einsenlohr (1966)	M_3^A	T, RH, u
	Fitzgerald (1966)	M_4^A	T, RH, u
	Marciano and Harbeck (1952)	M_5^A	T, RH, u
	McMillan (1971)	M_6^A	T, RH, u
	Meyer (1915)	M_7^A	T, RH, u
	Rohwer (1931)	M_8^A	T, RH, u, P
	WMO US (Gangopadhyaya, 1966)	M_9^A	T, RH, u
	WMO USSR (Gangopadhyaya, 1966)	M_{10}^A	T, RH, u
Combination models (C)	De Bruin (1978)	M_1^C	T, RH, u
	Doorenbos-Pruitt (1977)	M_2^C	T, RH, u, P, R_{in}^s
	Kimberley-Penman (Wright, 1982)	M_3^C	T, RH, u, P, R_n
	Koerselman and Beltman (1988)	M_4^C	T, RH, u, P, R_n
	Lafleur (1990)	M_5^C	T, RH, u, P, R_n
	McColl (2020)	M_6^C	T, RH, u, P, R_{in}^s, R_n
	Penman (1948)	M_7^C	T, RH, u, P, R_n, G
	Penman-Monteith (1965)	M_8^C	T, RH, u, P, R_{in}^s, R_n
Temperature-based models (T)	Hamon (1963)	M_1^T	T
	Hargreaves-Samani (1985)*	M_2^T	T
	Hydro-québec (Bisson, 1983)*	M_3^T	T
	Kharrufa (1985)	M_4^T	T
	Linacre (1977)	M_5^T	T, RH
	Papadakis (1965)	M_6^T	T
	Romanenko (1961)	M_7^T	T, RH
	Thornthwaite (1948)	M_8^T	T
Temperature-hybrid models (T+)	Jensen-Haise (1963)	M_1^{T+}	T, R_{in}^s
	McGuinness-Bordne (1972)	M_2^{T+}	T, R_0
	Oudin (2005)	M_3^{T+}	T, R_0
	Rouse (1998)	M_4^{T+}	T, R_n
	Stephens-Stewart (1963)	M_5^{T+}	T, R_{in}^s
	Turc (1955)	M_6^{T+}	T, RH, R_{in}^s, R_{out}^s
Radiation-based models (R)	Abtew 1 (1996)	M_1^R	R_{in}^s
	Abtew 2 (1996)*	M_2^R	T, R_{in}^s
	Abtew 3 (1996)*	M_3^R	T, R_{in}^s
	De Bruin-Keijman (1978)	M_4^R	T, P, R_n, G
	Makkink (1957)	M_5^R	T, R_{in}^s
	Přibáň net radiation (1985)	M_6^R	T, R_n
	Přibáň relative humidity (1985)	M_7^R	T, RH, R_n
	Priestley & Taylor (1972)	M_8^R	R_n,, G

Table 5: The equations of aerodynamic evapotranspiration models used in this study

Model	Equation
M_1^A	$PET = 180(1.35 * 10^2 + 1.54 * 10^2 * u)(e_a^* - e_a)$
M_2^A	$PET = 33.27(e_a^* - e_a)(1 + 4.66 * 10^{-5}\, u)$
M_3^A	$PET = 1.023\, u\, (e_a^* - e_a)$
M_4^A	$PET = 160.43(e_a^* - e_a)(1 + 0.0208u)$
M_5^A	$PET = 1.0057\, u(e_a^* - e_a)$
M_6^A	$PET = \frac{0.8640}{\lambda_v}(4.0 + 2.44\, u)(e_a^* - e_a)$
M_7^A	$PET = 12.49(1 + 0.00415u)\, (e_a^* - e_a)$
M_8^A	$PET = 6.630 * (1.465 - 0.0630A)(0.44 + 0.0022u)(e_a^* - e_a)$
M_9^A	$PET = 1.31 * u(e_a^* - e_a)$
M_{10}^A	$PET = 1.3 * (1 + 0.72u)(e_a^* - e_a)$

Table 6: The equations of temperature-hybrid evapotranspiration models used in this study

Model	Equation
M_1^{T+}	$PET = \left(0.014\left(\frac{9}{5}T_a + 32\right) - 0.37\right) * Q_s * 3.523 * 10^{-2}$
M_2^{T+}	$PET = 1000 * \frac{0.0864R_0}{\lambda_v \rho_w}\frac{T+5}{68}$
M_3^{T+}	$PET = 10\frac{0.0864R_0(T+5)}{\lambda_v \rho_w}$
M_4^{T+}	$PET = 86.4 * 10^6\, (0.59\, R_n + 1.083T)(\rho_w \lambda_v)^{-1}$
M_5^{T+}	$PET = (0.0082(\frac{9}{5}T_a + 32) - 0.19) * \frac{8.486R_{sin}}{\lambda_v \rho_w}$
M_6^{T+}	$PET = \frac{1000}{\lambda_v \rho_w}\frac{\left(\frac{T_a}{T_a+15}\right)(0.0864(R_{sin} - R_{sout}) + 24)}{1.3} * c$ $c = 1 + \frac{50 - RH}{70}\ for\ RH < 50\%; c = 1\ for\ RH \geq 50\%$

Table 7: The equations of combination evapotranspiration models used in this study

Model	Equation
M_1^C	$PET = \frac{864}{\rho_w \lambda_v}\left(\frac{\alpha}{\alpha-1}\right)\frac{\gamma}{\Delta+\gamma}(2.9+2.1u)(e_a^*-e_a)$
M_2^C	$PET = 0.0864K_d * \frac{\frac{1}{\lambda_v}\Delta R_s}{\Delta+\gamma} - 0.3;$ $K_d = 1.066 - \frac{0.13RH}{100} + 0.045u - \frac{0.02RH}{100}u - 0.00315\left(\frac{RH}{100}\right)^2 - 0.0011u^2$
M_3^C	$PET = \frac{1}{\lambda_v}\left(\frac{\Delta}{\Delta+\gamma}0.0864R_n + 2.62\frac{\Delta}{\Delta+\gamma} * (e_a^*-e_a) * K_p\right)$ $K_p = 0.4 + 0.14\exp\left(-\left(\frac{J_D-173}{58}\right)^2\right) + 0.605 + 0.345\exp\left(-\left(\frac{J_D-243}{80}\right)^2\right) * u$
M_4^C	$ET = 0.73 * \frac{\frac{\Delta}{\lambda_v} * R_n + 10\gamma(3.7+4u)(e_a^*-e_a)}{\Delta+\gamma} + 0.16$
M_5^C	$ET = 0.85 * \left(\frac{\Delta}{\lambda_v} * R_n + 10\gamma(3.7+4u)(e_a^*-e_a)\right)(\Delta+\gamma)^{-1} + 0.18$
M_6^C	$ET = 86.4(\lambda_v\rho_w)^{-1}[461T^2\ \lambda_v^{-1}c_a\ \rho_a\ C_{at}W_0 * \left\{\frac{\lambda_v^2}{c_a}\frac{10^{-6}0.622e_a^*}{461*T^2A}\frac{C_{can}}{C_{can}+C_{at}}\exp\left(\frac{10^{-6}\lambda_v}{461T^2}\frac{R_n - G + \frac{C_{can}C_{at}}{C_{can}+C_{at}}\frac{\rho_a\lambda_v 0.622e_a}{A}}{\rho_a c_a C_{at}}\right)\right\}$ $-\rho_a\lambda_v 10^{-6}\frac{C_{can}C_{at}}{C_{can}+C_{at}}\frac{0.622e_a}{A}]$
M_7^C	$PET = \lambda^{-1}(\Delta+\gamma)^{-1}\left(0.0864\Delta R_n + 2.62\gamma(e_a^*-e_a)(1+0.537u)\right)$
M_8^C	$ET = \frac{0.0864\Delta R_n + 86400\ c_a\ \rho_a\ C_{at}e_a^*\ [1-RH]}{\rho_w\ \lambda_v\left(\Delta+\gamma*\left(1+\frac{C_{at}}{C_{can}}\right)\right)}$

Table 8: The equations of temperature-based evapotranspiration models used in this study

Model	Equation
M_1^T	$PET = 29.8D * \frac{e_a^*}{T + 273.2}$
M_2^T	$PET = 0.0023 \left(\frac{0.1987R_0}{\lambda_v \rho_w}\right)(T_{max} - T_{min})^{0.5}(T + 17.8)$
M_3^T	$PET = 0.02978\,(T_{max} - T_{min})\, exp\left(0.019(\frac{9}{5}(T_{max} + T_{min}) + 64\right)$
M_4^T	$PET = 0.34 * \left(100 * \frac{D}{365 * 12}\right) * T^{1.3}$
M_5^T	$PET = \frac{k(T + 0.006z)(100 - y)^{-1} + 15(T - T_{dew})}{80 - T}$ $where\ k_{lake} = 500\ and\ k_{marsh} = 700$
M_6^T	$PET = 0.1844\,(e^*_{max} - e^*_{min-2})$ $where\ e^*_{min-2}: saturation\ vapor\ pressure\ at\ T_{min} - 2^oC$
M_7^T	$PET = 4.5\left(1 + \frac{T}{25}\right)^2\left(1 - \frac{e_a}{e_a^*}\right)$
M_8^T	$PET = 16 * \left(\frac{D}{360}\right)\left(\frac{10T}{I}\right)^K$ $I = \sum_{n=1}^{12}\left(\frac{T_{mo}}{5}\right)^{1.514}, T_{mo}: mean\ monthly\ temperature$ $K = 0.49239 + 1.792\ 10^{-2}I - 0.771\ 10^{-4}I^2 + 6.75\ 10^{-7}I^{-3}$

Table 9: The equations of radiation-based evapotranspiration models used in this study

Model	Equation
M_1^R	$PET = 0.0449\frac{R_{sin}}{\lambda_v}$
M_2^R	$PET = \frac{0.012(2.064R_{sin}+50)T_{max}}{T_{max}+15}$
M_3^R	$PET = 0.00154\frac{R_{sin}T_{max}}{\lambda_v}$
M_4^R	$PET = 1000\frac{1.11\left(\frac{\Delta}{\Delta+\gamma} * 0.0864(R_n - G)\right)+10.3}{\rho_w\lambda_v}$
M_5^R	$PET = \left(52.6 * \frac{\Delta}{\Delta+\gamma} * \frac{R_{sin}}{\lambda_v\rho_w\ 10^{-6}}\right) - 0.12$
M_6^R	$PET = (-4.66 + 0.0306\ R_n\ ) * 30.5^{-1}$
M_7^R	$PET = 0.00107\ R_n(1-RH)^{0.038}$
M_8^R	$PET = 1000\alpha\frac{0.0864(R_n - \mathrm{G})\ \Delta}{(\Delta+\gamma)\lambda_v\rho_w}$

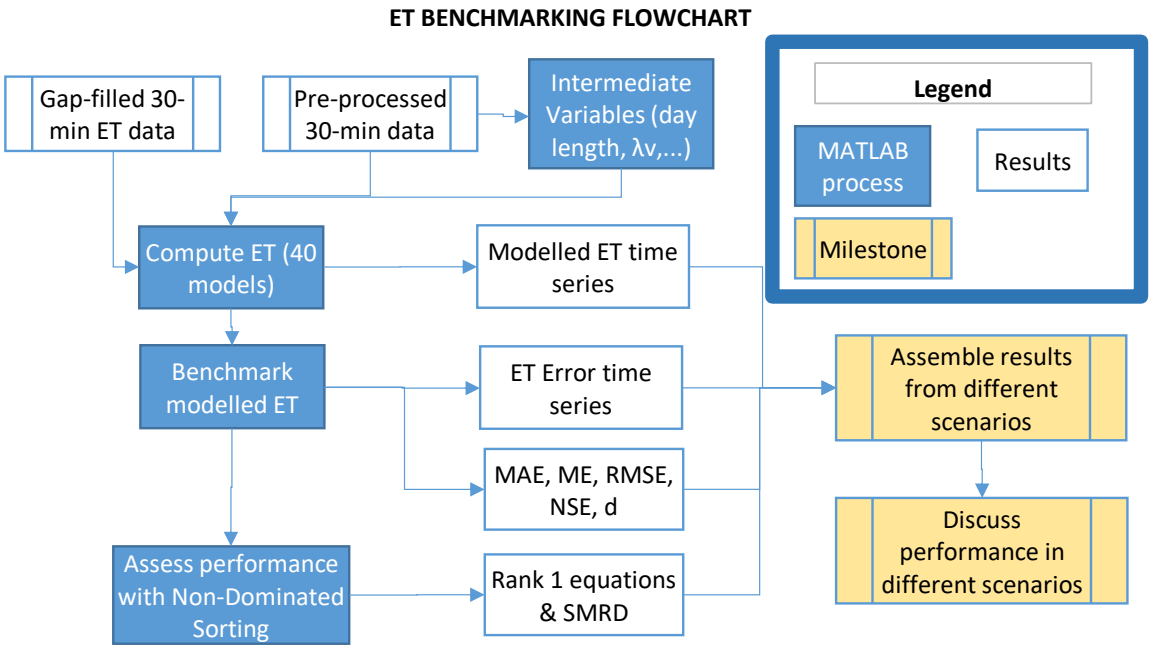

Figure 13. ET benchmarking computations methodology flowchart.

Our benchmarking focuses on assessing the combined effects of land cover (vegetated *vs.* open-water), timescale (half-hourly to monthly) as well as the diurnal (daytime *vs.* nighttime *vs.* full day) and seasonal segments (beginning *vs.* middle *vs*. end of the growing season) on the skills of empirical ET models. This benchmarking exercise is executed through three independent experiments that are applied in the two sites. Our first experiment focuses on the effect of timescale in determining the skill of ET models. It is known that the dependence of ET on meteorological variables (e.g., net radiation) changes across time scales (Jansen and Teuling, 2020; Rimmer et al., 2009). Consequently, it is important to investigate the range of timescales in which different models are relevant. Our second experiment is performed solely at the half-hourly timescale – the finest timescale in which observed ET is available – but considers ET signals at different diurnal segments, i.e. daytime and nighttime. This is to address the skills of empirical ET models in capturing observed signal when there are major changes in incoming shortwave radiation and photosynthetic activities in the course of day (Aubinet et al., 2012; Wang and Dickinson, 2012). Finally, our third experiment looks at how the efficiency of ET models can vary across different segments of the growing season. For instance, albedo changes in the marsh during the growing season (and hence the ratio of transpiration to the total ET), along with the heat storage in the lake (see Drexler et al., 2004; van Emmerik et al., 2013). It is still unclear how empirical models can capture the seasonal trajectory of ET in response to an evolving environment during the growing season. This experiment is performed at a daily timescale and considers months of May, July and September as the representative of the beginning, middle and the end of the growing season.

Table 10: Summary of Goodness of Fit measures, their formulation and purpose in this study

Goodness of Fit Measure	Equation	Purpose
Mean absolute error (MAE)	$\frac{\sum_{i=1}^{N}(\lvert ET_{mod} - ET_{obs}\rvert)}{N}$	Multiobjective ranking
Mean error (ME)	$\frac{\sum_{i=1}^{N}(ET_{mod} - ET_{obs})}{N}$	Multiobjective ranking
Root mean square error (RMSE)	$\sqrt{\frac{\sum_{i=1}^{N}(ET_{mod} - ET_{obs})^2}{N}}$	Multiobjective ranking
Index of agreement (d)	$1 - \frac{\left(\sum_{i=1}^{N}(ET_{mod} - ET_{obs})^2\right)}{\sum_{i=1}^{N}(\lvert ET_{mod} - \overline{ET_{obs}}\rvert - \lvert ET_{obs} - \overline{ET_{obs}}\rvert)^2}$	Multiobjective ranking
Standardized Mean Range per Day (SMRD)	$\frac{\sum_{i=1}^{N}(ET^{*}_{max} - ET^{*}_{\min})}{N\Delta t}$	Independent proxy of uncertainty
Nash Sutcliffe Efficiency (NSE)	$1 - \frac{\left(\sum_{i=1}^{N}(ET_{mod} - ET_{obs})^2\right)}{\sum_{i=1}^{N}(ET_{obs} - \overline{ET_{obs}})^2}$	Independent proxy of skill

3.3 Results

3.3.1 Skills of empirical models across a range of time scales

The focus here is on identifying non-falsified ET models in the marsh and the lake sites across a range of timescales, extended from half-hourly to monthly. Figure 14 summarizes the results in the marsh. In panel (a), the non-falsified models across different timescales are shown, revealing that there is no timescale in which a single ET model can dominate over all other models. At the finest timescale, there is at least one model from each category among non-falsified models. From 1- to 6-hour, the non-falsified models mainly include aerodynamic and combination models. This indicates the importance of radiative and wind forcing in driving ET at the marsh site across finer timescales. The most versatile aerodynamic models in the marsh at timescales smaller than 12-hour are M_2^A (time scales smaller or equal to 3-hour) and M_6^A (all time scales except 3-hour). Combination methods are also seen in timescales finer than 12-hour, where the model M_3^C is the most versatile model across these timescales.

The most versatile aerodynamic models in the marsh at timescales smaller than 12-hour are M_2^A (time scales smaller or equal to 3-hour) and M_6^A (all time scales except 3-hour). Combination methods are also seen in timescales finer than 12-hour, where the model M_3^C is the most versatile model across these timescales. At time scales coarser than 12-hour, RMSE, MAE and SMRD are generally improved; inter-modal variability decreases; and, the non-falsified models are dominated by aerodynamic and temperature-hybrid models, except at the biweekly timescale. The most versatile models across coarser timescales are M_8^A and M_5^{T+}. This indicates a critical range – in this case between 12-hour to weekly, in which the skill in representing ET declines with the shift from aerodynamic to temperature-hybrid models. However, it should be noted that ME shows a conflicting pattern, indicating the importance of adopting a multi-objective sorting for benchmarking modeling performance. Figure 15 shows the benchmarking analysis for the lake. Similarly, no single ET model can dominate over all other models in any of the considered timescales. While ET at finer scales is best captured by aerodynamic models, temperature-based and radiation models dominate at coarser timescales. The most versatile aerodynamic models in the lake and at the finer time scales include M_6^A, M_2^A and M_{10}^A. Similar to the marsh, as the timescale gets coarser, RMSE, MAE and SMRD values decrease. This trend is also observed in NSE and d with more gradual improvement over time. There are few models that are shared in both lake and the marsh (e.g. M_2^A and M_6^A in daily and sub-daily timescales. Differences can be also witnessed between the two sites, e.g. M_5^{T+} performs better at timescales coarser than 12-hour in the marsh, but at finer timescales in the lake. However, in scales finer than weekly, non-falsified models provide negative NSE, indicating poor simulations at the lake.

3.3.2 Skills of empirical models across different diurnal segments

As the incoming radiation is absent during nighttime, the mechanisms that drive ET, and accordingly the nature and skills of non-falsified models, can alter during different time of day. In

order to better investigate this, we use the non-dominating sort algorithm to rank half-hourly ET models during daytime, nighttime and a full day, separately.

Figure 16 summarizes the findings of this experiment in the lake and marsh. In the marsh, there are at least six non-falsified models during each segment of a day. During the daytime and full day, the first-rank models include all categories. In the nighttime though, the non-falsified models are mainly limited to aerodynamic models as well as several combination equations, in response to the absence of incoming radiation during the nighttime. In the lake, nine models are non-falsified during the full day, containing all categories except radiation-based models. During the daytime and nighttime though, the number of non-falsified models extensively declines. During the daytime, there are only three non-falsified models that are either temperature-based or temperature hybrid. In the nighttime, one temperature-based model dominates all other options.

The behaviour of GoFs during different time of day are also different. In the marsh the value of RMSE and MAE are improved moving from full day to daytime to nighttime, whereas this is not the case for other GoFs. In the lake though, the expected skill along with the range of uncertainty in GoFs is strictly improved moving from full day to daytime to nighttime.

It is worthwhile to note that although in both the lake and the marsh, there is an ET model that is non-falsified in the three diurnal segments, the non-falsified model is different in the lake (M_1^T) and the marsh (M_6^A), indicating that a unique empirical model that can be relevant to both lake and marsh during the whole day cannot be found.

3.3.3 Skills of empirical models across different segments of the growing season

As the growing season continues, vegetation evolves in the marsh and heat storage increases in the lake. As a result, the performance of empirical models may change; and thus non-falsified models during different segments of the growing season. To address this, we consider assessing the skill of non-falsified models in simulating daily ET signal in the beginning, middle and the end of the growing season, represented by the months May, July and September, respectively (Figure 17). First and foremost, the expected ME values in both sites and in all months are above zero, indicating that the ET is overestimated by all non-falsified models. In both landscapes, there is no ET model that remains non-falsified during all segments of the growing season. In the marsh, aerodynamic models are only present in May, when vegetation is still in its early stage, and canopy resistance is low, allowing wind to have more impacts on ET. As the growing season continues, however, temperature-based and temperature hybrid models become more skillful.

In the lake, there is an absolute dominance in months May and September by M_5^A and M_1^R, respectively, meaning that there is one ET model that can dominate all other modeling options. In month July, however, there is at least one model from each category that is not falsified. The larger number of non-falsified models in July is also associated with a wider range of GoFs and a SMRD of nearly 2 mm/day. Considering that the total ET is 100 mm, this uncertainty is quite considerable and can include around 60% of the total monthly ET flux. In the marsh, in contrary, the best modeling performance is observed in the month July, when the monthly ET is the maximum. In the lake though the skill is improved in the month September when thermal storage is declining.

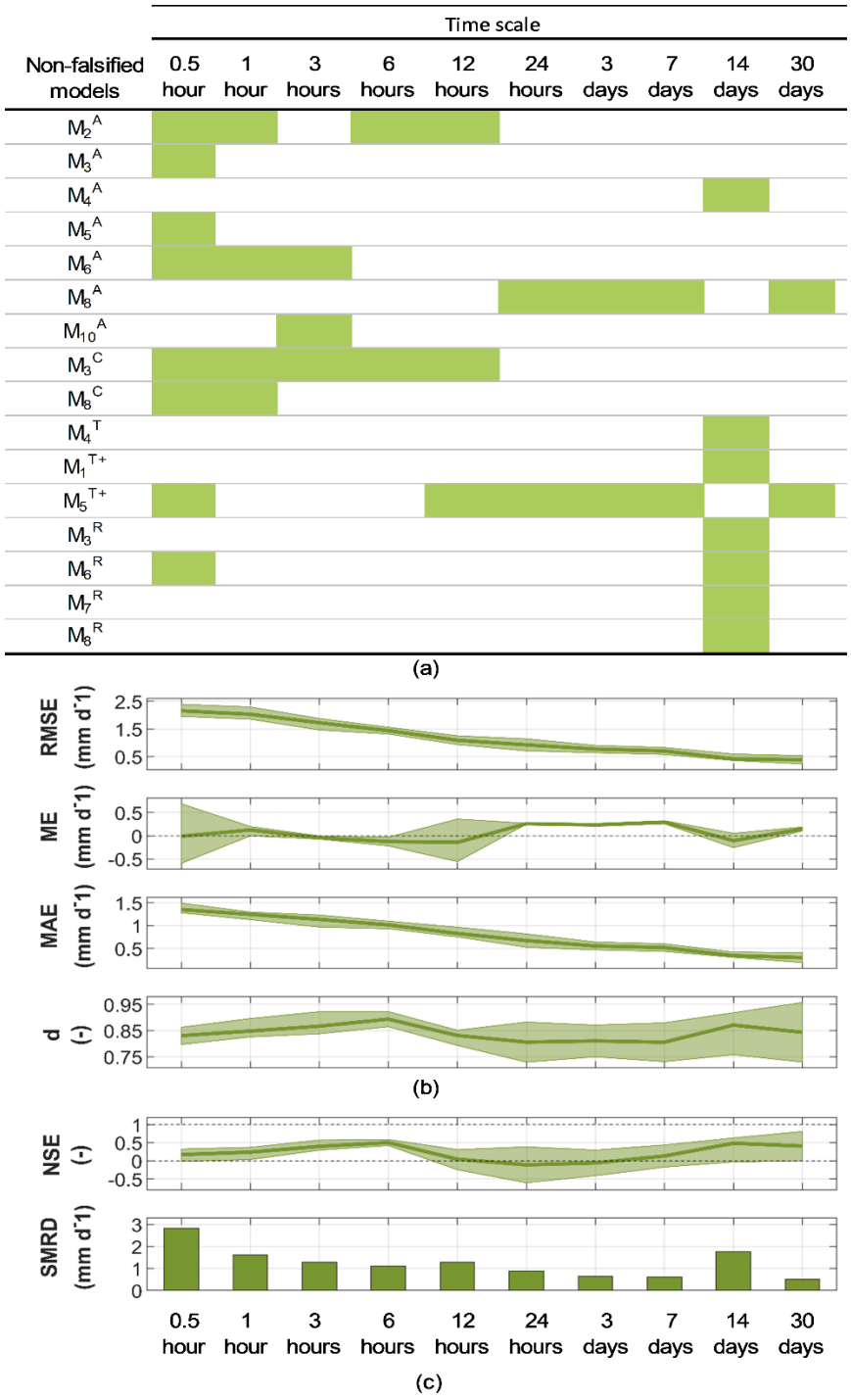

Figure 14. Results of non-dominated sorting for benchmarking the performance of ET models across a range of time scales in the marsh illustrated by (a) the list of the non-falsified models at each time scale, (b) the associated GoF envelopes along with expected performances shown in solid lines, and (c) the independent monitoring of accuracy quantified by NSE and SMRD.

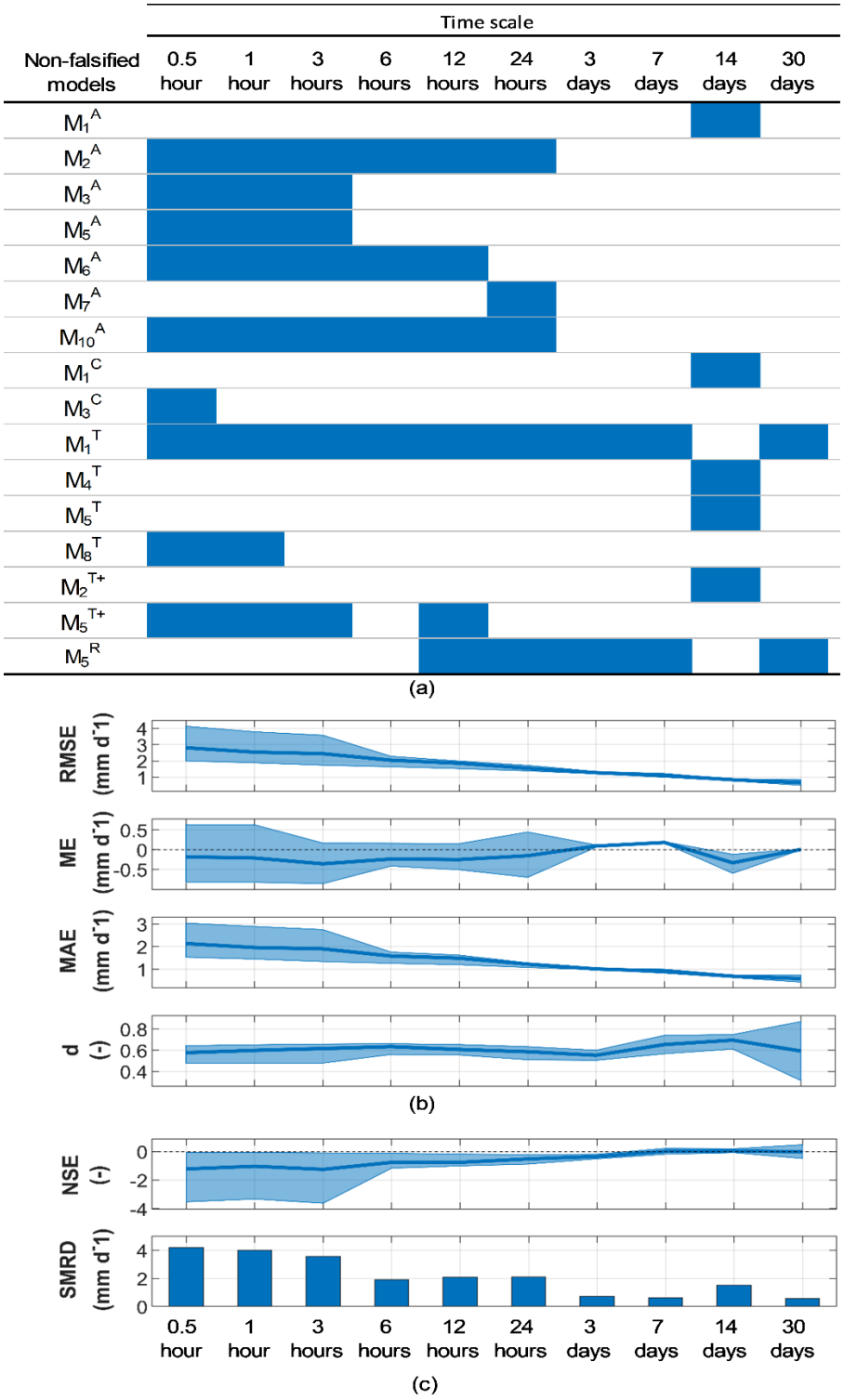

Figure 15. The results of non-dominated sorting for benchmarking the performance of ET models across a range of time scales in the lake illustrated by (a) the list of the non-falsified models at each time scale, (b) the associated GoF envelopes along with expected performances shown in solid lines, and (c) the independent monitoring of accuracy quantified by NSE and SMRD.

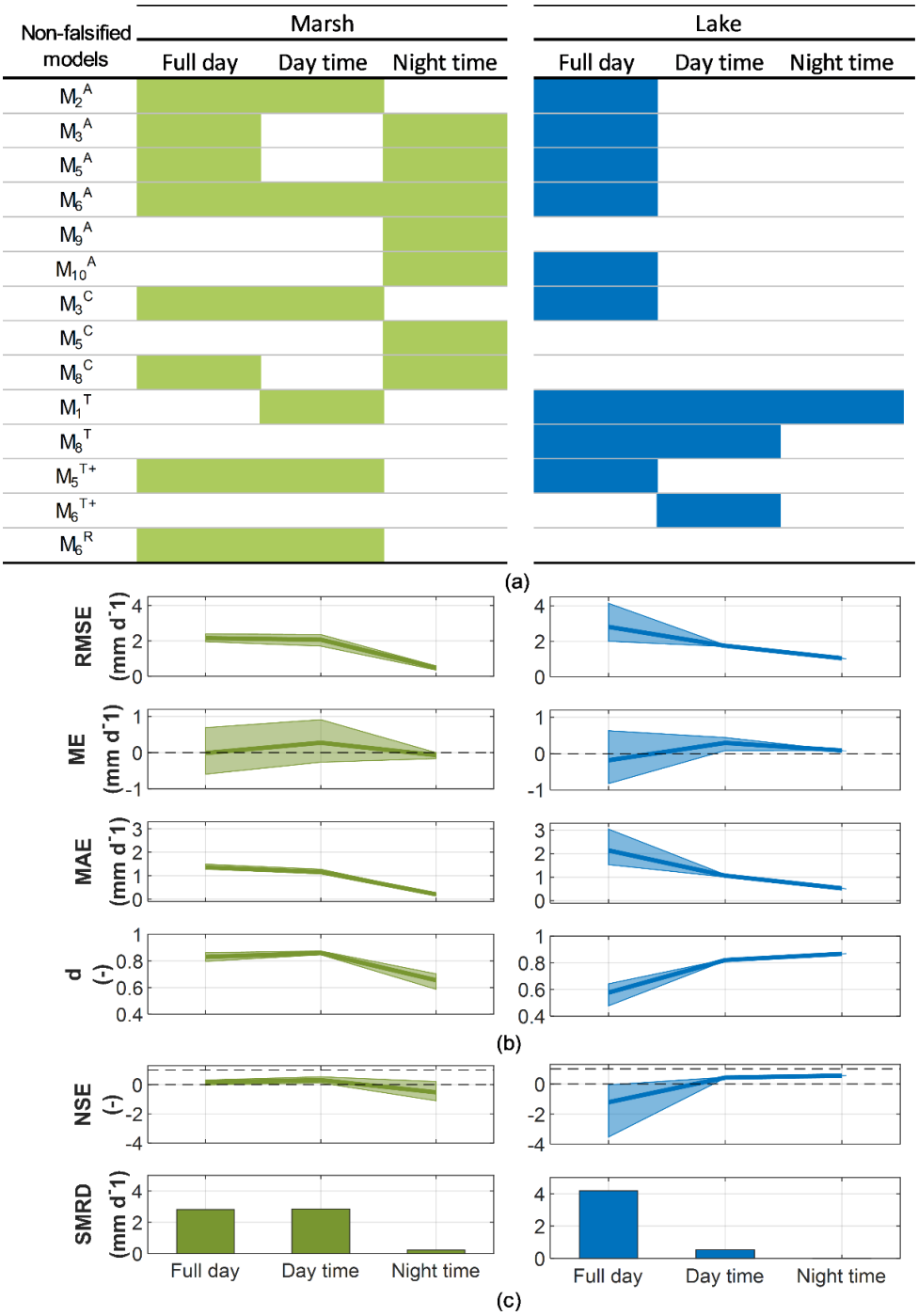

Figure 16. Benchmarking non-dominated sorting results in the marsh and lake illustrated by (a) the non-falsified models at each time of the day, (b) the associated GoF envelopes along with expected performances shown in solid lines, and (c) the associated monitoring measures NSE and SMRD.

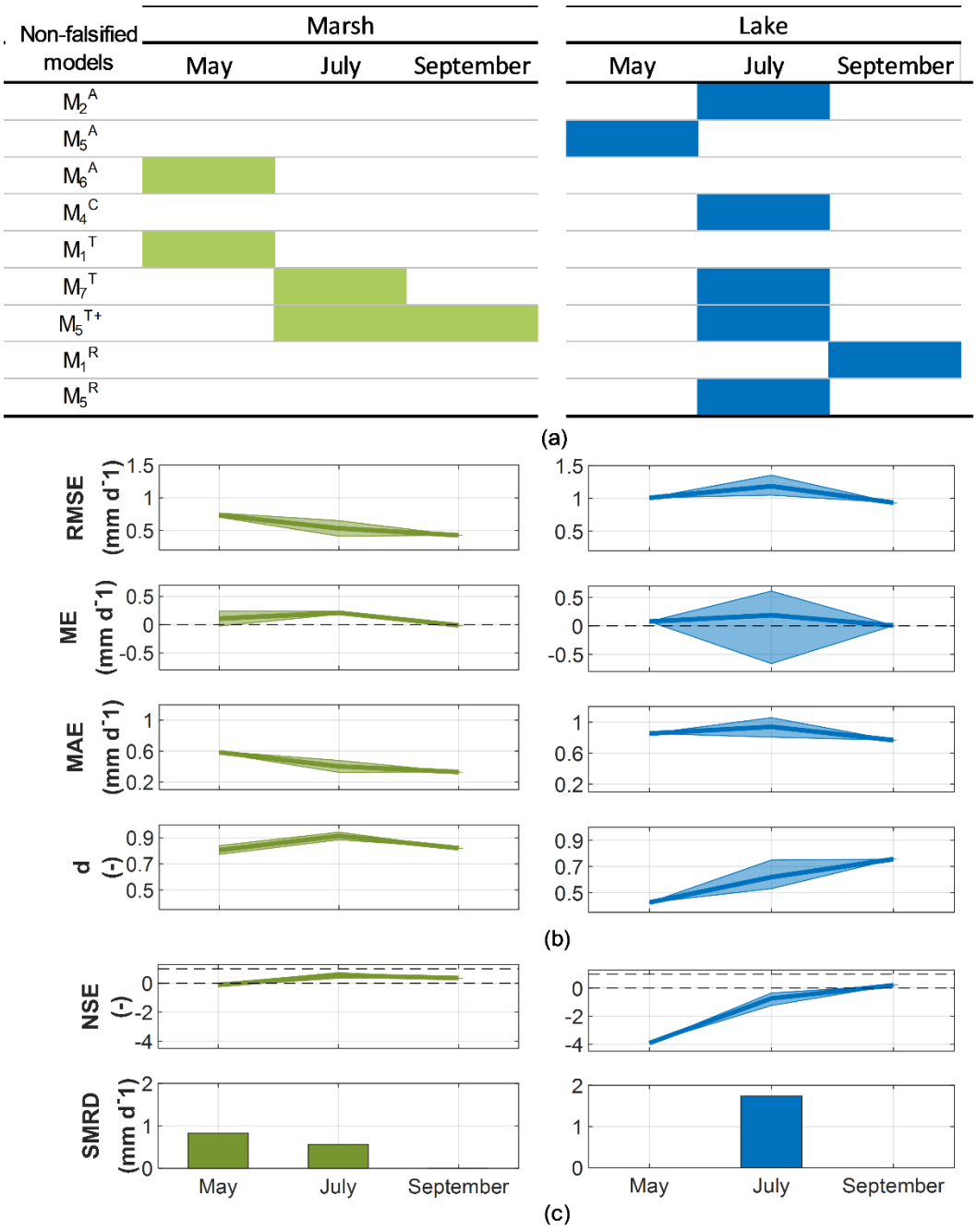

Figure 17. Benchmarking non-dominated sorting results in the marsh and lake illustrated by (a) a list of the non-falsified models at each month, (b) the associated GoF envelopes along with expected performances shown in solid lines, and (c) the associated monitoring measures NSE and SMRD.

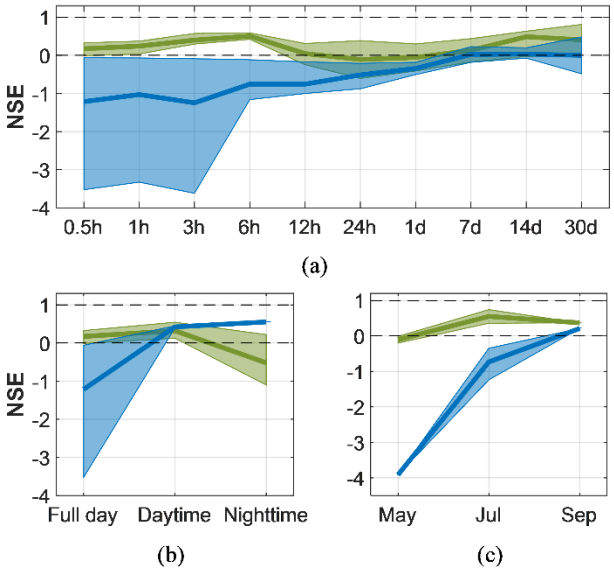

Figure 18. Comparison between performance of non-falsified models in the marsh and lake at different (a) time scales, (b) times of the day and (c) times of the season. In each panel, the solid line is the expected NSE by the non-falsified models, while the envelope represents the corresponding inter-model range of NSE values.

3.4 Discussion

Our study is indeed not the only benchmarking study available in the literature on lakes and wetlands. Thanks to so many pioneering works with which we can verify our finding. For instance, at the marsh site and at coarser times scales, our results are consistent with the previous findings on the role of wind speed and net radiation in driving ET (Jansen and Teuling, 2020; Priestley and Taylor, 1972; Sun and Song, 2008). Note that net radiation has a direct influence on surface temperature when heat storage is small; therefore, temperature becomes a proxy for ET. However, models solely based on temperature or radiation do not perform well as wind is an important driver of ET in waterbodies. Decreasing inter-model variability and improving RMSE at coarser timescales is also indicated in the literature (Jansen and Teuling, 2020; Liou and Kar, 2014).

At the like site due to the large heat storage and thermal inertia, the response to changes in net radiation (or its proxy air temperature) is not quick; however, extended fetches provide an ideal setting for wind to become the dominant driver of ET, which lead to several aerodynamic models being consistently dominant in many sub-daily timescales. This is in agreement with earlier studies (Jansen and Teuling, 2020; Přibáň and Ondok, 1985; Rosenberry et al., 2007). Having said that, it should be noted the simulation performance is extremely poor in the lake at time scales finer than weekly. This points at the importance of thermal inertia in driving ET at the lake.

Using the results provided in Section 4, we can intercompare the skills of empirical models in the marsh and the lake. Figure 18 shows this analysis. The base results related to this intercomparison

are already presented in Figure 14 to Figure 17. Up to 12-hour, the non-falsified ET models are strictly more skillfull in the marsh than the lake, meaning that the lowest performance of the non-falsified models in the marsh is higher than the best performance of those in the lake. The expected NSE of non-falsified models are also higher in the marsh across all timescales considered. Similarly considering different periods of the growing season, again the skills of non-falsified models are strictly higher in the marsh compared to the lake. Considering different diurnal segments, modelling performance is again strictly higher in the marsh considering full days. During daytime and nighttime individually, however, the skill of non-falsified models becomes comparable and even strictly better than the performance of non-falsified models in the marsh. This might be due to different thermal behavior of the lake as it switches between day and night from being the sink to the source of heat (Gan and Liu, 2020; Nordbo et al., 2011). This may prevent simple empirical models to consistently capture ET with the same skill during full days.

To have a better understanding of errors and corresponding microclimatic conditions, we look directly at the error signal, considering $Error = ET_{simulated} - ET_{measured}$. Figure 19 shows the timeseries of the error of the first-rank models at half-hourly to biweekly timescales in the marsh (left) and the lake (right). These error envelopes correspond to the non-falsified models presented in Figure 14 and Figure 15 for the marsh and the lake, respectively. As it is clear, errors are higher and more variable at finer timescales. Error envelopes are generally wider in the lake than in the marsh, except in weekly and biweekly timescales. Magnitudes of error are also higher in the lake, where ET is overestimated in the beginning and underestimated in the end of the season. Large errors in lake were also witnessed in Section 4 by expected NSE values being negative up to weekly timescale, which can be attributed to the lake's heat storage (Gan and Liu, 2020). Large errors in the marsh are observed in late May as well as mid- June and mid-August, coinciding with high temperature peaks, prolonged periods with high net radiation and no precipitation – see Figure 20. In such condition, energy needed for ET is available; however, the non-falsified ET models overestimate the observed ET by up to 4 mm/day. This may be due to the stomata closure, preventing excessive drying of plants (Collatz et al., 1991), not considered explicitly in ET models.

To have a better look at the skills of ET models across times of the day, we also analyze the relative error signal for non-falsified models during daytime and nighttime – see Figure 21, showing higher uncertainty in estimating ET signal in the marsh than the lake in both times of a day. A closer look at the error and uncertainty in ET signal in the marsh reveals poor skills coincide with high net radiation during time (overestimation) and windy nights (underestimation), respectively. Also as noted in Figure 18, the skill of non-falsified ET models during nighttime is strictly lower in the marsh than the lake. Comparable or even better modeling skills in the lake during daytime and nighttime, but strictly poorer skills during the full day, can show the trade-off in skills of empirical ET models between days and night and the fact that considered models are not able the capture the diurnal cycle of ET in the lake. This is another line of evidence for the limitations in the empirical ET models to capture ET signals from open water.

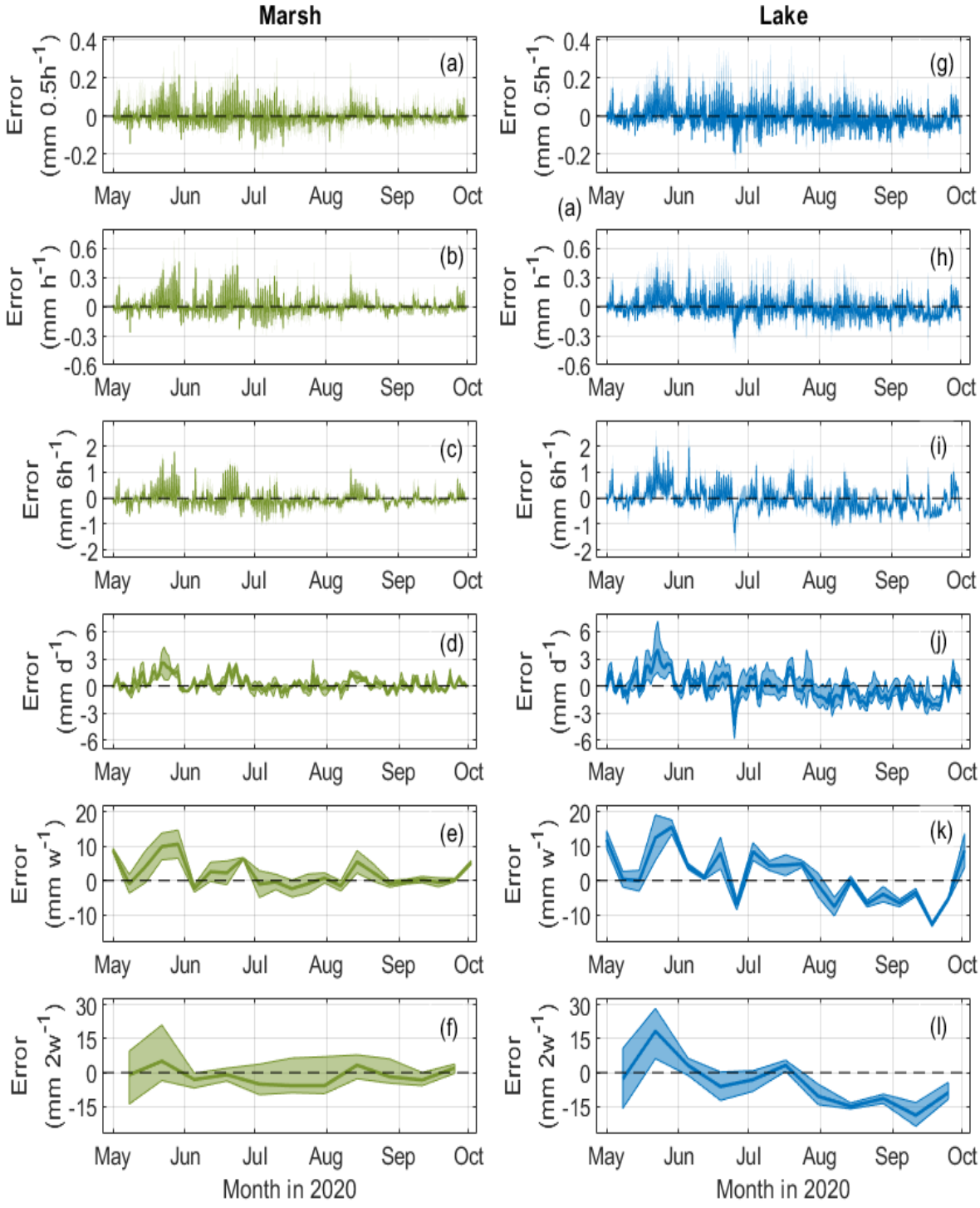

Figure 19. The envelope of errors in the non-dominated simulations of evapotranspiration in the marsh (left) and in the lake (right) during full days at 0.5 hour, 1 hour, 6 hours, 24 hours, 7 days and 14 days simulation steps, sorted from top to bottom respectively ($\boldsymbol{Error = ET_{modelled} - ET_{measured}}$). In each panel, the solid line is the expected simulation by the non-falsified models at the given location timescale.

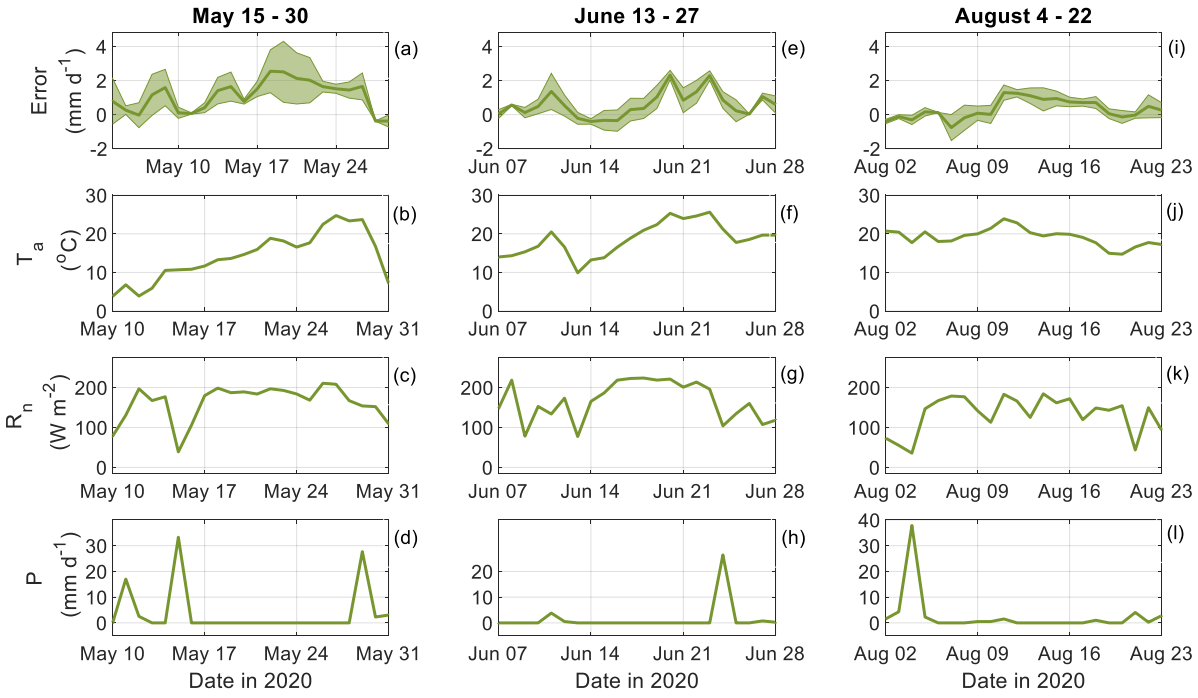

Figure 20. Peak errors during the 3 heatwave events in the marsh during the study period, where ET is overestimated after a prolonged period of high net radiation with no precipitation, leading to higher temperatures.

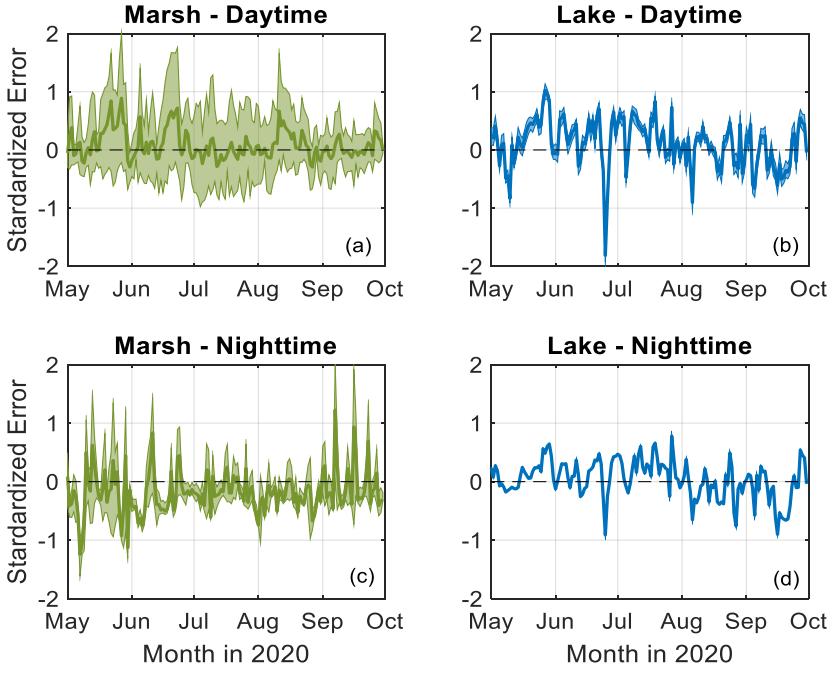

Figure 21**.** Half-hourly relative error of non-falsified models presented at a daily time scale during daytime and nighttime in the marsh and lake between May and October. The solid line represents the models' mean while the shaded area represents inter-model range.

4 Conclusion

Despite impacting a wide range of environmental and societal activities, quantifying ET is one of the grand challenges in the field on hydrology and hydroclimatology (Trenberth and Asrar, 2014). A truly physically-based model for ET requires coupling water, energy and carbon budgets, resulting into formation of complex models that often cannot be handled in practice. As a result, ET is still quantified mainly in relation to some conceptual variables such as PET that can be estimated using empirical equations derived from commonly measured meteorological variables. By putting earlier reviews and intercomparison studies in perspective (e.g., Rosenberry et al., 2007, 2004; Seiller and Anctil, 2016; Singh and Xu, 1997; Winter et al., 1995), we consider 40 empirical models to make the most comprehensive benchmarking study of empirical ET models in a lake-wetland due, located in Magog in Estrie region of Québec, in which not only the theoretical foundation for applying such models (i.e. unlimited water availability) is satisfied; but also, ET is measured using a fully consistent EC approach. We use a multi-objective ranking algorithm as a basis of our benchmarking and pursue this exercise through three experiments that assess the performance of considered models across a range of timescales, time of day and seasonal segments.

Our findings shed light on the complexities associated with modeling ET using empirical models in lakes and wetland. We show that in majority of comparison cases, there is no single ET model that can dominate over all other models. Having said that, some general patterns can be seen. For instance, in the marsh site and from 1- to 6-hour, the non-falsified models mainly include aerodynamic and combination models, indicating the importance of radiative and wind forcing in driving ET. At longer time scales, the non-falsified models mainly consist of aerodynamic and temperature-hybrid models. In the lake and at finer scales, ET is best captured by aerodynamic models, whereas temperature-based and radiation models dominate other model types in coarser timescales. In both sites, error envelops are wider and more variant at finer timescales; and inter-model variability decreases by moving from finer to coarser timescales. In the marsh, we have observed that the most versatile models across time scales were M_2^A, Carpenter (1888), M_6^A, McMillan (1971), M_3^C, Kimberley-Penman (Wright, 1982) and M_5^{T+}, Stephens-Stewart (1963). In the lake, sub-daily time scales are often dominated by aerodynamic models, while supra-daily time scales are dominated by temperature- and radiation-based models; overall, M_1^T, Hamon's (1963) equation was the most versatile, being always dominant except at the 2-week time scale. While the exact dominant models can be consulted for each time scale, time of the day and time of the growing season in Chapter 3, Table 11 below summarizes for each site the models which were the most often dominant.

Table 11: Summary of most dominant evapotranspiration models

Landscape	Model	0.5h – 12h	12h – 3-day	1-week – 1-month	Full day	Daytime	Nighttime
Marsh	McMillan (M_6^A)		✔	✔	✔	✔	✔
	Kimberly-Penman (M_3^C)	✔			✔	✔	
Lake	Hamon (M_1^T)	✔	✔	✔	✔	✔	✔

As far as the comparison between the skills of the continuous ET models are concerned, the expected NSE of non-falsified models are consistently higher in the marsh and across all timescales considered. Within different periods of the growing season, again the skills of non-falsified models are strictly higher and associated with less uncertainty in the marsh. Continuous ET simulations in the lake remain practically non-informative in timescale finer than weekly, as expected NSE of non-falsified models remain negative. Magnitudes of error are also higher in the lake, where ET is overestimated in the beginning and underestimated in the end of the growing season.

However, when ET models are ranked separately in daytime and nighttime, the skill of non-falsified models in the marsh and the lake becomes comparable, and even strictly better in the lake. The uncertainty is also substantially higher in the marsh than the lake in both times of day, particularly during daytime. When shifting from day time and full days to night time, we observed a shift towards more wind-based models which is consistent with the negligible net radiation during the night. In the lake, both daytime and nighttime ET are better modelled by temperature-based equations, with Hamon's equation being dominant across all times of the day. An important detail to observe is that the dominant temperature-based equations observed in the lake use day length as input, which is a proxy of average solar radiation, and Thornthwaite's equation is based on long-term records of air temperature. An interesting future step would be to attempt to create an unprecedented equation using wind speed, which is a known strong driver of lake evaporation, along with day length, which has demonstrated Based on our observations of the error signal, we argue that capturing diurnal and seasonal dynamics of ET in the lake requires more physically-based models that can take into the account the thermal role of water stored in the lake.

Large errors in the marsh across different temporal scales coincide with high temperature peaks, prolonged periods with high net radiation and no precipitation. These errors may be associated to stomata closure, which is not represented in empirical ET models. In addition, One known source of uncertainty in ET estimation during the night is condensation (Cuxart et al., 2019; Liu et al., 2018), which is not seen in any of the ET models. We suggest better representations of plant functions and physiology to account for ET from wetlands in the development of future models. This requires a leap to combine the fields of geophysics with biology.

Although the Cherry River Marsh and Lake Memphremagog are located in the same local climate, we have observed that their measured ET differs mainly due to differences in presence of

vegetation and possibly in heat storage capacity. However, our understanding of the effect of heat storage and transpiration on ET is one of the grand challenges of the decade according to GEWEX, and additional studies specifically investigating these effects are warranted. One interesting observation was that during daytime and nighttime, when lakes are best modelled, the two most dominant models contained the parameter of day length. Among existing equations, day length is only combined with temperature or radiation, but never with wind speed (Djaman et al., 2015; Sartori, 2000; Seiller and Anctil, 2016; Shuttleworth, 2007). Recall that day length is calculated as a function of geographical location and time of the year, and is therefore a proxy of long-term temperature and radiation –such equations are ideally calibrated based on many years of data to improve their coefficient's representativeness. Therefore, it would be interesting to investigate the combination of day length with wind speed which represent the two fundamental evapotranspiration drivers (free and forced evaporation) in a very simple formulation.

An alternative method of estimating evapotranspiration is through the use of integrated numerical models coupling land-atmosphere processes instead of empirical models. In such case, water balance and energy balance processes are also coupled using partial differential equations and may better represent heat storage. However, at the same time this adds another level of uncertainty due to additional modelling assumptions which is discussed in other works, and partially explains the limited use of numerical models in the literature (Courault et al., 2005). In addition, existing numerical models attempting to estimate evapotranspiration make use of empirical models somewhere in their process – for example Hostetler and Bartlein's numerical model (Hostetler and Bartlein, 1990; Lenters et al., 2005), which uses the Harbeck equation to estimate ET based on temperature, relative humidity and wind speed. Other models are available, but this coupling between land-atmosphere has proved more challenging than empirical models (Sharma et al., 2018).

Last but not the least, under climate change conditions, better understanding of ET from wetlands and lakes is essential for understanding extremes, whether quantifying natural or anthropogenic droughts (see AghaKouchak et al., 2021), or understanding and simulating heavy convective precipitation is concerned (Coppola et al., 2020; Sillmann et al., 2017). Convective precipitation is strongly related to extreme weather events such as flooding and tornadoes (Prein et al., 2020), and will be stronger in a warmer climate (Peleg et al., 2018; Yin et al., 2018). We hope our study can contribute into revealing the state of modeling ET from waterbodies and pave the way for development of more advanced empirical and/or physically-based ET models. In the context of a changing climate, one might ask what effect climate change may have on the parameterization of evapotranspiration models. It is important to first clarify the distinction between the representation of physics in models, and evapotranspiration physics itself. The former is dependent on our capacity to represent reality, which improves with time due to scientific advances (Sartori, 2000; Shuttleworth, 2007), while the latter is fundamental and unchanging. The physics of evapotranspiration are not expected to change, but the observed historical changes in forcing variables such as temperature and other meteorological variables are (Hartmann et al., 2013; Seneviratne et al., 2006), hence affecting evapotranspiration. Consequently, when the physical representation of an evapotranspiration variable is proxied by a statistically created coefficient,

such coefficients would change. A future quantitative investigation could determine the sensitivity of existing equations to expected changes in main variables, such as an increase of 1ºC, 2ºC, 3ºC and 4ºC in air temperature.

As described in previous chapters, Eddy Covariance processing steps determine the final measurements of evapotranspiration. Consequently, the calibration of models is dependent on processing steps, which have been improving over time during the last decades (Seiller and Anctil, 2016; Shuttleworth, 2007). In addition, existing equations have been calibrated based on different measurement techniques such as pan evaporation, lysimeter, Eddy Covariance and other methods. Consequently, sensitivity analyses are warranted to better understand the impacts of different measurement techniques and processing techniques, and existing studies already investigate this question and can guide the reader to previous strategies used in similar efforts (Aubinet et al., 2012; Gebler et al., 2015; Mauder and Foken, 2006; Papale et al., 2006).

Previous benchmarking studies have attempted to determine best models in wetlands and lakes. In wetlands, Rosenberry et al. (2003) compare 12 empirical models and conclude that the Priestley & Taylor (radiation) and DeBruin-Keijman are best during full days using the means and standard deviations of errors as benchmarking measures with approximately 0.1 mm/day of error at a monthly time scale, which is almost identical to the measure we have in the marsh. In Valipour's review (2015), 40 previous studies are considered, where a total of 31 different models are considered dominant, showing the large heterogeneity in conclusions. Only 9 of these 40 studies considered 5 or more models in their benchmarking. In lakes, Rosenberry et al. (2005) compare 15 empirical models and conclude that the Priestley-Taylor, DeBruin-Keijman and Penman (combination) equations are best with a mean error of 0.2 mm/day at a monthly time scale, while we report the same goodness of fit measure at almost 0 mm/day. As mentioned, the wide heterogeneity in the literature with respect to measurement type, goodness-of-fit measure used, and equations selected for the benchmarking exercise make it even more difficult to extract general insights. The abovementioned Rosenberry's two studies for marshes and lakes, for example, are both based on Bowen Ratio Energy Balance estimations as the ET benchmarking measurement dataset, which biases results into including an overwhelming number of dominant radiation-based equations in both sites. A more standardized approach should be implemented by authors to add uniformity and improve consensus.

In retrospect, adopting a robust intercomparison approach with a large number of models and assessing several Goodness-of-Fit measures simultaneously allows to eliminate the methodological uncertainty which is present in the literature due to the selective use of specific equations and Goodness-of-Fit measures by different studies. Also, the selected goodness-of-fit measures were also chosen based on their complementary representation of different parts of the error signal. For example, the mean average error is better representative of the center of the error distributions while the root mean square error exacerbates the importance of very large and very small errors, consequently being better representative of tails. To facilitate communication of ET benchmarking studies in different marshes and lakes, a non-dominated sorting framework can be implemented systematically to achieve higher consensus about best models in ET literature.

These investigations have marked the beginning of a series of microclimatological investigations at the Cherry River Marsh and Lake Memphremagog by Concordia University. From an academic perspective, pursuing research in these two landscapes will allow to deepen our understanding about land-atmospheric interactions of marshes and lakes, which are gaining societal importance due to our changing climate as discussed. From a societal perspective, the City of Magog is formally committed to adapting itself to be resilient to future climate through its Climate Change Adaptation Plan (Côté and Pouliot, 2021). In this plan, heatwaves, floods, droughts, freeze and thaw patterns and forest fires are identified as direct impacts to their community, which are all potential research topics with global significance and local benefits. The mitigation effects by the marsh and lake related to these risks can be studied and expanded to other regional water bodies. Now that an evapotranspiration portrait is prepared and recommended equations are provided by modelling, the establishment of more accurate hydrological models is also possible; this work is currently being initiated by another graduate student and will allow to improve water management plans. This is especially important considering that Lake Memphremagog is in a transboundary watershed, where international collaboration between Canada and the United States is required to ensure that water quantity and quality is guaranteed on both sides through adequate management.

5 References

AghaKouchak, A., Mirchi, A., Madani, K., Baldassarre, G.D., Nazemi, A., Alborzi, A., Anjileli, H., Azarderakhsh, M., Chiang, F., Hassanzadeh, E., Huning, L.S., Mallakpour, I., Martinez, A., Mazdiyasni, O., Moftakhari, H., Norouzi, H., Sadegh, M., Sadeqi, D., Loon, A.F.V., Wanders, N., 2021. Anthropogenic Drought: Definition, Challenges, and Opportunities. Reviews of Geophysics 59, e2019RG000683. https://doi.org/10.1029/2019RG000683

Alavi, N., Warland, J.S., Berg, A.A., 2006. Filling gaps in evapotranspiration measurements for water budget studies: Evaluation of a Kalman filtering approach. Agricultural and Forest Meteorology 141, 57–66. https://doi.org/10.1016/j.agrformet.2006.09.011

Allen, R.G., Pereira, L.S. (Eds.), 1998. Crop evapotranspiration: guidelines for computing crop water requirements, FAO irrigation and drainage paper. FAO, Rome.

Allen, R.G., Pereira, L.S., Howell, T.A., Jensen, M.E., 2011. Evapotranspiration information reporting: I. Factors governing measurement accuracy. Agricultural Water Management 98, 899–920. https://doi.org/10.1016/j.agwat.2010.12.015

Anderson-Nichols & Company, Inc., 1978. Lake Memphremagog - Vermont - A Hydrologic and Hydraulic Analysis - The Capability and Procedure to Regulate Lake Memphremagog. New York District - Corps of Engineers.

Ashraf, B., Yazdani, R., Mousavi-Baygi, M., Bannayan, M., 2014. Investigation of temporal and spatial climate variability and aridity of Iran. Theor Appl Climatol 118, 35–46. https://doi.org/10.1007/s00704-013-1040-8

Ashraf, S., Nazemi, A., AghaKouchak, A., 2021. Anthropogenic drought dominates groundwater depletion in Iran. Sci Rep 11, 9135. https://doi.org/10.1038/s41598-021-88522-y

Aubinet, M., Vesala, T., Papale, D., 2012. Eddy covariance: a practical guide to measurement and data analysis. Springer Science & Business Media.

Bao, C., Xu, L., Goodman, E.D., Cao, L., 2017. A novel non-dominated sorting algorithm for evolutionary multi-objective optimization. Journal of Computational Science 23, 31–43. https://doi.org/10.1016/j.jocs.2017.09.015

Barry, R.G., Blanken, P.D., 2016. Microclimate and local climate. Cambridge University Press.

Bedient, P.B., Huber, W.C., Vieux, B.E., 2012. Hydrology and Floodplain Analysis, 5th ed. Pearson Upper Saddle River, NJ, USA.

Blanken, P., Rouse, W., Culf, A., Spence, C., Boudreau, L., Jasper, J., Kochtubajda, B., Schertzer, W., Marsh, P., Verseghy, D., 2000. Eddy covariance measurements of evaporation from Great Slave Lake, Northwest Territories, Canada. WATER RESOURCES RESEARCH 36, 1069–1077.

Bolund, P., Hunhammar, S., 1999. Ecosystem services in urban areas. Ecological Economics 29, 293–301. https://doi.org/10.1016/S0921-8009(99)00013-0

Bormann, H., Holländer, H.M., Blume, T., Buytaert, W., Chirico, G.B., Exbrayat, J.-F., Gustafsson, D., Hölzel, H., Kraft, P., Krauße, T., others, 2011. Comparative discharge

prediction from a small artificial catchment without model calibration: Representation of initial hydrological catchment development. Die Bodenkultur 62, 23–29.

Bourdeau-Goulet, S.-C., Hassanzadeh, E., 2021. Comparisons Between CMIP5 and CMIP6 Models: Simulations of Climate Indices Influencing Food Security, Infrastructure Resilience, and Human Health in Canada. Earth's Future 9, e2021EF001995. https://doi.org/10.1029/2021EF001995

Burba, G., 2013. Eddy covariance method for scientific, industrial, agricultural and regulatory applications: A field book on measuring ecosystem gas exchange and areal emission rates. LI-Cor Biosciences.

Campbell Scientific Inc., 2007. LoggerNet Instruction Manual Version 3.4.

Carpenter, 1888. Annual Report - Colorado Agricultural Experiment Station, Colorado State University, Colorado Agricultural Experiment Station. Colorado State University.

Cheng, R., He, C., Jin, Y., Yao, X., 2018. Model-based evolutionary algorithms: a short survey. Complex Intell. Syst. 4, 283–292. https://doi.org/10.1007/s40747-018-0080-1

Chu, R., Li, M., Islam, A.R.M.T., Fei, D., Shen, S., 2019. Attribution analysis of actual and potential evapotranspiration changes based on the complementary relationship theory in the Huai River basin of eastern China. International Journal of Climatology 39, 4072–4090. https://doi.org/10.1002/joc.6060

Clement, R.J., 2004. Mass and energy exchange of a plantation forest in Scotland using micrometeorological methods (PhD Thesis). University of Edinburgh.

Collatz, G.J., Ball, J.T., Grivet, C., Berry, J.A., 1991. Physiological and environmental regulation of stomatal conductance, photosynthesis and transpiration: a model that includes a laminar boundary layer. Agricultural and Forest Meteorology 54, 107–136. https://doi.org/10.1016/0168-1923(91)90002-8

Coppola, E., Sobolowski, S., Pichelli, E., Raffaele, F., Ahrens, B., Anders, I., Ban, N., Bastin, S., Belda, M., Belusic, D., Caldas-Alvarez, A., Cardoso, R.M., Davolio, S., Dobler, A., Fernandez, J., Fita, L., Fumiere, Q., Giorgi, F., Goergen, K., Güttler, I., Halenka, T., Heinzeller, D., Hodnebrog, Ø., Jacob, D., Kartsios, S., Katragkou, E., Kendon, E., Khodayar, S., Kunstmann, H., Knist, S., Lavín-Gullón, A., Lind, P., Lorenz, T., Maraun, D., Marelle, L., van Meijgaard, E., Milovac, J., Myhre, G., Panitz, H.-J., Piazza, M., Raffa, M., Raub, T., Rockel, B., Schär, C., Sieck, K., Soares, P.M.M., Somot, S., Srnec, L., Stocchi, P., Tölle, M.H., Truhetz, H., Vautard, R., de Vries, H., Warrach-Sagi, K., 2020. A first-of-its-kind multi-model convection permitting ensemble for investigating convective phenomena over Europe and the Mediterranean. Clim Dyn 55, 3–34. https://doi.org/10.1007/s00382-018-4521-8

Côté, J.-N., Pouliot, J., 2021. Plan d'adaptation aux changements climatiques pour la Ville de Magog. Ville de Magog.

Courault, D., Seguin, B., Olioso, A., 2005. Review on estimation of evapotranspiration from remote sensing data: From empirical to numerical modeling approaches. Irrigation and Drainage Systems 19, 223–249. https://doi.org/10.1007/s10795-005-5186-0

Cuxart, J., Verhoef, A., Marthews, T.R., Evans, J., 2019. Current Challenges in Evapotranspiration Determination. GEWEX Quarterly 29.

Dalton, J., 1802. Experimental essays on the constitution of mixed gases; on the force of steam or vapor from water and other liquids in different temperatures, both in a Torricellian vacuum and in air; on evaporation and on the expansion of gases by heat. Mem. Manchester Liter. and Phil. Soc 5, 535–602.

de Bruin, H.A.R., 1978. A Simple Model for Shallow Lake Evaporation. Journal of Applied Meteorology and Climatology 17, 1132–1134. https://doi.org/10.1175/1520-0450(1978)017<1132:ASMFSL>2.0.CO;2

Deb, K., Pratap, A., Agarwal, S., Meyarivan, T., 2002. A fast and elitist multiobjective genetic algorithm: NSGA-II. IEEE Transactions on Evolutionary Computation 6, 182–197. https://doi.org/10.1109/4235.996017

Dingman, S.L., 2015. Physical hydrology, 3rd ed. Waveland press.

Djaman, K., Balde, A.B., Sow, A., Muller, B., Irmak, S., N'Diaye, M.K., Manneh, B., Moukoumbi, Y.D., Futakuchi, K., Saito, K., 2015. Evaluation of sixteen reference evapotranspiration methods under sahelian conditions in the Senegal River Valley. Journal of Hydrology: Regional Studies 3, 139–159. https://doi.org/10.1016/j.ejrh.2015.02.002

Doorenbos, J., Pruitt, W., 1977. Crop water requirements. Irrigation and drainage paper (FAO) 24.

dos Santos, C.A.C., Mariano, D.A., das Chagas A. do Nascimento, F., da C. Dantas, F.R., de Oliveira, G., Silva, M.T., da Silva, L.L., da Silva, B.B., Bezerra, B.G., Safa, B., de S. Medeiros, S., Neale, C.M.U., 2020. Spatio-temporal patterns of energy exchange and evapotranspiration during an intense drought for drylands in Brazil. International Journal of Applied Earth Observation and Geoinformation 85, 101982. https://doi.org/10.1016/j.jag.2019.101982

Drexler, J., Snyder, R., Spano, D., Paw, K., 2004. A review of models and micrometeorological methods used to estimate wetland evapotranspiration. HYDROLOGICAL PROCESSES 18, 2071–2101. https://doi.org/10.1002/hyp.1462

ECCC, 2020. Historical Climate Data - Climate [WWW Document]. Environment and Climate Change Canada. URL https://climate.weather.gc.ca/index_e.html (accessed 9.29.20).

Emilsson, T., Sang, Å., 2017. Impacts of climate change on urban areas and nature-based solutions for adaptation. Nature-based Solutions to Climate Change Adaptation in Urban Areas.

Falge, E., Baldocchi, D., Olson, R., Anthoni, P., Aubinet, M., Bernhofer, C., Burba, G., Ceulemans, R., Clement, R., Dolman, H., Granier, A., Gross, P., Grünwald, T., Hollinger, D., Jensen, N.-O., Katul, G., Keronen, P., Kowalski, A., Lai, C.T., Law, B.E., Meyers, T., Moncrieff, J., Moors, E., Munger, J.W., Pilegaard, K., Rannik, Ü., Rebmann, C., Suyker, A., Tenhunen, J., Tu, K., Verma, S., Vesala, T., Wilson, K., Wofsy, S., 2001. Gap filling strategies for defensible annual sums of net ecosystem exchange. Agricultural and Forest Meteorology 107, 43–69. https://doi.org/10.1016/S0168-1923(00)00225-2

Fan, S.-M., Wofsy, S.C., Bakwin, P.S., Jacob, D.J., Fitzjarrald, D.R., 1990. Atmosphere-biosphere exchange of CO2 and O3 in the central Amazon Forest. Journal of Geophysical Research: Atmospheres 95, 16851–16864. https://doi.org/10.1029/JD095iD10p16851

Finnigan, J.J., Clement, R., Malhi, Y., Leuning, R., Cleugh, H.A., 2003. A Re-Evaluation of Long-Term Flux Measurement Techniques Part I: Averaging and Coordinate Rotation. Boundary-Layer Meteorology 107, 1–48. https://doi.org/10.1023/A:1021554900225

Fitzgerald, D., 1886. Evaporation. Van Nostrand's Engineering Magazine (1879-1886) 35, 41.
Foken, T., 2017. Micrometeorology. Springer Berlin Heidelberg, Berlin, Heidelberg. https://doi.org/10.1007/978-3-642-25440-6
Foken, T., 2008. The Energy Balance Closure Problem: An Overview. Ecological Applications 18, 1351–1367. https://doi.org/10.1890/06-0922.1
Foken, T., Göockede, M., Mauder, M., Mahrt, L., Amiro, B., Munger, W., 2004. Post-Field Data Quality Control, in: Lee, X., Massman, W., Law, B. (Eds.), Handbook of Micrometeorology: A Guide for Surface Flux Measurement and Analysis, Atmospheric and Oceanographic Sciences Library. Springer Netherlands, Dordrecht, pp. 181–208. https://doi.org/10.1007/1-4020-2265-4_9
Foken, Th., Wichura, B., 1996. Tools for quality assessment of surface-based flux measurements. Agricultural and Forest Meteorology 78, 83–105. https://doi.org/10.1016/0168-1923(95)02248-1
Gan, G., Liu, Y., 2020. Heat Storage Effect on Evaporation Estimates of China's Largest Freshwater Lake. Journal of Geophysical Research: Atmospheres 125, e2019JD032334. https://doi.org/10.1029/2019JD032334
Gebler, S., Hendricks Franssen, H.-J., Pütz, T., Post, H., Schmidt, M., Vereecken, H., 2015. Actual evapotranspiration and precipitation measured by lysimeters: a comparison with eddy covariance and tipping bucket. Hydrology and Earth System Sciences 19, 2145–2161. https://doi.org/10.5194/hess-19-2145-2015
Ghiasi, H., Pasini, D., Lessard, L., 2011. A non-dominated sorting hybrid algorithm for multi-objective optimization of engineering problems. Engineering Optimization 43, 39–59. https://doi.org/10.1080/03052151003739598
Gunawardhana, M., Silvester, E., Jones, O.A.H., Grover, S., 2021. Evapotranspiration and biogeochemical regulation in a mountain peatland: insights from eddy covariance and ionic balance measurements. Journal of Hydrology: Regional Studies 36, 100851. https://doi.org/10.1016/j.ejrh.2021.100851
Guo, D., Westra, S., Maier, H.R., 2016. An R package for modelling actual, potential and reference evapotranspiration. Environmental Modelling & Software 78, 216–224. https://doi.org/10.1016/j.envsoft.2015.12.019
Guo, Y., Zhang, Y., Ma, N., Xu, J., Zhang, T., 2019. Long-term changes in evaporation over Siling Co Lake on the Tibetan Plateau and its impact on recent rapid lake expansion. Atmospheric Research 216, 141–150. https://doi.org/10.1016/j.atmosres.2018.10.006
Gurjanov, A., Zubkovskij, S., Fedorov, M., 1984. Mnogokanalnaja avtomatizirovannaja sistema obrabotki signalov na baze EVM (Automatic multi-channel system for signal analysis with electronic data processing). Geod Geophys Veröff 2, 26.
Harding, K.J., Snyder, P.K., 2012a. Modeling the Atmospheric Response to Irrigation in the Great Plains. Part I: General Impacts on Precipitation and the Energy Budget. Journal of Hydrometeorology 13, 1667–1686. https://doi.org/10.1175/JHM-D-11-098.1
Harding, K.J., Snyder, P.K., 2012b. Modeling the Atmospheric Response to Irrigation in the Great Plains. Part II: The Precipitation of Irrigated Water and Changes in Precipitation Recycling. Journal of Hydrometeorology 13, 1687–1703. https://doi.org/10.1175/JHM-D-11-099.1

Hartmann, D.L., Tank, A.M.G.K., Rusticucci, M., Alexander, L.V., Brönnimann, S., Charabi, Y.A.R., Dentener, F.J., Dlugokencky, E.J., Easterling, D.R., Kaplan, A., Soden, B.J., Thorne, P.W., Wild, M., Zhai, P., 2013. Observations: Atmosphere and surface. Climate Change 2013 the Physical Science Basis: Working Group I Contribution to the Fifth Assessment Report of the Intergovernmental Panel on Climate Change 159–254. https://doi.org/10.1017/CBO9781107415324.008

Harwell, G.R., 2012. Estimation of evaporation from open water - A review of selected studies, summary of U.S. Army Corps of Engineers data collection and methods, and evaluation of two methods for estimation of evaporation from five reservoirs in Texas (Report No. 2012–5202), Scientific Investigations Report. USGS, Reston, VA. https://doi.org/10.3133/sir20125202

Hassanzadeh, E., Elshorbagy, A., Nazemi, A., Jardine, T.D., Wheater, H., Lindenschmidt, K.-E., 2017. The ecohydrological vulnerability of a large inland delta to changing regional streamflows and upstream irrigation expansion. Ecohydrology 10, e1824. https://doi.org/10.1002/eco.1824

Hassanzadeh, E., Elshorbagy, A., Wheater, H., Gober, P., Nazemi, A., 2016. Integrating Supply Uncertainties from Stochastic Modeling into Integrated Water Resource Management: Case Study of the Saskatchewan River Basin. Journal of Water Resources Planning and Management 142, 05015006. https://doi.org/10.1061/(ASCE)WR.1943-5452.0000581

Heinesch, B., Yernaux, M., Aubinet, M., 2007. Some methodological questions concerning advection measurements: a case study. Boundary-Layer Meteorol 122, 457–478. https://doi.org/10.1007/s10546-006-9102-4

Herman, M.R., Nejadhashemi, A.P., Abouali, M., Hernandez-Suarez, J.S., Daneshvar, F., Zhang, Z., Anderson, M.C., Sadeghi, A.M., Hain, C.R., Sharifi, A., 2018. Evaluating the role of evapotranspiration remote sensing data in improving hydrological modeling predictability. Journal of Hydrology 556, 39–49. https://doi.org/10.1016/j.jhydrol.2017.11.009

Hojstrup, J., 1993. A statistical data screening procedure. Meas. Sci. Technol. 4, 153–157. https://doi.org/10.1088/0957-0233/4/2/003

Hostetler, S.W., Bartlein, P.J., 1990. Simulation of lake evaporation with application to modeling lake level variations of Harney-Malheur Lake, Oregon. Water Resour. Res. 26, 2603–2612. https://doi.org/10.1029/WR026i010p02603

International Joint Commission (IJC), 2019. International Joint Commission Lake Memphremagog Study Science and Policy Workshop.

Jansen, F.A., Teuling, A.J., 2020. Evaporation from a large lowland reservoir – (dis)agreement between evaporation models from hourly to decadal timescales. Hydrology and Earth System Sciences 24, 1055–1072. https://doi.org/10.5194/hess-24-1055-2020

Jensen, M.E., Burman, R.D., Allen, R.G., 1990. Evapotranspiration and Irrigation Water Requirements. American Society of Civil Engineers.

Jia, W., Yin, L., Zhang, M., Zhang, J., Zhang, X., Gu, X., Dong, J., 2021. Modified method for the estimation of groundwater evapotranspiration under very shallow water table conditions based on diurnal water table fluctuations. Journal of Hydrology 597, 126193. https://doi.org/10.1016/j.jhydrol.2021.126193

Kaimal, J., Finnigan, J., Derbyshire, S., 1994. Atmospheric boundary layer flows–Their structure and measurement. Oxford University Press.

Karimi, P., Bastiaanssen, W.G.M., 2015. Spatial evapotranspiration, rainfall and land use data in water accounting - Part 1: Review of the accuracy of the remote sensing data. Hydrology and Earth System Sciences 19, 507–532. https://doi.org/10.5194/hess-19-507-2015

Kljun, N., Calanca, P., Rotach, M.W., Schmid, H.P., 2015. A simple two-dimensional parameterisation for Flux Footprint Prediction (FFP). Geoscientific Model Development 8, 3695–3713. https://doi.org/10.5194/gmd-8-3695-2015

Kljun, N., Calanca, P., Rotach, M.W., Schmid, H.P., 2004. A Simple Parameterisation for Flux Footprint Predictions. Boundary-Layer Meteorology 112, 503–523. https://doi.org/10.1023/B:BOUN.0000030653.71031.96

Köppen, W., Geiger, R., 1936. Handbuch der klimatologie. Verlag von Gebrüder Borntraeger, Berlin.

LAMRAC, 2021. Conservation & mise en valeur [WWW Document]. L'Association du Marais de la Rivière aux Cerises. URL https://maraisauxcerises.com/conservation/o-conservation.php (accessed 6.11.21).

Lee, X., Massman, W., Law, B., 2004. Handbook of micrometeorology: a guide for surface flux measurement and analysis. Springer Science & Business Media.

Legates, D.R., McCabe Jr, G.J., 1999. Evaluating the use of "goodness-of-fit" measures in hydrologic and hydroclimatic model validation. Water resources research 35, 233–241. https://doi.org/10.1029/1998WR900018

Lenters, J.D., Kratz, T.K., Bowser, C.J., 2005. Effects of climate variability on lake evaporation: Results from a long-term energy budget study of Sparkling Lake, northern Wisconsin (USA). Journal of Hydrology 308, 168–195. https://doi.org/10.1016/j.jhydrol.2004.10.028

Li, Z.-L.(1, 2), Tang, R.(1, 2,3), Zhou, C.(1), Tang, B.(1), Bi, Y.(2, 5), Wan, Z.(4), Yan, G.(6), Zhang, X.(7), 2009. A review of current methodologies for regional Evapotranspiration estimation from remotely sensed data. Sensors 9, 3801–3853. https://doi.org/10.3390/s90503801

LI-COR Inc., 2019. EddyPro Software Instruction Manual V.07. LI-Cor Biosciences, Nebraska.

Liou, Y.-A., Kar, S.K., 2014. Evapotranspiration estimation with remote sensing and various surface energy balance algorithms-a review. Energies 7, 2821–2849. https://doi.org/10.3390/en7052821

Liu, H., Blanken, P.D., Weidinger, T., Nordbo, A., Vesala, T., 2011. Variability in cold front activities modulating cool-season evaporation from a southern inland water in the USA. Environ. Res. Lett. 6, 024022. https://doi.org/10.1088/1748-9326/6/2/024022

Liu, X., Xu, C., Zhong, X., Li, Y., Yuan, X., Cao, J., 2017. Comparison of 16 models for reference crop evapotranspiration against weighing lysimeter measurement. Agricultural Water Management 184, 145–155. https://doi.org/10.1016/j.agwat.2017.01.017

Liu, X., Xu, J., Yang, S., Zhang, J., Wang, Y., 2018. Vapor Condensation in Rice Fields and Its Contribution to Crop Evapotranspiration in the Subtropical Monsoon Climate of China. Journal of Hydrometeorology 19, 1043–1057. https://doi.org/10.1175/JHM-D-17-0201.1

Liu, X., Zhang, D., 2013. Trend analysis of reference evapotranspiration in Northwest China: The roles of changing wind speed and surface air temperature. Hydrological Processes 27, 3941–3948. https://doi.org/10.1002/hyp.9527

Lobell, D.B., Bala, G., Duffy, P.B., 2006. Biogeophysical impacts of cropland management changes on climate. Geophysical Research Letters 33. https://doi.org/10.1029/2005GL025492

Lott, R.B., Hunt, R.J., 2001. Estimating evapotranspiration in natural and constructed wetlands. Wetlands 21, 614–628. https://doi.org/10.1672/0277-5212(2001)021[0614:EEINAC]2.0.CO;2

Ma, N., Zhang, Y., Xu, C.-Y., Szilagyi, J., 2015. Modeling actual evapotranspiration with routine meteorological variables in the data-scarce region of the Tibetan Plateau: Comparisons and implications. Journal of Geophysical Research: Biogeosciences 120, 1638–1657. https://doi.org/10.1002/2015JG003006

Marie-Victorin, F., 1964. Flore Laurentienne. Les Presses de l'Université de Montréal, Montréal.

Mauder, M., Foken, T., 2006. Impact of post-field data processing on eddy covariance flux estimates and energy balance closure. Meteorologische Zeitschrift 597–609. https://doi.org/10.1127/0941-2948/2006/0167

McColl, K.A., 2020. Practical and Theoretical Benefits of an Alternative to the Penman-Monteith Evapotranspiration Equation. Water Resources Research 56, e2020WR027106. https://doi.org/10.1029/2020WR027106

Metcalfe, R.A., Petzold, H., Luce, J.J., Buttle, J.M., 2019. Evaluating seasonal and regional calibration of temperature-based methods for estimating potential evaporation in Ontario. Canadian Water Resources Journal / Revue canadienne des ressources hydriques 44, 2–21. https://doi.org/10.1080/07011784.2018.1493399

Minville, M., Cartier, D., Guay, C., Leclaire, L.-A., Audet, C., Le Digabel, S., Merleau, J., 2014. Improving process representation in conceptual hydrological model calibration using climate simulations. Water Resources Research 50, 5044–5073.

Moncrieff, J., Clement, R., Finnigan, J., Meyers, T., 2004. Averaging, Detrending, and Filtering of Eddy Covariance Time Series, in: Lee, X., Massman, W., Law, B. (Eds.), Handbook of Micrometeorology: A Guide for Surface Flux Measurement and Analysis, Atmospheric and Oceanographic Sciences Library. Springer Netherlands, Dordrecht, pp. 7–31. https://doi.org/10.1007/1-4020-2265-4_2

Moncrieff, J.B., Massheder, J.M., de Bruin, H., Elbers, J., Friborg, T., Heusinkveld, B., Kabat, P., Scott, S., Soegaard, H., Verhoef, A., 1997. A system to measure surface fluxes of momentum, sensible heat, water vapour and carbon dioxide. Journal of Hydrology, HAPEX-Sahel 188–189, 589–611. https://doi.org/10.1016/S0022-1694(96)03194-0

Monteith, J.L., 1965. Evaporation and environment. Symposia of the Society for Experimental Biology 19, 205–234.

Nakayama, T., Shankman, D., 2013. Evaluation of uneven water resource and relation between anthropogenic water withdrawal and ecosystem degradation in Changjiang and Yellow River basins. Hydrological Processes 27, 3350–3362. https://doi.org/10.1002/hyp.9835

Nazemi, A., Chan, A.H., Yao, X., 2008. Selecting representative parameters of rainfall-runoff models using multi-objective calibration results and a fuzzy clustering algorithm, in: BHS 10th National Hydrology Symposium, Exeter, UK. pp. 13–20.

Nazemi, A., Wheater, H.S., 2015a. On inclusion of water resource management in Earth system models - Part 1: Problem definition and representation of water demand. Hydrology and Earth System Sciences 19, 33–61. https://doi.org/10.5194/hess-19-33-2015

Nazemi, A., Wheater, H.S., 2015b. On inclusion of water resource management in Earth system models - Part 2: Representation of water supply and allocation and opportunities for improved modeling. Hydrology and Earth System Sciences 19, 63–90. https://doi.org/10.5194/hess-19-63-2015

Nazemi, A., Yao, X., Chan, A.H., 2006. Extracting a set of robust Pareto-optimal parameters for hydrologic models using NSGA-II and SCEM, in: 2006 IEEE International Conference on Evolutionary Computation. IEEE, pp. 1901–1908.

Nazemi, A., Zaerpour, M., Hassanzadeh, E., 2020. Uncertainty in Bottom-Up Vulnerability Assessments of Water Supply Systems due to Regional Streamflow Generation under Changing Conditions. Journal of Water Resources Planning and Management 146, 04019071. https://doi.org/10.1061/(ASCE)WR.1943-5452.0001149

Nazemi, A.-R., Akbarzadeh, M.-R., Hosseini, S.-M., 2002. Fuzzy-stochastic linear programming in water resources engineering, in: 2002 Annual Meeting of the North American Fuzzy Information Processing Society Proceedings. NAFIPS-FLINT 2002 (Cat. No. 02TH8622). Presented at the 2002 Annual Meeting of the North American Fuzzy Information Processing Society Proceedings. NAFIPS-FLINT 2002 (Cat. No. 02TH8622), pp. 227–232. https://doi.org/10.1109/NAFIPS.2002.1018060

Nordbo, A., Launiainen, S., Mammarella, I., Leppäranta, M., Huotari, J., Ojala, A., Vesala, T., 2011. Long-term energy flux measurements and energy balance over a small boreal lake using eddy covariance technique. Journal of Geophysical Research: Atmospheres 116. https://doi.org/10.1029/2010JD014542

Novick, K.A., Biederman, J.A., Desai, A.R., Litvak, M.E., Moore, D.J.P., Scott, R.L., Torn, M.S., 2018. The AmeriFlux network: A coalition of the willing. Agricultural and Forest Meteorology 249, 444–456. https://doi.org/10.1016/j.agrformet.2017.10.009

Oke, T.R., 1987. Boundary Layer Climates, 2nd ed. Taylor & Francis.

Pan, S., Pan, N., Tian, H., Friedlingstein, P., Sitch, S., Shi, H., Arora, V.K., Haverd, V., Jain, A.K., Kato, E., Lienert, S., Lombardozzi, D., Nabel, J.E.M.S., Ottlé, C., Poulter, B., Zaehle, S., Running, S.W., 2020. Evaluation of global terrestrial evapotranspiration using state-of-the-art approaches in remote sensing, machine learning and land surface modeling. Hydrology and Earth System Sciences 24, 1485–1509. https://doi.org/10.5194/hess-24-1485-2020

Papale, D., Reichstein, M., Aubinet, M., Canfora, E., Bernhofer, C., Kutsch, W., Longdoz, B., Rambal, S., Valentini, R., Vesala, T., Yakir, D., 2006. Towards a standardized processing of Net Ecosystem Exchange measured with eddy covariance technique: algorithms and uncertainty estimation. Biogeosciences 3, 571–583. https://doi.org/10.5194/bg-3-571-2006

Paul-Limoges, E., Wolf, S., Schneider, F.D., Longo, M., Moorcroft, P., Gharun, M., Damm, A., 2020. Partitioning evapotranspiration with concurrent eddy covariance measurements in a mixed forest. Agricultural and Forest Meteorology 280, 107786. https://doi.org/10.1016/j.agrformet.2019.107786

Peel, M.C., Finlayson, B.L., McMahon, T.A., 2007. Updated world map of the Köppen-Geiger climate classification. Hydrology and Earth System Sciences 11, 1633–1644. https://doi.org/10.5194/hess-11-1633-2007

Peleg, N., Marra, F., Fatichi, S., Molnar, P., Morin, E., Sharma, A., Burlando, P., 2018. Intensification of Convective Rain Cells at Warmer Temperatures Observed from High-Resolution Weather Radar Data. Journal of Hydrometeorology 19, 715–726. https://doi.org/10.1175/JHM-D-17-0158.1

Penman, H.L., 1948. Natural evaporation from open water, bare soil and grass. Proceedings of the Royal Society of London. Series A. Mathematical and Physical Sciences 193, 120–145. https://doi.org/10.1098/rspa.1948.0037

Peterson, T.C., Golubev, V.S., Groisman, P.Y., 1995. Evaporation losing its strength. Nature 377, 687–688. https://doi.org/10.1038/377687b0

Pilegaard, K., Mikkelsen, T.N., Beier, C., Jensen, N.O., Ambus, P., Ro-Poulsen, H., 2003. Field measurements of atmosphere-biosphere interactions in a Danish beech forest. Boreal Environment Research 8, 315–334.

Prein, A.F., Liu, C., Ikeda, K., Bullock, R., Rasmussen, R.M., Holland, G.J., Clark, M., 2020. Simulating North American mesoscale convective systems with a convection-permitting climate model. Clim Dyn 55, 95–110. https://doi.org/10.1007/s00382-017-3993-2

Prein, A.F., Liu, C., Ikeda, K., Trier, S.B., Rasmussen, R.M., Holland, G.J., Clark, M.P., 2017. Increased rainfall volume from future convective storms in the US. Nature Clim Change 7, 880–884. https://doi.org/10.1038/s41558-017-0007-7

Priestley, C.H.B., Taylor, R.J., 1972. On the Assessment of Surface Heat Flux and Evaporation Using Large-Scale Parameters. Monthly Weather Review 100, 81–92. https://doi.org/10.1175/1520-0493

Rasmussen, A.H., Hondzo, M., Stefan, H.G., 1995. A Test of Several Evaporation Equations for Water Temperature Simulations in Lakes. JAWRA Journal of the American Water Resources Association 31, 1023–1028. https://doi.org/10.1111/j.1752-1688.1995.tb03418.x

Reichstein, M., Falge, E., Baldocchi, D., Papale, D., Aubinet, M., Berbigier, P., Bernhofer, C., Buchmann, N., Gilmanov, T., Granier, A., Grünwald, T., Havránková, K., Ilvesniemi, H., Janous, D., Knohl, A., Laurila, T., Lohila, A., Loustau, D., Matteucci, G., Meyers, T., Miglietta, F., Ourcival, J.-M., Pumpanen, J., Rambal, S., Rotenberg, E., Sanz, M., Tenhunen, J., Seufert, G., Vaccari, F., Vesala, T., Yakir, D., Valentini, R., 2005. On the separation of net ecosystem exchange into assimilation and ecosystem respiration: review and improved algorithm. Global Change Biology 11, 1424–1439. https://doi.org/10.1111/j.1365-2486.2005.001002.x

Rimmer, A., Samuels, R., Lechinsky, Y., 2009. A comprehensive study across methods and time scales to estimate surface fluxes from Lake Kinneret, Israel. Journal of Hydrology 379, 181–192. https://doi.org/10.1016/j.jhydrol.2009.10.007

Roderick, M.L., Rotstayn, L.D., Farquhar, G.D., Hobbins, M.T., 2007. On the attribution of changing pan evaporation. Geophysical Research Letters 34. https://doi.org/10.1029/2007GL031166

Rosenberry, D.O., Stannard, D.I., Winter, T.C., Martinez, M.L., 2004. Comparison of 13 equations for determining evapotranspiration from a prairie wetland, Cottonwood Lake Area, North Dakota, USA. Wetlands 24, 483–497. https://doi.org/10.1672/0277-5212

Rosenberry, D.O., Winter, T.C., Buso, D.C., Likens, G.E., 2007. Comparison of 15 evaporation methods applied to a small mountain lake in the northeastern USA. Journal of Hydrology 340, 149–166. https://doi.org/10.1016/j.jhydrol.2007.03.018

Roulet, N.T., Woo, M.-K., 1986. Wetland and Lake Evaporation in the Low Arctic. Arctic and Alpine Research 18, 195–200. https://doi.org/10.1080/00040851.1986.12004077

Rouse, W.R., 1998. A water balance model for a subarctic sedge fen and its application to climatic change. Climatic change 38, 207–234.

Sartori, E., 2000. A critical review on equations employed for the calculation of the evaporation rate from free water surfaces. Solar Energy 68, 77–89. https://doi.org/10.1016/S0038-092X(99)00054-7

Schmid, H.P., Grimmond, C.S.B., Cropley, F., Offerle, B., Su, H.-B., 2000. Measurements of CO2 and energy fluxes over a mixed hardwood forest in the mid-western United States. Agricultural and Forest Meteorology 103, 357–374. https://doi.org/10.1016/S0168-1923(00)00140-4

Seiller, G., Anctil, F., 2016. How do potential evapotranspiration formulas influence hydrological projections? Hydrological Sciences Journal 61, 2249–2266. https://doi.org/10.1080/02626667.2015.1100302

Seneviratne, S.I., Lüthi, D., Litschi, M., Schär, C., 2006. Land–atmosphere coupling and climate change in Europe. Nature 443, 205–209. https://doi.org/10.1038/nature05095

Sharma, A., Hamlet, A.F., Fernando, H.J.S., Catlett, C.E., Horton, D.E., Kotamarthi, V.R., Kristovich, D. a. R., Packman, A.I., Tank, J.L., Wuebbles, D.J., 2018. The Need for an Integrated Land-Lake-Atmosphere Modeling System, Exemplified by North America's Great Lakes Region. Earth's Future 6, 1366–1379. https://doi.org/10.1029/2018EF000870

Shuttleworth, W.J., 2007. Putting the "vap" into evaporation. Hydrology and Earth System Sciences 11, 210–244. https://doi.org/10.5194/hess-11-210-2007

Sigut, L., 2017. [Toolbox] - A rolling list of software/packages for flux-related data processing [WWW Document]. FLUXNET. URL https://fluxnet.org/2017/10/10/toolbox-a-rolling-list-of-softwarepackages-for-flux-related-data-processing/ (accessed 5.26.21).

Sillmann, J., Thorarinsdottir, T., Keenlyside, N., Schaller, N., Alexander, L.V., Hegerl, G., Seneviratne, S.I., Vautard, R., Zhang, X., Zwiers, F.W., 2017. Understanding, modeling and predicting weather and climate extremes: Challenges and opportunities. Weather and Climate Extremes 18, 65–74. https://doi.org/10.1016/j.wace.2017.10.003

Singh, V., Xu, C.-Y., 1997. Evaluation and generalization of 13 mass-transfer equations for determining free water evaporation. Hydrological Processes 11, 311–323.

Stannard, D.I., Rosenberry, D.O., 1991. A comparison of short-term measurements of lake evaporation using eddy correlation and energy budget methods. Journal of Hydrology 122, 15–22. https://doi.org/10.1016/0022-1694(91)90168-H

Tanny, J., Cohen, S., Assouline, S., Lange, F., Grava, A., Berger, D., Teltch, B., Parlange, M.B., 2008. Evaporation from a small water reservoir: Direct measurements and estimates. Journal of Hydrology 351, 218–229. https://doi.org/10.1016/j.jhydrol.2007.12.012

Tasumi, M., 2005. A Review of Evaporation Research on Japanese Lakes, in: Impacts of Global Climate Change. Presented at the World Water and Environmental Resources Congress, ASCE, pp. 1–10. https://doi.org/10.1061/40792(173)555

Thornthwaite, C.W., 1948. An approach toward a rational classification of climate. Geographical review 38, 55–94. https://doi.org/10.2307/210739

Trenberth, K.E., Asrar, G.R., 2014. Challenges and Opportunities in Water Cycle Research: WCRP Contributions, in: Bengtsson, L., Bonnet, R.-M., Calisto, M., Destouni, G., Gurney, R., Johannessen, J., Kerr, Y., Lahoz, W.A., Rast, M. (Eds.), The Earth's Hydrological Cycle. Springer Netherlands, Dordrecht, pp. 515–532. https://doi.org/10.1007/978-94-017-8789-5_3

Valipour, M., 2015. Temperature analysis of reference evapotranspiration models. Meteorological Applications.

Valipour, Mohammad, 2015. Evaluation of radiation methods to study potential evapotranspiration of 31 provinces. Meteorol Atmos Phys 127, 289–303. https://doi.org/10.1007/s00703-014-0351-3

van Emmerik, T.H.M., Rimmer, A., Lechinsky, Y., Wenker, K.J.R., Nussboim, S., van de Giesen, N.C., 2013. Measuring heat balance residual at lake surface using Distributed Temperature Sensing. Limnology and Oceanography Methods 11, 79–90. https://doi.org/10.4319/lom.2013.11.79

Verhoef, A., Cuxart, J., Marthews, T., Evans, J., van Oevelen, P., 2020. Report on the First Determining Evapotranspiration Workshop. GEWEX Quarterly 30.

Vickers, D., Mahrt, L., 1997. Quality Control and Flux Sampling Problems for Tower and Aircraft Data. Journal of Atmospheric and Oceanic Technology 14, 512–526. https://doi.org/10.1175/1520-0426(1997)014<0512:QCAFSP>2.0.CO;2

Vieira, H., Nazemi, A., 2020. The cooling function of the Cherry River Marsh. Memphrémagog Conservation Inc. 7.

Ville de Magog, 2021. Environnement - Protection des sources d'eau potable [WWW Document]. Ville de Magog. URL https://www.ville.magog.qc.ca/informations-services/environnement/ (accessed 7.16.21).

Wang, H., Olhofer, M., Jin, Y., 2017. A mini-review on preference modeling and articulation in multi-objective optimization: current status and challenges. Complex Intell. Syst. 3, 233–245. https://doi.org/10.1007/s40747-017-0053-9

Wang, K., Dickinson, R.E., 2012. A review of global terrestrial evapotranspiration: Observation, modeling, climatology, and climatic variability. Reviews of Geophysics 50. https://doi.org/10.1029/2011RG000373

Wang, W., Xiao, W., Cao, C., Gao, Z., Hu, Z., Liu, S., Shen, S., Wang, L., Xiao, Q., Xu, J., Yang, D., Lee, X., 2014. Temporal and spatial variations in radiation and energy balance across a large freshwater lake in China. Journal of Hydrology 511, 811–824. https://doi.org/10.1016/j.jhydrol.2014.02.012

Webb, E.K., Pearman, G.I., Leuning, R., 1980. Correction of flux measurements for density effects due to heat and water vapour transfer. Quarterly Journal of the Royal Meteorological Society 106, 85–100. https://doi.org/10.1002/qj.49710644707

Wei, Z., Yoshimura, K., Wang, L., Miralles, D.G., Jasechko, S., Lee, X., 2017. Revisiting the contribution of transpiration to global terrestrial evapotranspiration. Geophysical Research Letters 44, 2792–2801. https://doi.org/10.1002/2016GL072235

Wilczak, J.M., Oncley, S.P., Stage, S.A., 2001. Sonic Anemometer Tilt Correction Algorithms. Boundary-Layer Meteorology 99, 127–150. https://doi.org/10.1023/A:1018966204465

Willmott, C.J., Ackleson, S.G., Davis, R.E., Feddema, J.J., Klink, K.M., Legates, D.R., O'Donnell, J., Rowe, C.M., 1985. Statistics for the evaluation and comparison of models. Journal of Geophysical Research: Oceans 90, 8995–9005. https://doi.org/10.1029/JC090iC05p08995

Wilson, K., Goldstein, A., Falge, E., Aubinet, M., Baldocchi, D., Berbigier, P., Bernhofer, C., Ceulemans, R., Dolman, H., Field, C., Grelle, A., Ibrom, A., Law, B.E., Kowalski, A., Meyers, T., Moncrieff, J., Monson, R., Oechel, W., Tenhunen, J., Valentini, R., Verma, S., 2002. Energy balance closure at FLUXNET sites. Agricultural and Forest Meteorology, FLUXNET 2000 Synthesis 113, 223–243. https://doi.org/10.1016/S0168-1923(02)00109-0

Winter, T.C., Rosenberry, D.O., Sturrock, A.M., 1995. Evaluation of 11 Equations for Determining Evaporation for a Small Lake in the North Central United States. Water Resources Research 31, 983–993. https://doi.org/10.1029/94WR02537

Yin, J., Gentine, P., Zhou, S., Sullivan, S.C., Wang, R., Zhang, Y., Guo, S., 2018. Large increase in global storm runoff extremes driven by climate and anthropogenic changes. Nat Commun 9, 4389. https://doi.org/10.1038/s41467-018-06765-2

Yuling, F., 2005. Energy balance closure at ChinaFLUX sites. Sci. China Earth Sci 48, 2005.

Zandmoghaddam, S., Nazemi, A., Hassanzadeh, E., Hatami, S., 2019. Representing Local Dynamics of Water Resource Systems through a Data-Driven Emulation Approach. Water Resour Manage 33, 3579–3594. https://doi.org/10.1007/s11269-019-02319-3

Zhang, W., Zhu, Y., Jiang, J., 2016. Effect of the urbanization of wetlands on microclimate: a case study of Xixi Wetland, Hangzhou, China. Sustainability.

Zhang, Y., Peña-Arancibia, J.L., McVicar, T.R., Chiew, F.H.S., 2016. Multi-decadal trends in global terrestrial evapotranspiration and its components. Scientific reports. https://doi.org/10.1038/srep19124

Zhou, L., Zhou, G., 2009. Measurement and modelling of evapotranspiration over a reed (Phragmites australis) marsh in Northeast China. Journal of Hydrology 372, 41–47. https://doi.org/10.1016/j.jhydrol.2009.03.033

Appendix A – Stations' Geometry

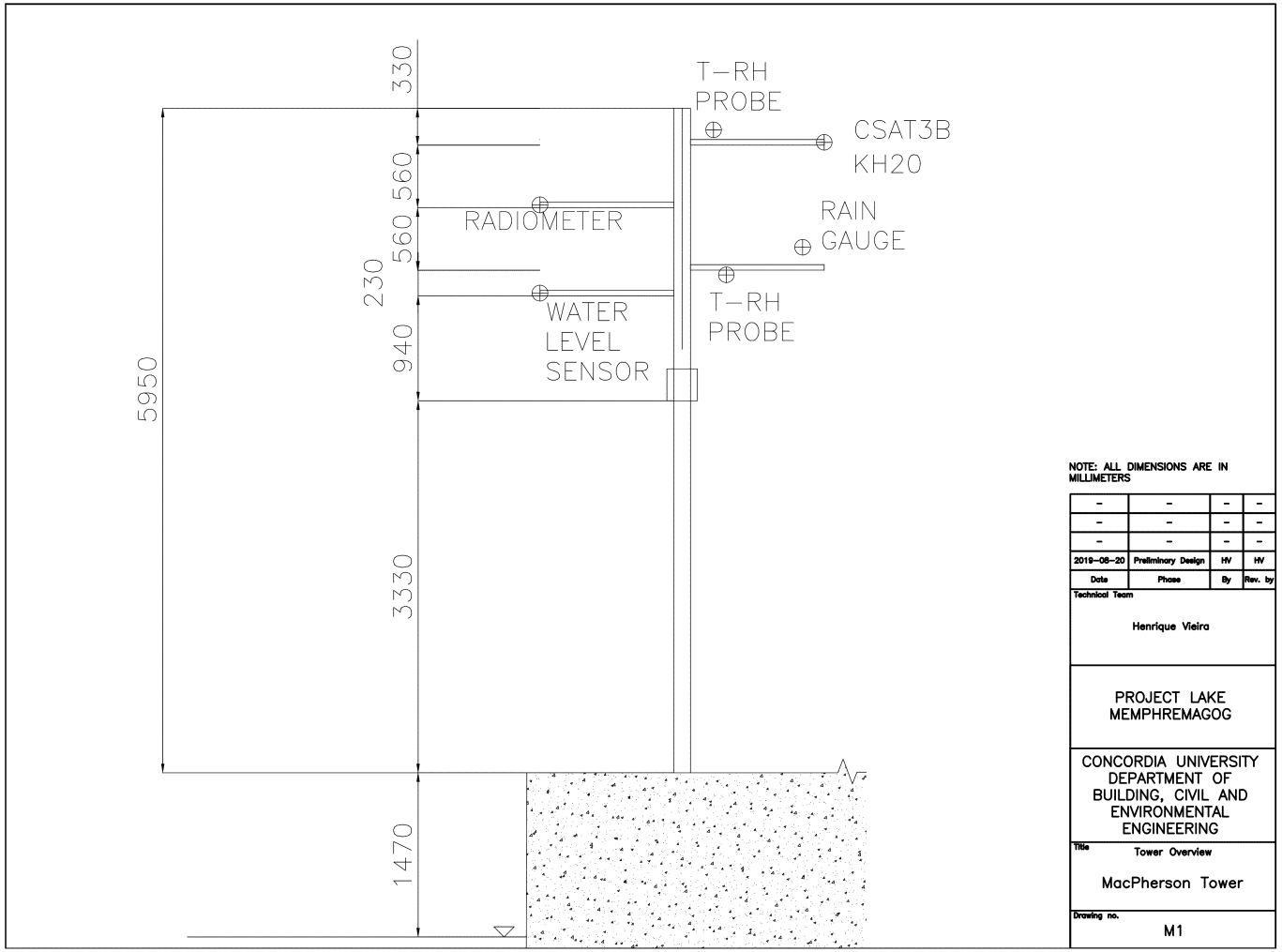

Figure A-1: Geometry of the Lake Macpherson's station – profile view

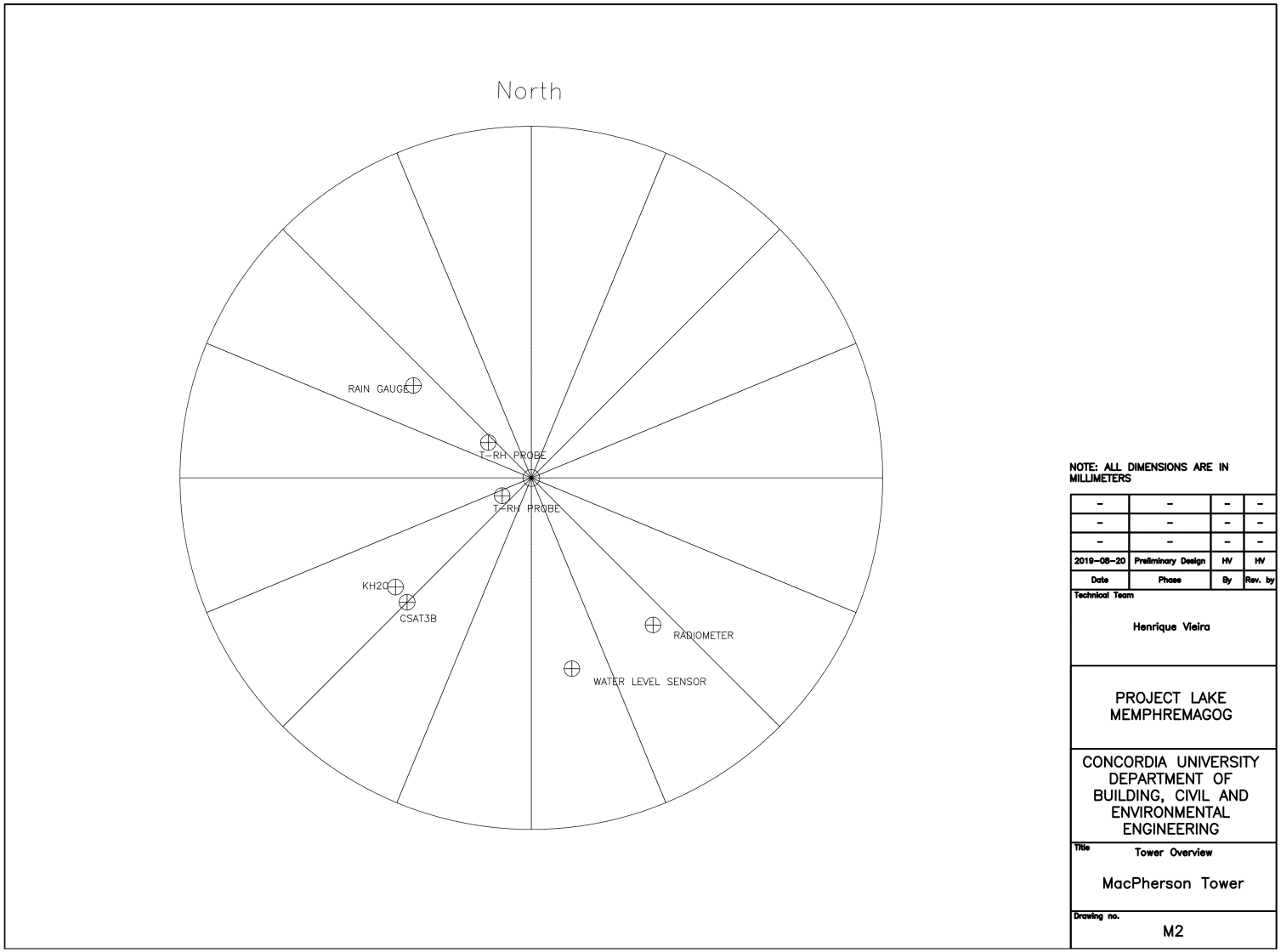

Figure A-2: Geometry of the Lake Macpherson's station – plan view

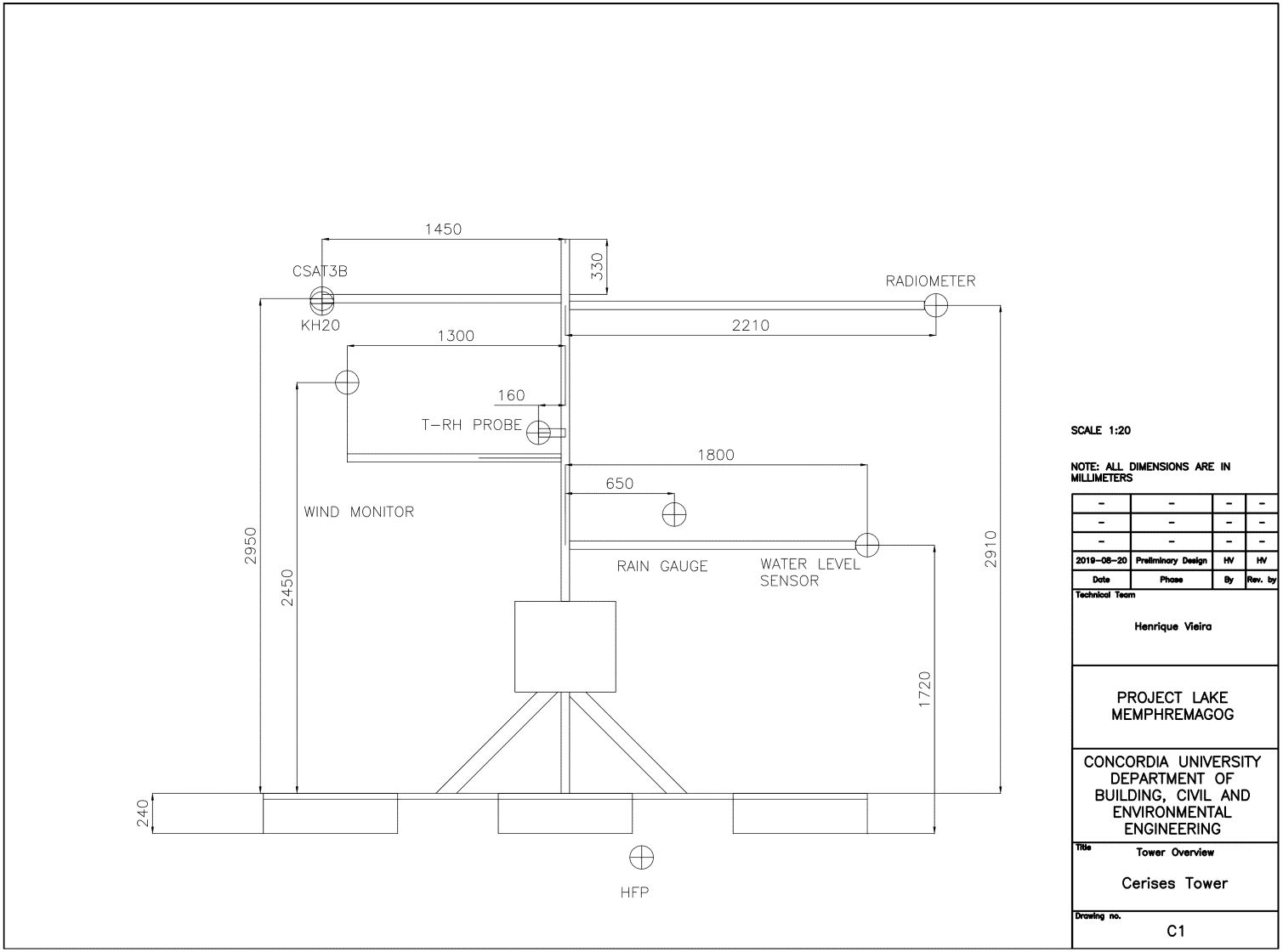

Figure A-3: Geometry of the Cherry River Marsh's station – profile view

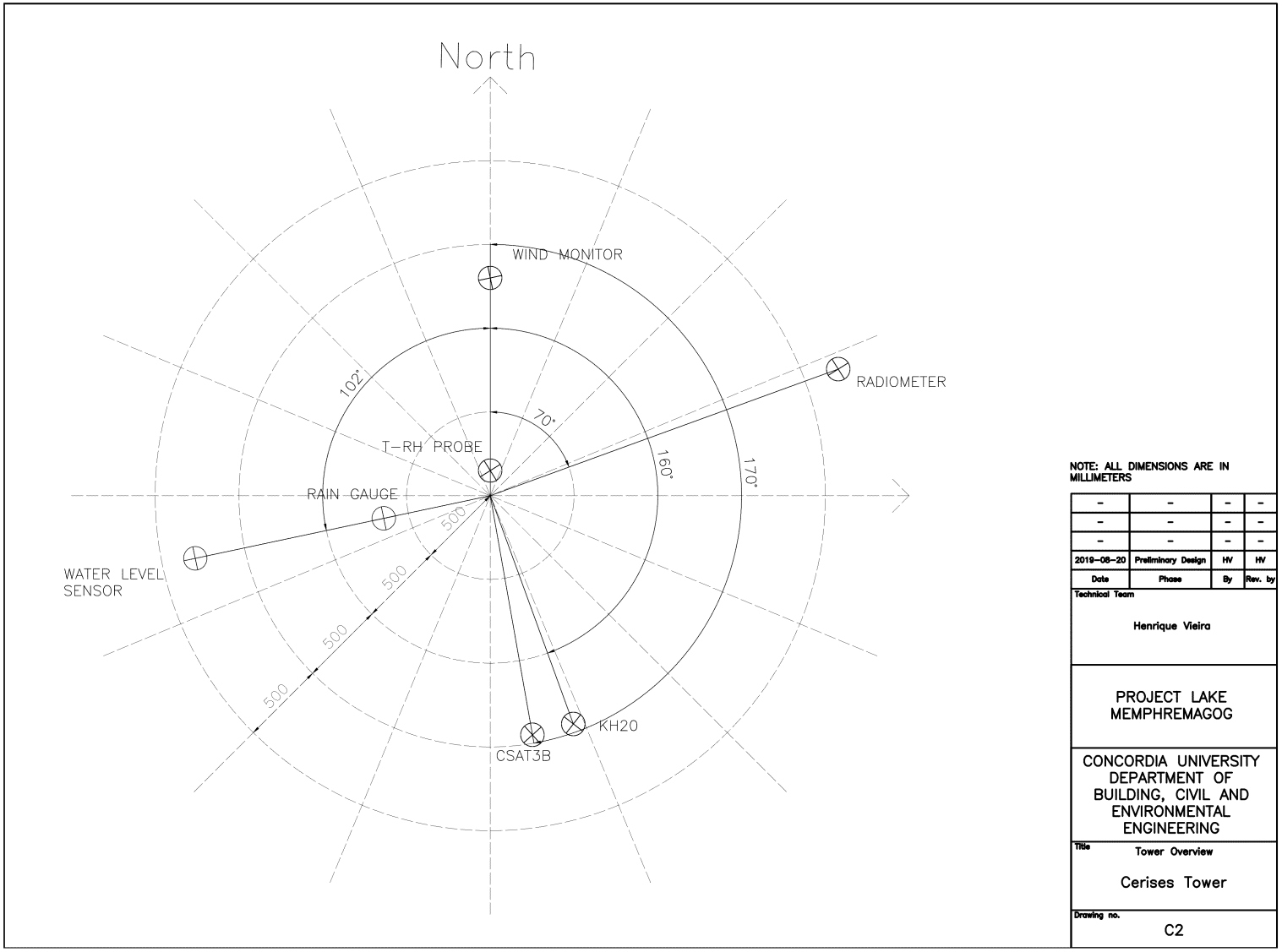

Figure A-4: Geometry of the Cherry River Marsh's station – profile view

Appendix B – The Cooling Function of Cherry River Marsh

The ecosystem services of aquatic environments, such as lakes and wetlands, are not fully understood particularly in urban settings. Conventionally, urban development has often followed a "clear and build" philosophy, where services provided by the ecosystem were undermined and assumed negligible. Recently, the negative consequences of such approaches are being recognized by large and small communities worldwide. In the case of wetlands and shorelines, it has been common practice to excavate, drain and fill these natural bodies in various development projects, but a wealth of problems related to flooding, erosion and water quality follow.

As part of a larger research program, Ali Nazemi – an assistant professor at the Department of Building, Civil and Environmental Engineering, Concordia University – and his team at the Water Security and Climate Change Lab are trying to understand the hydrologic and climatic functions of Lake Memphremagog. His team is composed of engineers and hydrologists who work on understanding the impacts of hydroclimatic, hydrological and management changes on both ecosystem and society, sharing insights and recommending best practices to ensure sustainable resource management.

In collaboration with the city of Magog, two state-of-the-art weather stations were installed in March 2019 to collect fine-scale and detailed microclimatic data at the lake Memphremagog and the nearby Cherry River Marsh. In a preliminary analysis, executed by Henrique Vieira, Dr. Nazemi's MASc student, on a quality-controlled data period, it was found that in the majority of months, particularly in the summer, the marsh system is acting as a natural cooling system for the City of Magog. In fact, the air temperature on the marsh was cooler than on Quai MacPherson during a good portion of 2019, as seen in the graph with the solid line shown below. This shows the significant impact of this marsh system on reducing the surplus heat in summer months that are progressively warming due to climate change. Considering the expected growth in the number of heat-related complications due to more frequent extreme temperature events observed in our changing climate, a nature-based cooling system like the Cherry River Marsh system is a valuable natural asset. Further analysis has shown that the observed decreases in temperature is associated with higher relative humidity in the marsh system, which may be due to higher transpiration rates at the marsh compared to evaporation rates at Lake Memphremagog – see the graph with the dashed line shown below. The team is now looking for formal proof of this hypothesis using the upcoming data in 2020.

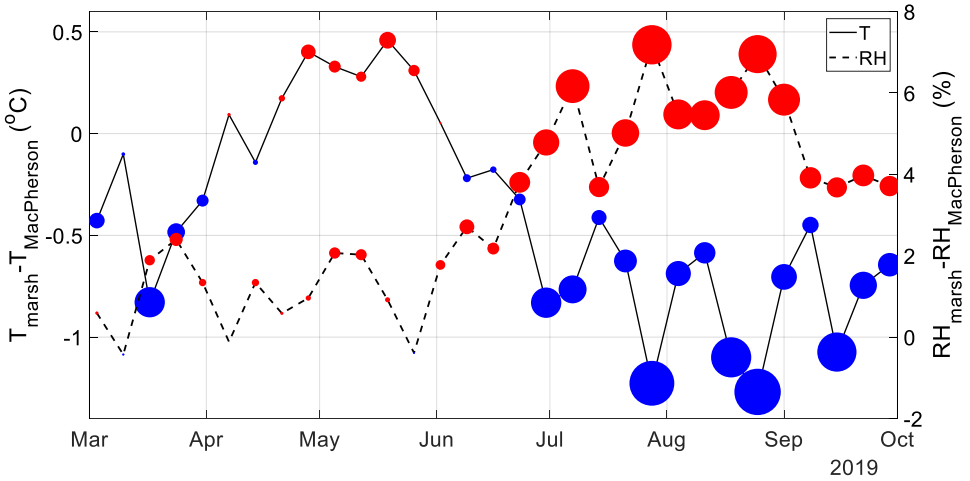

Figure 1. *Differences in temperature (solid line) and relative humidity (dashed line) measured at the Cherry River Marsh and Quai MacPherson. The size of circles is proportional to the difference between temperatures and relative humidity in the two sites. Higher/lower values in the marsh are represented by the red/blue colors.*